THE SKULL OF THE TITANOSAUR *TAPUIASAURUS MACEDOI* (DINOSAURIA: SAUROPODA), A BASAL TITANOSAUR FROM THE LOWER CRETACEOUS OF BRAZIL

Jeffrey A. Wilson[1,2]
Diego Pol[3]
Alberto B. Carvalho[4]
Hussam E. D. Zaher[3]

1. Museum of Paleontology & Department of Earth and Environmental Sciences, University of Michigan, Ann Arbor, MI, U.S.A.
2. Corresponding author: E-mail: wilsonja@umich.edu
4. Consejo Nacional de Investigaciones Científicas y Técnicas (CONICET), Museo Paleontológico Egidio Feruglio, Trelew, Argentina
3. Museu de Zoologia da Universidade de São Paulo, Serviço de Vertebrados, São Paulo, SP, Brasil

This is the author manuscript accepted for publication and has undergone full peer review but has not been through the copyediting, typesetting, pagination and proofreading process, which may lead to differences between this version and the Version of Record. Please cite this article as doi: 10.1111/zoj.12420

Received Date : 22-Jul-2015
Revised Date : 04-Feb-2016
Accepted Date : 09-Feb-2016
Article type : Original Article

ABSTRACT— Although Titanosauria is the most diverse and late-surviving sauropod lineage, cranial elements are known for just over 24 of its 70+ genera—the vast majority of which are fairly fragmentary and restricted to the Late Cretaceous. Only three complete titanosaur skulls have been described to date; two of these are from the latest Cretaceous (Nemegtosaurus, Rapetosaurus), and the third, Tapuiasaurus, is from the Early Cretaceous (Aptian). In this contribution, we build on the initial treatment of the taxon by providing a complete description of the cranial elements that benefits from additional preparation and Computed Tomography imaging. We identify 6 additional features diagnosing Tapuiasaurus macedoi, including a jugal with an elongate lacrimal process forming much of the posteroventral border of the antorbital fenestra, a lateral temporal fenestra divided by a second squamosal-postorbital contact, and upper jaw teeth with labial wear facets. We directed the new morphological data in Tapuiasaurus as well as other observations towards a re-analysis of its phylogenetic position within Titanosauria. Our analysis yielded 34 most parsimonious trees, most of which recovered Tapuiasaurus in a basal position adjacent the Early Cretaceous taxa Malawisaurus and Tangvayosaurus, but two recovered it within Late Cretaceous nemegtosaurids. We explored the effects of missing data and missing stratigraphic ranges on our results, concluding that (1) when missing data levels are high, resolution of even small amounts of that missing data can have dramatic effects on topology, (2) taxa that are mostly scored for characters that cannot be scored in other taxa may be topologically unstable, and (3) there were several slightly suboptimal trees that had greatly improved stratigraphic fit with relatively little compromise in terms of treelength.

Keywords: Gondwana—Mesozoic—MIG—missing data—morphology—Sauropodomorpha—South America—systematics—vertebrate palaeontology

INTRODUCTION

The recent discovery of a complete skull and partial postcranial skeleton of Tapuiasaurus macedoi (Zaher et al., 2011) offered the first glimpse at the skull of a titanosaur from South America, where the greatest documented diversity of that group has steadily accumulated since the first species were named in the late 19th Century (Lydekker, 1893; Ameghino, 1898). Currently there are 30–38 valid titanosaur species known from South America (J.A. Wilson & M.D. D'Emic, unpubl. data), the vast majority of which were recovered from Upper Cretaceous sediments of Argentina. South American species account for approximately half of the global diversity of Titanosauria (70+ species).

Cranial remains of titanosaurs, including braincases, teeth, and mandibular fragments, have been recovered for approximately one-third of titanosaur species (Table 1), but until quite recently no complete titanosaur skull had been described, although two were briefly mentioned more than 15 years ago (Calvo et al., 1997; Martínez, 1998). Ironically, two complete but isolated titanosaur skulls from the latest Cretaceous of Mongolia spent some 35 years misclassified as diplodocoids (Nemegtosaurus, Nowinski, 1971; Quaesitosaurus, Kurzanov & Bannikov, 1983) due to the absence of comparable material and the mistaken assumption that titanosaurs were restricted to or predominant on southern landmasses. It wasn't until the discovery of a nearly complete skull in association with a bone fide titanosaur skeleton that titanosaur cranial anatomy was definitively known (Rapetosaurus, Curry Rogers & Forster, 2001).

<<Table 1 approximately here>>

Tapuiasaurus is one of only two Early Cretaceous titanosauriforms preserved with a complete skull, the other being the brachiosaurid Abydosaurus mcintoshi (Chure et al., 2010). Although they share general similarities consistent with their placement within Titanosauriformes, their skulls do not closely resemble one another—Abydosaurus has a more boot-shaped profile that recalls the skull of Giraffatitan, whereas Tapuiasaurus has a more elongate skull with a downwardly deflected snout more similar to the Late Cretaceous titanosaurs Rapetosaurus and Nemegtosaurus (Zaher et al., 2011). The sister-taxon relationship recovered between Tapuiasaurus and these Late Cretaceous titanosaurs implies (1) a minimum 55 million-year stratigraphic debt, potentially double that depending on topological relationships, and (2) the 8 other valid titanosaur species analyzed, known from no or very fragmentary cranial remains, did not possess this 'classic' titanosaur skull morphology possessed by nemegtosaurids. But what of the ca. 60 other valid titanosaur species known from no or very fragmentary cranial remains? Did their skulls resemble those of Tapuiasaurus, Rapetosaurus, and Nemegtosaurus or were they distinct?

In this paper, we provide a detailed description of the skull of Tapuiasaurus macedoi based the holotypic and only exemplar. Our goal is to provide morphological data that can be used in subsequent phylogenetic analyses and studies of titanosaur feeding. We rescore Tapuiasaurus and certain other titanosaur taxa and re-analyze the original matrix, and we discuss the distribution of missing data within Titanosauria and how this and similar patterns affect phylogenetic analysis.

ABBREVIATIONS

Institutions. BP, Bernard Price Institute for Palaeontological Research, University of Witwatersrand, Johannesburg, South Africa; MML, Museo Municipal de Lamarque, Río Negro, Argentina; MZSP-PV, Museu de Zoologia da Universidade de São Paulo, Brazil.

DISPOSITION OF CRANIAL ELEMENTS IN QUARRY

The holotypic skeleton of Tapuiasaurus macedoi was collected in lacustrine claystone sediments of the Quiricó Formation exposed near Coração de Jesus, Minas Gerais, Brazil. The skull was found articulated to the mandibles and neck, and the hyoid bones were preserved in a position close to their expected life position (Fig. 1). The left side of the skull, which is the more distorted, was found in the 'up' position in the field. It was rotated slightly ventrolaterally such that the ventral "U"-shaped outline of the mandible was exposed first. This was followed by the left maxillary teeth and parts of the left side of the skull. The right side of the skull was preserved face-down in the field. It was protected by sediments and is the better preserved side. The mandible was found attached to the skull, swung open at an angle of approximately 30˚, with a small part of the surangular found underneath the anteroventral projection of the quadratojugal. The two hyoid elements were found between and below the posterior ends of the mandibles. The left element was preserved closer to the mandibles than the right element. The longer, anterior branches were aligned with the upper tooth row, whereas the shorter, posterodorsal branches were aligned with the squamosal process of the quadratojugal. In relation to the anteroposterior position, the anterior extremities of the hyoid bones were coincident with the posterior end of the dentary bones.

The proatlas was found attached to the basicranium, covering the foramen magnum. The atlas-axis complex was found just posterior to the proatlas. Due to deformation, the axis,

and not the paroccipital process, was found attached to the posterior projection of the squamosal in the right side.

<<Figure 1 approximately here >>

DESCRIPTION

The description of the skull that follows is based on the holotypic skeleton, which includes an articulated anterior cervical region and other postcranial bones (see Zaher et al., 2011). The postcranium is not treated in this description because it is not yet fully prepared, but it will be the subject of a subsequent contribution.

We utilize Romerian orientational descriptors (i.e., anterior, posterior) rather than standardized terms (i.e. cranial, caudal), and we employ an eclectic terminology for skull bones rather than NAA/NAV terms (for more discussion on terminology, please see Harris, 2004; Wilson 2006). There is no standardized terminology for sauropod skull bones and their various processes, despite numerous excellent descriptions (e.g., Diplodocus, Holland, 1924; Giraffatitan, Janensch, 1935-6; Camarasaurus, Madsen et al., 1995). For example, the rami of the postorbital often recieve orientational descriptors (e.g., "anterior process of the postorbital"), even though the orientations are not always consistent or unambiguous. Even when they are consistent, however, the orientation of the skull with respect to the axial column can vary between sauropod taxa (e.g., Camarasaurus vs. Diplodocus), which creates further problems with this sort of orientational descriptor. Less commonly used are morphological descriptors (i.e., "frontal process of the postorbital"), but these too have drawbacks. Morphological descriptors for processes are not always informative when a certain process contacts multiple bones or when different processes each contact the same bone, which usually requires some additional orientational descriptor. There is no practical solution for this issue yet, but we consider the orientational ambiguity more severe than the morphological ambiguity. Where convenient, we use morphological, rather than orientational, terms for cranial processes to avoid orientational confusion. In certain cases however, it was more practical to use orientational terms (e.g., anteromedial process of the maxilla; anterior process of the lacrimal).

GENERAL

The skull of Tapuiasaurus macedoi (MZSP-PV 807) is approximately half a meter long and nearly half as tall (Fig. 2; Table 2). In general form, the skull most closely resembles that of

other narrow-crowned sauropods, such as the titanosaur Nemegtosaurus and the diplodocoid Diplodocus. The dentigerous portion of the skull in Tapuiasaurus represents 28% its total length, which is slightly greater than in Diplodocus (17.5%) or Nemegtosaurus (20%). The values for these narrow crowned forms differ significantly from those of broad-crowned forms (e.g., Camarasaurus = 50%), which have a comparable number of broad teeth, and from those of basal sauropodomorphs (e.g., Plateosaurus = 60%), which have a larger number of medium-breadth teeth.

<<Figure 2 approximately here>>

<<Table 2 approximately here>>

The skull in T. macedoi is very well preserved and nearly complete, lacking only portions of the bones bordering the narial region (viz. maxilla, premaxilla, nasal, lacrimal). Neither stapes was preserved, but the ceratobranchials were preserved with the skull.

The skull has been deformed by transverse compression and anterodorsal shearing. As a result, the transverse dimension of the skull is reduced, and bones in the palate, skull roof, and occiput have been damaged. The skull roof in particular has suffered extensive fracturing, rendering more difficult the interpretation of the shape of and connections between bones. The preservational distortion to the skull of Tapuiasaurus resembles that of the Nemegtosaurus holotype, which was likewise compressed transversely and slightly sheared anteriorly on one side (Nowinski, 1971: pl. 8).

Most cranial sutures are readily visible in this specimen of Tapuiasaurus. Individual braincase bones, which typically completely coossify in adult sauropods, are readily distinguishable. Other bones that fuse to one another in some adult sauropods, such as the parietals and the frontals, remain unfused in this specimen of T. macedoi.

Most cranial elements were readily visible in at least one view in the articulated skull. Due to the compression and shearing of the skull, however, certain regions of the skull were difficult to visualize, including the palate and braincase. Computed Tomography (CT) images of the skull were obtained in a Siemens Somaton Emotion scanner (slice: 0.63 mm; inter-slices: 0.3 mm; FOV: 281; kV: 110) at the Centro de Diagnóstico por Imagem (Unidade Nova América) in Rio de Janeiro, Brazil. The scans aided description of the areas of the skull that are difficult to visualize and provided additional clarity on particularly difficult areas to interpret (e.g., braincase, palate).

DERMAL ROOF COMPLEX

The dermal roof complex consists of median roofing bones (premaxilla, maxilla, nasal, frontal, parietal) and the circumorbital series (postorbital, prefrontal, lacrimal, jugal, squamosal, quadratojugal), which we describe in that order.

Premaxilla (Figs. 3, 4)

Completeness: The left and right premaxillae are nearly complete; each lacks only the distal end of its narial process.

Contacts/Borders: The premaxilla contacts its opposite on the midline and the maxilla and vomer. It forms the anterior margin of the external naris.

Morphology: The premaxilla is a tooth-bearing bone in the upper jaw that consists of a quadrangular body and an elongate, posteriorly-directed narial process.

The premaxillary body and narial process are distinguished from one another by a marked change in surface bone texture. The body of the premaxilla, which contains alveoli for four teeth, is pitted with small foramina and, like the maxilla, bears elongate, low ridges associated with the alveoli. The narial process of the premaxilla, in contrast, has the smooth, unpitted texture present in non-dentigerous cranial bones. A conspicuous foramen (ca. 5 mm long) marks this transition near the base of alveoli for the second and third premaxillary teeth. The premaxillary body is fairly narrow transversely, owing to the slenderness of the four tooth crowns it houses. Its contact with the maxilla is the most elongate suture in the skull, extending for more than half its length. For most of the premaxilla-maxilla suture, the two bones contact along a simple butt-joint, but near the transition between the pitted and smooth portions of the premaxilla, an anteromedially-directed process of the maxilla extends posterior to the premaxilla. Just below this overlapping contact is a small opening that we tentatively identify as the subnarial foramen, based on the position of and bones enclosing this structure in other sauropodomorphs (e.g., Eoraptor; Sereno et al., 2013). This identification differs from that of Zaher et al. (2011: fig. 1), who identified a larger opening enclosed by the maxilla as the subnarial foramen. As discussed below, we identify the latter opening as the anterior maxillary foramen.

The base of the narial process of the premaxilla is approximately 3.5 cm broad. It tapers quickly to nearly half that breadth and then very gradually narrows towards its distal terminus, which is incomplete but extends posteriorly as far as does the jugal process of the maxilla. The length and morphology of the missing portion of the narial process is difficult to

reconstruct, because the premaxilla is not completely preserved in any described titanosaur, neither in disarticulated elements (e.g., Malawisaurus; Narambuenatitan) nor in intact skulls (e.g., Nemegtosaurus; Quaesitosaurus). In the basal titanosauriform Abydosaurus, the narial process of the premaxilla is nearly complete, and it tapers to less than half a centimeter as an internarial bar that contacts the nasal (Chure et al., 2010). Although we cannot rule out the presence of a short internarial process of the premaxilla, we consider it unlikely based on the absence of an internarial process on the nasal (see below).

Posteriorly and medially, the premaxilla is successively overlapped by the anteromedial process of the maxilla and the vomer. There is a small, tab-like posteromedial process of the premaxilla, which is best preserved on the left side (Fig. 4).

Comments: The premaxilla is transversely narrow and the narial process is elongate, as in other narrow-crowned forms. The apparent reduction of the subnarial foramen in Tapuiasaurus, if correctly identified, is a feature shared with Nemegtosaurus and Diplodocus.

<< Figures 3 & 4 approximately here >>

Maxilla (Figs. 3–6)

Completeness: The right and left maxilla are nearly complete on both sides of the skull; each lacks only the tip of its nasal process.

Contacts/Borders: The maxilla contacts other dermal roof complex elements, including the premaxilla, jugal, lacrimal, and probably the prefrontal, as well as palatal elements, such as the palatine, ectopterygoid, and vomer. The maxilla participates in the margins of the antorbital fenestra and external naris.

Morphology: The maxilla consists of a main body, which is dentigerous, an elongate narial process, and a slightly shorter jugal process.

The body of the maxilla is set off from its jugal and nasal processes by a series of openings extending across the top of the snout. The posteriormost of these, positioned near the base of the jugal process, is the preantorbital fenestra, which is large (5.4 x ca. 3 cm) and bordered posteriorly and ventrally by a shallow fossa. Although the preantorbital fenestra is positioned near to the antorbital fenestra, it has no connection to it. Rather, the preantorbital fenestra opens into the maxillary canal and connects to two smaller foramina (long axis 1.1

cm, 0.7 cm) that lie in front of it, as well as to the relatively large anterior maxillary foramen (1.1 x 0.6 cm) positioned near the contact with the premaxilla (Fig. 5).

The body of the maxilla bears light pitting and a ridged texture resulting from the undulations formed by between adjacent alveoli. The body of the maxilla contacts the premaxillary body along a suture that is oriented nearly orthogonal to the alveolar margin. This ventral portion of the suture is straight, differing from the sinuous suture in Nemegtosaurus (Wilson 2005) and Abydosaurus (Chure et al., 2010). There is a small opening in the premaxilla–maxilla suture positioned approximately 0.5 cm anteroventral to the anterior maxillary foramen, which we identify as the subnarial foramen. Its position and size resemble the condition in Diplodocus (Wilson & Sereno, 1998) and Nemegtosaurus (Wilson et al., 2005). The subnarial foramen typically opens between the premaxilla and maxilla in saurischian dinosaurs (e.g., Eoraptor; Sereno et al., 2013), rather than within the maxilla itself (see Zaher et al., 2011: fig. 1).

The maxilla holds 12 alveoli; within each of these is a functional tooth and at least two replacing teeth (Fig. 6). Posterior to its dentigerous portion, the maxilla is dorsally embayed approximately 4 cm relative to a line connecting the posterior alveolar margin and the anteroventral corner of the quadratojugal. This post-dentigerous embayment on the maxilla consists of a roughly horizontal portion and a more vertically-oriented portion. The horizontal portion extends posteriorly as the jugal process of the maxilla. The more vertically-oriented portion projects posteriorly as a convex tab of bone that tapers to a narrow edge (3 mm). It bears a pitted lateral surface and a striated, spiculated medial surface.

The medial portion of the maxillary body is well exposed in ventral view (Fig. 4). A series of 12 replacement foramina are evenly spaced approximately 1.5 cm above the alveolar margin. The replacement foramina are roughly circular to D-shaped (0.5 x 0.5 cm) and arranged in a gently arched line that drops off dramatically at the 12th replacement foramen. Dorsal to the replacement foramina is a well-marked palatal shelf that extends its length; its posterior end furnishes the articulation for the palatine and ectopterygoid. The anteromedial process of the maxilla is dorsoventrally deep and tongue-shaped anteriorly. It underlaps the premaxilla posteromedially and is backed posteriorly by the vomer. Just below the anteromedial process is the subnarial foramen, which is visible at the same level laterally.

The jugal process of the maxilla is triangular and tapers sharply towards its distal end. It is overlain by the elongate, anteriorly-directed maxillary process of jugal, which nearly excludes the maxilla from the ventral margin of the antorbital fenestra. The distal tip of the

jugal process of the maxilla was not completely preserved, but it does not appear to have contacted the quadratojugal.

The narial process of the maxilla is dorsoventrally deep. A small process extends from its ventrolateral edge to overlap the lacrimal and approach (and probably contact) the prefrontal. This relatively short process is set off sharply by a well-marked narial fossa, which becomes quite shallow medially and anteriorly. The maxilla clearly overlaps the lacrimal in Tapuiasaurus, as it does in other titanosauriforms (e.g., Nemegtosaurus, Abydosaurus), but the nature of that overlap is not clear. The shape of the lacrimal (see below) suggests that a small portion of it was exposed medial to the narial process of the maxilla and would have formed part of the margin of the external naris, as was suggested for Rapetosaurus (Curry Rogers & Forster, 2004).

Comments: Tapuiasaurus has an autapomorphically elongate, tapering post-dentigerous process of the maxilla that is elevated above the alveolar margin. The presence of a tab-like process near the base of that process is shared with Rapetosaurus (Curry Rogers & Forster, 2004: fig. 3) and possibly with the second specimen of Nemegtosaurus (J.A. Wilson, unpubl. data), an undescribed specimen that has been attributed to Ampelosaurus (J. Le Loeuff, per. comm.), and Narambuenatitan (Filippi et al., 2011: fig. 4). The narial process of the maxilla of Tapuiasaurus is dorsoventrally deeper than is the post-dentigerous process and expands distally to house a well demarcated narial fossa. This feature is distinct from titanosauriforms such as Abydosaurus as well as Rapetosaurus, which is the only other titanosaur for which these parts of the maxilla are known. The palatal shelf of the maxilla in Tapuiasaurus extends the length of its jugal process, as it does in Rapetosaurus (Curry Rogers & Forster, 2004: figs. 3, 4).

<<Figures 5, 6 approximately here >>

Nasal (Fig. 7)

Completeness: The nasals are poorly preserved. Their contact with the frontals are obscured by matrix and bone fragments, and their midline contact is broken away. Their contact with the prefrontal is well-preserved.

Contacts/Borders: The nasal contacts its opposite on the midline, the frontal, and the prefrontal. The nasal forms the posterolateral margin of the external naris.

Morphology: The nasal is a small, L-shaped bone. The base and anterior process of the nasal form the short and long arms of the "L," respectively, with the external naris filling the angle between the two. The anterior process of the nasal is elongate and tapers distally from its medial side only; its lateral margin is straight and contacts the prefrontal along its entire length (Fig. 7).

The base of the nasal is anteroposteriorly elongate, probably indicating a substantial midline contact. Although the midline connection between the nasals is not quite completely preserved, there probably was no internarial bar because there is no hint of an anteriorly directed process. The base of the nasal appears to have been inset further posteriorly into the frontal than is the prefrontal.

Comments: The absence of an internarial bar in Tapuiasaurus resembles the condition reconstructed for Rapetosaurus (Curry Rogers & Forster, 2001), but differs from that of Nemegtosaurus and other titanosauriforms (e.g., Abydosaurus).

<<Figure 7 approximately here >>

Frontal (Figs. 7, 8)

Completeness: The frontals are the most damaged bones in the skull of Tapuiasaurus. Although the bones are physically present, they have been fragmented and jumbled. The right frontal is much better preserved than the left; its orbital margin and contacts with the adjacent bones can be reliably reconstructed.

Contacts: The frontal contacts its opposite on the midline, as well as the parietal, postorbital, prefrontal, nasal, laterosphenoid, and orbitosphenoid. The frontal forms the dorsal margin of the orbit and the anterior margin of the supratemporal fenestra.

Morphology: The frontal is the main skull roofing element. It is broader transversely than it is long anteroposteriorly (6.7 x 5.2 cm) and dorsally convex, forming the upper orbit. The lateral margin of the frontal is convex in dorsal view (Fig. 8), ca. 0.5 mm thick, and bears small, ridged ornamentation that is oriented radially with respect to the orbit. Medially, the frontal meets its opposite along a suture whose toothed margin is preserved in some broken fragments near the midline. Due to the significant damage near the midline, it is difficult to determine whether the frontals were domed or peaked there. The former seems less likely, because there is little elevation of the frontal immediately adjacent the broken median bone.

The shape of the outline of the frontal cannot be determined, and so it is not known whether the two frontals form a hexagon in dorsal view as they do in Nemegtosaurus (Wilson, 2005: fig. 7).

The frontal-prefrontal suture is moderately well preserved. These two elements contact along a slightly overlapping suture in which the prefrontal rests on the dorsal margin of the frontal. Unfortunately, the nasal and frontal are not well enough preserved to determine the exact course and nature of their overlap.

Posteriorly, the frontal contacts the parietal along a relatively short, straight, vertical suture that is contiguous with the suture for the postorbital, which begins near the medial margin of the supratemporal fenestra. In contast to the frontal-parietal contact, which is a vertical butt-joint, the frontal and postorbital meet along an overlapping suture that is slightly anteriorly inclined. The supratemporal fossa does not extend onto the frontal, being restricted to the parietal and postorbital.

The contacts between the frontal and braincase elements (i.e., laterosphenoid, orbitosphenoid) are not exposed.

Comments: The poor preservation of the frontals means that several characters cannot be reliably scored in Tapuiasaurus, such as the shape of the frontals in dorsal view or their doming at the midline.

<<Figure 8 approximately here >>

Parietal (Figs. 7–9)

Completeness: The parietals are nearly complete but damaged in the region of the frontal–parietal suture and near the midline.

Contacts/Borders: The parietal contacts its opposite on the midline, as well as the supraoccipital, exoccipital-opisthotic, prootic, squamosal, frontal, postorbital, and possibly the laterosphenoid. The parietal forms the posteromedial margin of the supratemporal fenestra.

Morphology: The parietal is a transversely elongate bone that forms the posterior part of the skull roof and the dorsal part of the occiput. The posterodorsal edge of the parietal, which forms the boundary between these two regions, is arched ventrally and sigmoid-shaped in dorsal view (Fig. 8). The edge is rounded and marked by roughened bone on the occipital

surface. The dorsally-facing skull roof portion of the parietal is embayed laterally by the supratemporal fenestra. The two arms bordering the embayment are unequal in length and anteroposterior thickness. The longer and thicker posterior arm of the parietal contacts the squamosal and posterior portion of the postorbital, and the shorter and thinner anterior arm contacts the frontal and the anterior portion of the postorbital. The distance between the supratemporal fenestrae is 5.7 cm, which is approximately the greatest diameter of each opening. The anterior arm of the parietal contacts the postorbital along a nearly vertically-oriented suture. The medial portions of the right and left parietals are just well-enough preserved to discern that they are sutured, rather than fused to one another, as they are to the frontal. They are not well enough preserved to rule out with certainty the presence of a median foramen within the parietal or between the parietal and frontal, but the presence of bone approaching the midline suggests this is unlikely.

The occipital portion of the parietal is narrow and gently arched ventrally, forming the dorsal portion of the occipital fossa. Ventrally, the occipital portion of the parietal borders the supraoccipital, exoccipital-opisthotic, and squamosal. Distally, this portion of the parietal contacts the postorbital.

Comments: The parietal of Tapuiasaurus contacts the postorbital to exclude the squamosal from the supratemporal fenestra, as in Nemegtosaurus and Quaesitosaurus. The occipital fossa of the parietal is oriented vertically, differing from the condition present in certain titanosaurs (e.g., Bonatitan) whose occipital fossa expanded anteriorly and exposed in dorsal view. The posttemporal fenestra in Tapuiasaurus appears to be absent.

<<Figure 9 approximately here >>

Postorbital (Figs. 7, 8, 10)

Completeness: The postorbital is complete and well preserved, but its medial surface, including the connection to the laterosphenoid, is not visible. The jugal process of the postorbital is twisted dextrally on the right side due to impingement of the quadrate and braincase bones; on the left side it is broken and displaced from its natural position.

Contacts: The postorbital contacts the squamosal, jugal, frontal, parietal, and laterosphenoid. The postorbital borders the orbit, lateral temporal fenestra, and supratemporal fenestra.

Morphology: The postorbital is a triradiate bone whose three processes each separate two skull openings. The elongate jugal process of the postorbital separates the orbit and lateral temporal fenestra, the abbreviate squamosal process separates the supratemporal and lateral temporal fenestrae, and the frontal process separates the orbit and supratemporal fenestra. The long axes of the jugal and squamosal processes are nearly collinear, and the frontal process extends nearly orthogonally to them. Near the junction among the three processes, the postorbital bears light orbital ornamentation consisting of small pits and ridges.

The jugal process of the postorbital is transversely deep (1.7 x 0.3 cm) and convex, and it gently bows posteriorly, forming the rounded posterior margin of the orbit. Towards its distal end, though, it becomes rod-like and ends in a blunt tip. The postorbital contacts the jugal along nearly half its length, meeting along a flat contact in which the postorbital overlaps the jugal anteriorly. On both the right and left sides of the skull, the gently bowed jugal process of the postorbital touches the squamosal, effectively dividing the lateral temporal fenestra into unequal portions. Although the collapsing of the temporal region around the braincase has distorted this region, we believe that this additional squamosal-postorbital contact and subdivided lateral temporal fenestra is natural.

The squamosal process of the postorbital is extremely short and triangular. It meets the squamosal along an inverted L-shaped articulation. As a result, the dorsal portion of the lateral temporal fenestra is anteroposteriorly narrow. The squamosal process of the postorbital has a small point contact with the parietal, which excludes the squamosal from participation in the supratemporal fenestra (see below, "Squamosal" and "Supratemporal Fenestra").

The frontal process of the postorbital is much more elongate than is the squamosal process (ca. 4.5 vs. 0.7 cm), and it is deeper transversely than long anteroposteriorly (ca. 2.5 vs. 1.0 cm). The portion of the frontal process bordering the orbit bears fine radial ridges and low, bumpy texture. Medially, the frontal process forms the anterior border of the supratemporal fenestra, overlapping the frontal and contacting the lateral edge of the parietal.

The postorbital-laterosphenoid contact is not visible on either side of the skull, but it was likely present based on the relationship of those bones in other titanosaurs.

Comments: Whereas in other titanosaurs such as Nemegtosaurus and Quaesitosaurus the three processes of the postorbital form a "T" shape with collinear squamosal and postorbital processes, in Tapuiasaurus it is the jugal and squamosal processes that are collinear, with the postorbital process extending at an oblique angle from them. Tapuiasaurus is unique among

titanosaurs in possessing an additional postorbital-squamosal contact, which subdivides the lateral temporal fenestra. The condition in Tapuiasaurus is similar to but distinct from that in rebbachisaurids such as Nigersaurus and Limaysaurus, which have reduced or completely closed both temporal openings (see Calvo & Salgado, 1995; Sereno et al., 2007).

<<Figure 10 approximately here >>

Prefrontal (Fig. 7)

Completeness: The prefrontal is nearly completely preserved, lacking only its distal tip and a small portion of its posteromedial margin.

Contacts/Borders: The prefrontal contacts the nasal, frontal, lacrimal, and probably the maxilla. The prefrontal forms the anterodorsal border of the orbit.

Morphology: The prefrontal is a triangular bone that is anteroposteriorly elongate and transversely narrow at its base (ca. 9.0 x 2.2 cm). It is flat posteriorly and tapers along its lateral margin towards a narrow anterior tip. The posterior margin of the prefrontal rests upon the dorsal surface of the anterior frontal. The prefrontals brace the nasals, which are approximately 25% broader transversely and perhaps slightly shorter anteroposteriorly. Distally, the prefrontal contacts the dorsolateral surface of the lacrimal in a region of the skull that is poorly preserved on both sides. It appears that the nasal and lacrimal exclude the prefrontal from the external naris, but there is a chance that a small stretch of the prefrontal is exposed on its margin.

A small foramen, trailed posteriorly by a narrow groove, is present on the dorsal margin of the right prefrontal (Fig. 7). The left prefrontal is not preserved well enough to determine whether the foramen was present. Near its contact with the frontal, the orbital margin of the prefrontal bears very light ornamentation that is developed to a similar extent as that on the jugal process of the postorbital.

Comments: The prefrontal of Tapuiasaurus resembles that of Rapetosaurus in its elongate, transversely narrow dorsal profile. In this respect, it differs from that of Nemegtosaurus and those of basal titanosauriforms (e.g., Abydosaurus, Giraffatitan), which are tranvsersely broader elements.

Lacrimal (Fig. 11)

Completeness: The right lacrimal is not complete, lacking its anterior process. The lacrimal is nearly complete on the left side of the skull, which for most other bones is the less-well-preserved side, but the bone has been fragmented and slightly displaced relative to the prefrontal and maxilla. As a consequence, the articulations between the lacrimal and the nasal, prefrontal, and maxilla are not well known.

Contacts/Borders: The lacrimal contacts the maxilla, jugal, prefrontal, and possibly the nasal (see below). The lacrimal participates in the borders of the orbit, antorbital fenestra, and external naris.

Morphology: The lacrimal is a 'figure-7' shaped bone whose two rami, the anterior process and the body, meet at an acute angle of ca. 26˚. The body of the lacrimal is a transversely flattened, anteroposteriorly expanded structure that separates the orbit from the antorbital fenestra. It is oriented nearly perpendicular to the upper tooth row and is overlapped anteriorly by the jugal, which nearly edges it out of the posterior margin of the antorbital fenestra. A fairly large lacrimal foramen (ca. 10 x 4 mm) opens on the dorsal half of the posterior surface of the lacrimal, as in all sauropods, but the anterior extension of the lacrimal canal cannot be traced in this specimen. Near the angle of the 'figure-7,' the lacrimal expands posterodorsally into a point, which was overlapped by the prefrontal and extends nearly to the frontal.

The anterior process of the lacrimal has complex contact with the maxilla and the prefrontal. The posterodorsal portion of the anterior process of the lacrimal is partially overlapped by a splint of the prefrontal. The articular surface on the lacrimal receiving this splint is set off by a narrow ridge. Further anteriorly, the anterior process of the lacrimal is overlapped by the narial process of the maxilla, which is not completely preserved on either side of the skull. We reconstructed the narial process of the maxilla based on its completely preserved margins, and it appears that the lacrimal had a small contribution to the margin of the external naris.

Comments: The presence of an anterior process of the lacrimal is a reversal from the condition in more basally-diverging sauropods, which possess only a lacrimal body (Wilson & Sereno 1998). The angulation between the anterior process and lacrimal body in T. macedoi is nearly identical to that of Bonitasaura (26 vs. 27˚; J.A. Wilson, unpubl. data.) but distinct from that of Rapetosaurus (73˚), which are the only other titanosaurs for which this

element is sufficiently well preserved to measure this angle. The elongate posterodorsal extension of the lacrimal, which nearly contacts the frontal, is also present in Bonitasaura (Gallina & Apesteguía, 2011: fig. 3) and possibly Nemegtosaurus, in which the base of the process can be observed but not its distal tip (Wilson, 2005: figs. 4, 8).

<<Figure 11 approximately here >>

Jugal (Fig. 12)

Completeness: The right jugal is nearly complete, but lacks a substantial portion of its lacrimal process and some of its ventral margin. The left jugal preserves more of the lacrimal process than does the right, but its postorbital and maxillary processes are much more fractured and deformed.

Contacts/Borders: The jugal contacts the quadratojugal, postorbital, lacrimal, and maxilla. It forms part of the margins of the lateral temporal fenestra, orbit, and antorbital fenestra.

Morphology: The jugal of Tapuiasaurus is an anteroposteriorly elongate and tetraradiate element. The processes of the jugal contacting the maxilla and postorbital are approximately anteriorly and posteriorly directed, respectively, meeting at an angle of ca. 145˚. The shorter, arched, and dorsally directed lacrimal process contacts the anterior side of the ventral lacrimal and borders the antorbital fenestra. A very short, posteroventrally directed process contacts the quadratojugal. The jugal is more than twice as long anteroposteriorly than it is dorsoventrally. It is excluded from the ventral margin of the skull.

The elongate maxillary process of the jugal forms a large portion of the ventral margin of the antorbital fenestra, which is an autapomorphy of the genus (Zaher et al., 2011). The jugal tapers gradually towards its anterior end, which nearly reaches the anterior margin of the antorbital fenestra, and rests upon the dorsal surface of the post-dentigerous process of the maxilla.

The quadratojugal process of the jugal is short and triangular, forming only a small portion of the anteroventral margin of the lateral temporal fenestra. Despite the brevity of the quadratojugal process, the jugal overlaps the quadratojugal along substantial contact that extends to the maxilla. As a consequence, the jugal is completely or nearly excluded from the ventral margin of the skull by the quadratojugal and maxilla.

The postorbital process of the jugal is rounded laterally, in contrast to the other jugal processes, all of which are transversely flat. The jugal-postorbital contact is extensive but not

tightly sutured. The postorbital process is oriented at an acute angle of ca. 33˚ with respect to the quadratojugal process, which itself is collinear to the maxillary process.

The lacrimal process of the jugal is dorsally oriented and slightly arched posteriorly. It wraps around the lacrimal anteriorly to form most of the posterior margin of the antorbital fenestra. The lacrimal rests on an external facet on the jugal, as it does in other sauropods (e.g., Giraffatitan; Janensch, 1935-6: fig. 21).

Comments: The jugal of basal sauropodomorphs such as Plateosaurus bears only three processes, which contact the postorbital, quadratojugal, and maxilla-lacrimal (e.g., Wilson & Sereno, 1998: fig. 5). Where in Plateosaurus there is only a single anteriorly-directed process that separates the lacrimal and maxilla and just reaches the margin of the antorbital fenestra, in Tapuiasaurus this process is modified into distinct contact surfaces for the lacrimal and maxilla that are separated by a lengthy antorbital fenestra margin. Although separate contacts for the maxilla and lacrimal are present in most sauropods (Diplodocus, Nemegtosaurus, Rapetosaurus, Camarasaurus, Giraffatitan, Abydosaurus) in none does the maxillary contact extend so far forward, nearly to the anterior margin of the antorbital fenestra.

<<Figure 12 approximately here >>

Squamosal (Figs. 8, 9, 13)

Completeness: The squamosal is complete on the left side of the skull and missing only a portion of its posterodorsal corner on the right.

Contacts: The squamosal contacts the quadrate, parietal, postorbital, quadratojugal, and exoccipital-opisthotic. It forms much of the posterior margin of the lateral temporal fenestra.

Morphology: The squamosal is a strap-like bone that forms part of the posterior margin of the skull and wraps around onto the occiput between the braincase and skull roof. The squamosal consists of three short processes and one elongate process extending from the posterodorsal corner of the skull. The elongate process is transversely thin, anteroposteriorly deep, and laterally convex. It overlaps the quadratojugal, with which it forms the posterior border of the lateral temporal fenesetra. The three short processes of the squamosal include a posteroventrally directed process that abuts the flat distal end of paroccipital process, an anterodorsal process that contacts the postorbital, and a narrow process that extends onto the occipital region of the skull between the exoccipital-opisthotic and the parietal.

The relatively short postorbital process of the squamosal bears a small, angled notch distally that receives the very reduced squamosal process of the postorbital. As a consequence, the dorsal portion of the lateral temporal fenestra is quite narrow. Just ventral to its articulation with the postorbital, the squamosal arches sharply to contact the postorbital a second time. As a result, the lateral temporal fenestra is figure-eight shaped with a smaller upper opening and a much larger ventral opening.

The quadratojugal process of the squamosal is platy, measuring 2.5–3.0 cm anteroposteriorly compared to ca. 0.2 cm transversely. In contrast to those of other sauropods, which taper to a point distally (e.g., Camarasaurus, Nemegtosaurus), the quadratojugal process of Tapuiasaurus expands distally. In addition, the squamosal overlaps the quadratojugal laterally in a contact that is manifest as an angled line laterally, as correctly identified by Zaher et al. (2011). The quadratojugal process of the squamosal also contacts the quadrate along its anterior edge, forming a deep lateral wall to the quadrate fossa.

The occipital process of the squamosal extends posterodorsally to contact the ventral edge of the lateral one-third of the parietal. This contact extends far enough laterally to exclude the squamosal from the margin of the supratemporal fenestra, as in Nemegtosaurus and Quaesitosaurus. From its articulation with the parietal, the squamosal continues posteroventrally to receive the paroccipital process. These elements abut each other along a fairly lengthy (ca. 3 cm) contact. Whereas in most sauropods the posttemporal fenestra opens between the parietal and exoccipital-opisthotic or between both these bones and the squamosal, in Tapuiasaurus, no such opening is found in this region, suggesting the posttemposal fenestra was closed. The region of the squamosal between its contacts with the paroccipital process and the postorbital bears light ornamentation consisting of small circular pits. A blunted spur is present just ventral and lateral to the contact with the paroccipital process.

Together, the squamosal and paroccipital process contact with the quadrate, which is not visible on either side of the skull. In other sauropods, the head of the quadrate articulates in a socket of the squamosal and is braced posteriorly by the paroccipital process (e.g., Abydosaurus).

Comments: The shape of the squamosal and its articulation with the quadratojugal and quadrate are autapomorphic for Tapuiasaurus. The quadratojugal process of the squamosal is transversely flattened and laterally convex, and it does not taper distally. Near its articulation with the postorbital it bears a relatively short, curved margin that borders the lateral temporal

fenestra that is truncated by contact with the descending ramus of the postorbital. This double postorbital contact does not appear to be present in a squamosal recently described from the Upper Cretaceous of Brazil (Martinelli et al., 2015). The quadratojugal process of the squamosal ends as a flattened plate of bone that is angled slightly relative to the axis of the process. The squamosal appears to have an end-on contact with the quadrate rather than an overlapping contact, and as a consequence forms part of the lateral wall of the quadrate fossa. Like Nemegtosaurus, the squamosal of Tapuiasaurus bears a small ventrally directed boss or spur.

Like the nemegtosaurids Nemegtosaurus and Quaesitosaurus, the squamosal is excluded from margin of supratemporal fenestra in Tapuiasaurus (Wilson, 2005: 311).

<< Figure 13 approximately here >>

Quadratojugal (Figs. 9, 13)

Completeness: The quadratojugal is completely preserved on the right side, but on the left side it is slightly damaged anteriorly.

Contacts/Borders: The quadratojugal contacts the squamosal, jugal, and quadrate. It forms part of the posterior and ventral margin of the lateral temporal fenestra.

Morphology: The quadratojugal forms the posteroventral corner of the skull, consisting of two rami that meet at an obtuse angle of ca. 137˚. The squamosal process of the quadratojugal continues the gentle posterior arch made by the squamosal, but near its base it curves back anteriorly to form a sharp hook, which is an autapomorphy of the species (Zaher et al., 2011). The squamosal process of the quadratojugal tapers distally to approximately 70% of its anteroposterior length. The jugal ramus of the quadratojugal is arched ventrally and expands towards its distal end, in contrast to the squamosal process. The jugal process ends in a flat edge, which comes very close to but probably did not contact the maxilla. The flat distal end of the jugal ramus of the quadratojugal bears no articulation for other bones and peers anteriorly towards the post-dentigerous maxilla.

The quadratojugal is platy and paper thin posteriorly (0.5–1 mm thick). It is involved in an overlapping suture with the squamosal that appears to be autapomorphic for the species (see above). The corner of the quadratojugal overlaps the quadrate along a suture that is ca. 3.5 cm long; it would have contributed to the lateral wall of the quadrate fossa.

Comments: The ventrally oriented hook of the quadratojugal is unique to Tapuiasaurus, as is the expanded, flat distal end that is exposed anteriorly.

Skull Openings (Figs. 2, 3, 5, 7, 10, 13)

Orbit: The orbit is bounded by the frontal, prefrontal, lacrimal, jugal, and postorbital bones. It is teardrop shaped, with its tapered end directed towards the contact between the quadratojugal and maxilla. The orbit is tipped posteriorly relative to the rest of the skull, and its long axis forms an angle of 137˚ with a chord stretching between the quadrate condyle and the alveolar end of the maxilla-premaxilla suture. The orbit is the largest cranial opening, occupying an area of approximately 80 cm^2 (measured on the better preserved, right side). The long axis of the orbit is nearly twice as long (15.2 cm) as its short axis (8.4 cm). The postorbital, frontal, and prefrontal bones, which surround the posterodorsal portion of the orbit, bear light ornamentation consisting of small bumps and ridges. The bumps are less than a millimeter in diameter and raised above the surface a similar amount. The ridges are similar to the bumps in elevation and width, but they typically extend for approximately 2 mm. The lacrimal, which borders the remainder of the orbit, is unornamented. The transverse thickness of the bones bordering the orbits varies around its circumference. The orbital margin ranges from approximately 1.5–3 cm deep transversely in the dorsal portion of the orbit, which extends approximately from the lacrimal foramen to the postorbital-jugal suture. In contrast, the remainder of the orbital margin is transversely thinner, typically less than 0.5 cm.

External Naris: The external naris is poorly preserved, but its margins, size, and shape can be reconstructed with varying degrees of certainty. It is very probable that the external nares were confluent (i.e., not divided by an internarial bar) and bounded by the nasal, lacrimal, maxilla, and premaxilla. The prefrontal, too, may have maintained a small margin on the external nares, but that region of the skull is damaged on both sides. The external nares form an elongate pentagon in anterodorsal view, with the a flat base of the pentagon extending across the nasals, the apex located where the premaxillae meet on the midline, and the remaining two angles at the junction of the lacrimal, prefrontal, and nasal bones. The height of the pentagon, which can be thought of as the distance from the nasal-nasal suture to the reconstructed position of the tips of the premaxillae (which are not fully preserved) is approximately 10 cm. The breadth of the pentagon is approximately one-fourth the height. The conjoined external nares is not the largest opening in skull, unlike the basally-diverging

macronarians Camarasaurus and Giraffatitan, but similar to more later-diverging taxa such as Abydosaurus and nemegtosaurids.

Antorbital Fenestra: The antorbital fenestra is bounded by the maxilla, jugal, and lacrimal. It is positioned between the orbit and preantorbital fenestra, as can be seen in lateral view (Fig. 2). The antorbital fenestra does not embay the maxilla nearly as much as in Rapetosaurus, in which it extends anterior to the preantorbital fenestra to the third maxillary tooth (Curry Rogers & Forster, 2004: fig. 1B). The antorbital fenestra in Tapuiasaurus is subtriangular, with a sharp apex located at the contact between the maxilla and lacrimal, an acutely rounded corner within the body of the maxilla, and an obtusely rounded corner between the lacrimal and maxillary processes of the jugal. The area of the better preserved, right antorbital fenestra is approximately 51 cm^2. Its long axis, which extends between the sharply angled and acutely rounded corners, measures ca. 12 cm, with some uncertainty due to damage. There is no fossa surrounding any part of the antorbital fenestra, as is synapomorphic for eusauropods (Wilson & Sereno, 1998); the low ridge on the narial process of the maxilla bounds a narial fossa dorsally, but there is no recessed bone on the ventral side bordering the antorbital fenestra.

Preantorbital Fenestra: Neosauropods are characterized by a preantorbital fenestra that is completely enclosed within the maxilla (Wilson & Sereno, 1998). The preantorbital fenestra is relatively small in Camarasaurus, but it is enlarged in both diplodocoids and titanosaurs. In Tapuiasaurus, the preantorbital fenestra is elliptical, with a horizontally oriented long axis (5.4 cm). The length of the short axis (ca. 3 cm) is poorly defined because the ventral portion of the preantorbital fenestra grades into a fossa, making it difficult to identify the boundary.

Supratemporal Fenestra: The supratemporal fenestra is bounded by the postorbital, parietal, and frontal. As in Nemegtosaurus and Quaesitosaurus, the squamosal is excluded from the margin of the supratemporal fenestra in Tapuiasaurus. It is elliptical in shape, with a long axis (5.2 cm) approximately 4 times the length of its short axis (1.3 cm). The right and left supratemporal fenestrae are not quite oriented collinearly in dorsal view (Fig. 8); the long axes of the fenestrae intersect slightly anterior to and dorsal to the frontal-parietal suture. The supratemporal fenestrae are separated by a distance that is approximately equal to their greatest diameter.

Lateral Temporal Fenestra: The lateral temporal fenestra is bounded by the squamosal, quadratojugal, postorbital, jugal, and quadrate. Unlike other sauropods, the lateral temporal fenestra in T. macedoi has been subdivided by a secondary contact between the squamosal and postorbital bones, a unique feature preserved on both sides of the skull. As a result, the lateral temporal fenestra is figure-8 shaped, divided into a smaller posterodorsal opening (ca. 2 cm) and a larger, elongate anteroventral opening (ca. 7.5 cm). In addition to its unique shape, the lateral temporal fenestra is attenuated anteroposteriorly, with its long axis (12.7 cm) more than ten times longer than its short axis (1.7 cm). In this respect, Tapuiasaurus resembles Nemegtosaurus. Like other narrow-crowned forms (e.g., Diplodocus), the skull of T. macedoi is extended posterodorsally, such that the occiput lies well behind the jaw joint when the tooth row is used as the horizontal. As a consequence, the long axis of the lateral temporal fenestra forms an angle of approximately 142˚ with a chord stretching between the quadrate condyle and the alveolar end of the maxilla-premaxilla suture. This resembles the condition in Diplodocus (145˚) and Nemegtosaurus (131˚) more closely than that of the macronarians Camarasaurus (122˚) and Giraffatitan (119˚). Neosauropods differ substantially from the condition in more basally-diverging sauropodomorphs such as Melanorosaurus (87˚), Plateosaurus (91˚), and Eoraptor (97˚).

PALATAL COMPLEX

The palatal complex consists of five elements that are at least partially cartilage-derived (i.e., splanchnocranial in origin): the vomer, ectopterygoid, palatine, pterygoid, and quadrate. The palatal bones were preserved in place, but they are difficult to observe due to their inaccessibility to preparation and due to the transverse compression of the skull. The palate was examined in CT slices and the parts visible on the specimen (e.g., underside of palate; lateral palate viewed through the antorbital fenestra).

Vomer (Fig. 4)

Completeness: The vomer appears to be complete and well-preserved. Its posterior end and connection to the palatine could not be observed directly.

Contacts: The vomer contacts the premaxilla, maxilla, and palatine.

Morphology: The vomer is a strap-shaped bone that forms the anterior portion of the palate. Careful inspection of the anterior vomer reveals that it is a single, median element, rather

than two paired elements like those found in other sauropods (e.g, Camarasaurus, Nemegtosaurus). The absence of a midline suture in the vomer is telling, because early-fusing sutures (e.g., supraoccipital–exoccipital-opisthotic) are still open in this individual of T. macedoi.

The anterior vomer is gently concave in the transverse plane and tapers anteriorly towards a short tip that contacts both the anteromedial process of the maxilla and the posteromedial process of the premaxilla. The vomer does not contact any bones laterally, forming a midline strut connecting the snout to the rest of the palate. The vomer's connection to the palatine can be observed through the left antorbital fenestra, where its posterior end is clasped the vomer near the midline.

Comments: The vomer in Tapuiasaurus is a single, median element.

Ectopterygoid (Fig. 4)

Completeness: The ectopterygoid is completely preserved on both sides of the skull.

Contacts/Borders: The ectopterygoid contacts the palatine, pterygoid, and maxilla.

Morphology: The ectopterygoid is a small bone that forms part of the transverse pterygoid hook. The ectopterygoid consists of an anterior and a ventral ramus that meet at a right angle. The anterior ramus of the ectopterygoid contacts the underside of the jugal process of the maxilla. The ventral ramus of the ectopterygoid is slightly arched posteriorly and wraps around the anterior portion of the pterygoid and extends slightly beyond it ventrally. It tapers to a point distally, as does the pterygoid. Together, the pterygoid and ectopterygoid form the transverse pterygoid hook, which extends ventrally beyond the deeply emarginated lateral margin of the skull (see Maxilla, above).

Comments: The configuration of palatal bones in Tapuiasaurus appears to differ from that of the only other titanosaurs with complete palatal series, Nemegtosaurus and Quaesitosaurus. In both these Mongolian forms, a single right-angle shaped bone was preserved in the palate. This bone was identified as the ectopterygoid by Wilson (2005: 298), but it was suggested to be the palatine by Nowinski (1971: fig. 3). In fact, this bone preserves characteristics of both.

Palatine (Fig. 4)

Completeness: The palatine lacks only a portion of its dorsal blade and part of the edge of its maxillary process.

Contacts: The palatine contacts its opposite on the midline, as well as the maxilla, pterygoid, ectopterygoid, and probably the vomer.

Morphology: The palatine is shaped like a partially unfurled scroll that extends from the lateral margin of the skull towards its midline. It consists of anteriorly-directed process and a large, dorsomedially-directed process. The anterior process is narrow near its base (1.0 cm) and expands distally slightly (1.2 cm) before tapering towards a blunt end. This tongue-shaped process contacts the underside of the palatal shelf of the maxilla near the beginning of its dorsal embayment. The anterior process of the palatine is emarginated laterally, but there does not appear to be a postpalatine fenestra.

The dorsomedially-directed process of the palatine is blade shaped. It expands quite dramatically towards its distal end, which occupies much of the area of the antorbital fenestra in lateral view. The posterior margin of its distal end is contacted by the pterygoid and possibly the parasphenoid rostrum of the basisphenoid. The anterior margin of the distal end is contacted by the vomer.

Comments: No palatine was identified in the palate of the intact skulls Nemegtosaurus and Quaesitosaurus. Wilson (2005) identified the single, large bone in contact with the underside of the maxillary shelf as the ectopterygoid and reconstructed a comparably small palatine. If this interpretation is correct, then the palate of Tapuiasaurus differs from those of Nemegtosaurus and Quaesitosaurus, which have enlarged pterygoids and relatively small palatines.

The palatine has not yet been described in other titanosaurs (e.g., Rapetosaurus, Bonitasaura).

Pterygoid (Figs. 9, 12)

Completeness: The ventral and posterior portions of the pterygoid are well preserved. The anterior portion is not as well preserved and not easily visible due to its position and coverage by other bones and matrix.

Contacts/Borders: The pterygoid contacts its opposite on the midline, as well as the basipterygoid processes and parasphenoid rostrum of the basisphenoid, quadrate, ectopterygoid, and palatine.

Morphology: The pterygoid is a triradiate bone that forms the posterior part of the palate. Two of the processes are nearly colinear, and the third, anterodorsal process extends at a right angle from them.

The most conspicuous process of the pterygoid is directed anteroventrally and contacts the ectopterygoid and palatine to form the transverse palatal flange. This process is not strongly arched, unlike those of other titanosauriforms (e.g., Abydosaurus, Phuwiangosaurus, Euhelopus). The distal end is flat, transversely thin, and approximately 1.5 cm across. It rests in a small fossa on the posteromedial face of the distal ectopterygoid (Fig. 12).

The anterodorsal process of the pterygoid is poorly exposed in this exemplar. It can be seen in the antorbital fenestra, where it extends towards the midline to contact the posterior margin of the conjoined blades of the palatine. Posterodorsally, it probably contacted the parasphenoid process of the basisphenoid.

The posterior process of the pterygoid is quite short and rounded. It is overlapped laterally by the anterior process of the quadrate, and medially it bears a ledge that receives the basipterygoid process. As in Nemegtosaurus, this ledge forms a rocker-like articulation rather than a socket-like articulation (e.g., Giraffatitan) or hooked articulation (e.g., Camarasaurus, Dicraeosaurus).

Comments: The short posterior process of the pterygoid is shared by other titanosaurs that preserve this bone (e.g., Nemegtosaurus, Rapetosaurus, Quaesitosaurus). The anteroventral process of the pterygoid, which forms part of the pterygoid flange, is straight in Tapuiasaurus and Rapetosaurus, which differs from the gently curved condition in Quaesitosaurus and the more strongly curved condition in Nemegtosaurus.

Quadrate (Figs. 9, 13)

Completeness: The quadrate is completely preserved on both sides of the skull. The left quadrate appears to be complete and undistorted, but the right quadrate is fractured in at least two places, creating proximal, middle, and distal sections that are displaced relative to one another.

Contacts/Borders: The quadrate contacts the basal tubera (basioccipital + basisphenoid), squamosal, quadratojugal, pterygoid, and articular. It is covered posteriorly by the exoccipital-opisthotic.

Morphology: The quadrate forms part of the posterior portion of the skull, contributing to the posterior palate and occiput. It contacts the dermal skull, braincase, and lower jaw. The quadrate of Tapuiasaurus is visible almost exclusively in posterior view, where it is sandwiched between the dermal skull and braincase. Its posterior surface extends from approximately the height of the occipital condyle to be slightly below the ventral margin of the quadratojugal. The quadrate consists of the head dorsally, the condyle ventrally, the pterygoid flange anteriorly, and a body that joins them. The body of the quadrate is arched medially, with the apex of the arch contacting the ventrolateral corner of the basal tubera (Fig. 9). The quadrate houses a deep quadrate fossa, whose medial margin is rounded, owing to the arching of the quadrate body, and whose lateral margin is formed by the squamosal and quadratojugal. The pterygoid flange of the quadrate extends anteroventrally to overlap the lateral surface of the pterygoid. That contact is not completely visible on either side, but on the visible portion of the right side indicates that the pterygoid flange was probably fairly small.

Laterally, the quadrate contacts the squamosal and quadratojugal. Interestingly, these bones meet end on, such that the margin of the lateral temporal fenestra grades gently anteromedially, as visible in lateral view (Figs. 2, 13). The surface of the quadrate body in this region of the skull is pitted in a manner not seen in other skull bones.

The quadrate condyle hangs below quadratojugal by approximately 1 cm in lateral view. The better preserved left condyle is kidney-shaped in distal view. The long axis of the condyle is oriented anterolaterally to posteromedially, with the convex portion of the condyle facing posterolaterally and the concave portion facing anteromedially. The anterior portion of the condyle is slightly smaller than the posterior portion.

Comments: The end-on articulation between the quadrate and quadratojugal is currently restricted to Tapuiasaurus.

BRAINCASE

The braincase consists of median elements (supraoccipital, basioccipital, basisphenoid) and paired elements (exoccipital-opithotic, prootic, laterosphenoid, orbitosphenoid) that form the endocranial cavity. We have relatively limited access to the braincase due to coverage by other bones. Braincase bones are only visible in right lateral view (i.e., through the orbit) and in posterior-posteroventral view. Some portions of the occiput are difficult to interpret, due to the fracturing that has occurred between the braincase, skull roof, and temporal bones.

Supraoccipital (Fig. 9)

Completeness: The supraocccipital is complete but slightly damaged on its lateral edges, near its connection to the squamosal and exoccipital-opisthotic.

Contacts/Borders: The supraoccipital contacts the parietal, squamosal, exoccipital-opisthotic, and proatlas; it forms the dorsal median margin of the foramen magnum.

Morphology: The supraoccipital forms the dorsomedian portion of the occiput and contacts the posterior margin of the skull roof and temporal bones. The supraoccipital is pentagonal in shape, with a broad ventral base, relatively short ventrolateral sides, and elongate dorsolateral sides. The supraoccipital contacts the parietal along its dorsolateral sides, along an undulating suture that is concave medially and convex laterally. The lateral extremes of the supraoccipital are positioned slightly above the margin of the foramen magnum, near the distal tip of the occipital process of the squamosal. The supraoccipital makes a small contribution (ca. 2 cm) to the dorsal margin of the foramen magnum, to which it is subequal in height (3.2 cm). The supraoccipital contacts the exoccipital-opisthotic along a long, bent suture. The external surface of the supraoccipital bears little relief apart from a medial nuchal ridge that bears vertically-oriented striae. The nuchal ridge is 1.2 cm broad and extends along the length of the supraoccipital. Just lateral to its base is a low, rounded eminence that probably represents the articular surface for the proatlas.

Comments: The supraoccipital of Tapuiasaurus bears a median nuchal ridge, as in most titanosaurs (e.g., Jainosaurus). In this respect, it differs from Rapetosaurus, Bonatitan, and Muyelensaurus, which possess a median groove, and Pitekunsaurus, which lacks both the groove and the ridge (see Wilson et al., 2009: 25). The tight connection between the supraoccipital, exoccipital-opisthotic, and squamosal suggests that there is no posttemporal foramen in Tapuiasaurus.

Basioccipital (Fig. 9)

Completeness: The basioccipital is complete, but its dorsal surface forming the floor of the braincase is not visible because it is covered by the right proatlas, which could not be easily removed from the occiput without damage.

Contacts/Borders: The basioccipital contacts the exoccipital-opisthotic, basisphenoid, and probably the prootic and orbitosphenoid, based on comparisons with other sauropods (e.g., Jainosaurus). The basioccipital contacts the three components of the first cervical vertebra, including the neural arch and intercentrum of the atlas, and the odontoid process of axis (atlantal pleurocentrum).

Morphology: The basioccipital is the posteromedian braincase bone that forms the occipital condyle and the basal tubera. The suture between the basioccipital and basisphenoid is probably marked by a groove on the ventral surface of the basal tubera, such as the one present in other titanosaurs (e.g., Vahiny). The occipital condyle is subcircular in shape in posterior view; it is slightly broader transversely than it is tall dorsoventrally (3.0 x 2.5 cm). The approximate length of the convexity of the condyle is 1.7 cm, but its shape is not hemispherical. Rather, the condyle is bluntly pointed posteriorly. In posterolateral view, the articular surface of the condyle appears to wrap ventrally, but the degree to which it does so is accentuated by damage to this portion of the occiput. There is no basioccipital depression between the occipital condyle and the basal tubera.

The basal tubera are approximately 5 cm wide and extend ventrally approximately 3.5 cm. Their ventrolateral corners are expanded, triangular, and slightly pendant, as they are in Nemegtosaurus. From these corners, the ventral margin of the basal tubera curve dorsally towards the ventromedian point of contact. In posterior view, the basal tubera are both tranversely and dorsoventrally concave. The ventrolateral corner of the basal tubera contacts the medial surface of the quadrate, which bends inwards to meet it. This contact is present in titanosaurs and immediate outgroups (e.g., Phuwiangosaurus).

Comments: The basal tubera of Tapuiasaurus and Nemegtosaurus have expanded, triangular ventrolateral corners. This condition is distinct from that present in Rapetosaurus, Antarctosaurus, Bonatitan, and most other titanosaurs.

Basisphenoid (Figs. 9, 14)

Completeness: The basisphenoid appears to be completely preserved. The basipterygoid processes are damaged near their base. The posterior surface of the basisphenoid is exposed, but its other surfaces are not visible due to coverage or close approximation of adjacent bones.

Contacts/Borders: The basisphenoid contacts the basioccipital, orbitosphenoid, laterosphenoid, prootic, pterygoid, and quadrate.

Morphology: The basisphenoid forms part of the floor of the braincase and contacts the palate. The basisphenoid lies anterior to the basioccipital and extends forward to form the parasphenoid rostrum, which cannot be seen in this specimen. As mentioned above, a groove on the ventral surface of the basal tubera, is probably the boundary between basisphenoid and basioccipital. There does not appear to be a median opening along this suture; nor does there appear to be an opening for the internal carotid artery there, as there is in Bonatitan (Paulina Carabajal, 2012).

The basipterygoid processes are approximately 4 cm long and are oriented slightly anteriorly relative to the basal tubera. Due to damage to both sides, their cross-sectional shape cannot be determined. The basipterygoid processes are separated from one another by a U-shaped embayment that is crossed by a median ridge that extends from just below the suture with the basioccipital onto the ventral aspect of the skull. It is unknown whether it continues anterior to form part of the parasphenoid rostrum. This feature does not appear to be present in other titanosaurs.

In lateral view, the basisphenoid and its contact with neighboring braincase bones are visible. The basisphenoid extends dorsally as a raised peak between the laterosphenoid and orbitosphenoid, forming the lower margin of cranial nerve III. The opening for cranial nerve VI is completely enclosed by the basisphenoid. Just anterior to that opening are three smaller foramina of unknown identity. The basisphenoid continues anteriorly as the parasphenoid rostrum, the base of which is just visible through the orbit.

Comments: The median ridge on the basisphenoid appears to be autapomorphic of Tapuiasaurus. A tiny raised structure is present in the embayment between the basipterygoid processes of Rapetosaurus, but it does not extend onto the posterior surface of the skull.

<<Figure 14 approximately here >>

Exoccipital-Opisthotic (Fig. 9)

Completeness: The left exoccipital-opisthotic is complete but fractured in the region of its contact with the supraoccipital. The right exoccipital-opisthotic lacks the distal half of its paroccipital process.

Contacts/Borders: The exoccipital-opisthotic contacts the prootic, supraoccipital, basioccipital, squamosal, quadrate, and possibly the proatlas; it borders the foramen magnum.

Morphology: The exoccipital-opisthotic forms the lateral sides of the occiput and the paroccipital processes. It forms most of the border of the foramen magnum, apart from the small contributions by the supraoccipital dorsally and the basioccipital ventrally. Near midheight of the lateral margin of the foramen magnum, the exoccipital-opisthotic forms a small prominence. This structure may have contacted the proatlas, but this cannot be determined with certainty. More ventrally, the contact between the exoccipital-opisthotic and the basioccipital can be clearly seen, and it is certain that it forms the shoulders of the occipital condyle, as it does in other sauropods. Due to the overlying right proatlas, it cannot be determined for certain whether or not the left and right exoccipital-opisthotic contact one another on the floor of the braincase, but it is likely that there was a small basioccipital contribution to the foramen magnum.

The paroccipital processes extend towards the lateral margin of the skull, contacting the squamosal to brace the quadrate head posteriorly. The better preserved, left paroccipital process is slightly ventrally directed, but this is at least partly due to the inward and downward crushing of this side of the skull that have broken and separated dorsal and ventral portions of the exoccipital-opisthotic on this side. The distal paroccipital process is dorsoventrally deep (3.6 cm) and slightly thickened anteroposteriorly (0.8 cm), and its terminus is rounded. It meets the back of the squamosal along its length.

Comments: The paroccipital process of Tapuiasaurus does not have the pendant non-articular process that is present in most other titanosaurs (e.g., Bonatitan, Rapetosaurus, Antarctosaurus, Quaesitosaurus). The condition in Nemegtosaurus is not known with certainty because there is some damage to this region, but it may have lacked this process as well (see Wilson, 2005: fig. 9).

Prootic (Fig. 14)

Completeness: The prootic appears to be complete on the right side. Its connections to the skull roof and to the exoccipital-opisthotic cannot be observed; nor can the terminus of its ventral spur. The left prootic is not exposed.

Contacts/Borders: The prootic contacts the exoccipital-opisthotic, laterosphenoid, basisphenoid, and parietal.

Morphology: The prootic forms the posterolateral wall of the braincase. It is normally transversely oriented and tightly appressed to the paroccipital processes. In this exemplar, however, the paroccipital processes have been deflected posteriorly, and as a consequence the prootic is oriented posterolaterally. The prootic is an approximately triangular bone in lateral view, with a fairly narrow dorsal base that tapers towards a ventral apex. The prootic forms the posterior margin of the opening for cranial nerve V, and it also likely contained the openings of cranial nerves VII and VIII and bordered the jugular foramen, as it does in other titanosaurs (e.g., Jainosaurus), but these features cannot be observed directly in this specimen due to matrix cover.

The exit for cranial nerve V is ellipital and dorsoventrally elongate (1.2 x 0.6 cm) and continues as two grooves on the lateral surface of the braincase. These grooves are directed ventrally and posteriorly. The more ventrally-oriented groove, which is partially bounded by the laterosphenoid and basisphenoid, is commonly observed in sauropods and represents the path of the mandibular (CN V_3) or maxillomandibular (CN V_{2-3}) branch of the trigeminal nerve, but the more posteriorly-directed branch is less commonly observed. It probably represents the ophthalmic branch (CN V_1). A second trigeminal groove is also present in Quaesitosaurus (Kurazanov & Bannikov, 1983: fig. 2B), but it appears to be more ventrally oriented than it is in Tapuiasaurus.

Posteriorly, the prootic is developed into the crista prootica, which is gently arched sharp crest. There is no development of the tab-like posterolateral process that characterizes dicraeosaurids (Salgado & Calvo, 1992). The crista prootica continues ventrally as a spur that extends onto the basisphenoid. The portion of the prootic posterior to the crista prootica cannot be observed in this specimen.

Comments: The presence of a posteriorly directed groove for the one of the branches of the trigeminal nerve (probably V_1, the ophthalmic branch) is a feature that is currently restricted

to Tapuiasaurus and Quaesitosaurus. However, there is no prootic known from Rapetosaurus to compare, and that of Nemegtosaurus and is not visible.

Laterosphenoid (Fig. 14)

Completeness: The laterosphenoid is nearly completely preserved on the right side of the skull, lacking only its distal terminus. The anterodorsal part of the right laterosphenoid is covered by scleral ossicles, and the left laterosphenoid is not exposed.

Contacts/Borders: The laterosphenoid contacts the orbitosphenoid, prootic, basisphenoid, frontal, and postorbital.

Morphology: The laterosphenoid forms a portion of the lateral wall of the braincase and makes the posterior margin of cranial nerves III and IV and the anterior margin of the cranial nerve V. Like the prootic, the laterosphenoid is typically a transversely oriented element, and this specimen it has been distorted posteroventrally. It is broadest dorsally, where it contacts the frontal and forms a narrow, arched arm directed towards the postorbital. The contact between the postorbital and laterophenoid is not preserved in this specimen. The laterosphenoid tapers ventrally, reaching one-third its dorsal width at the level of the opening for cranial nerve III. It continues tapering ventrally, forming a short, recurved spur that edges part of the basisphenoid from the groove for the maxillo-mandibular or mandibular branch of cranial nerve V. It appears that the laterosphenoid does not participate in the margin of cranial nerve VI, which differs from the condition in other titanosaurs, such as Jainosaurus.

Comments: It is not known whether the laterosphenoids are pillarlike or if they extend medially to contact one another on the midline, as they do in Vahiny (Curry Rogers & Wilson, 2014).

Orbitosphenoid (Fig. 14)

Completeness: The portions of the orbitosphenoid that are visible laterally are complete; but its dorsal and anterior margins cannot be observed because they are covered by scleral ossicles.

Contacts/Borders: The orbitosphenoid contacts the laterosphenoid, basisphenoid, frontal, and its opposite on the midline.

Morphology: The orbitosphenoid forms the anterior portion of the braincase. Very little of it can be observed in the holotypic specimen of Tapuiasaurus macedoi. The nature of its contact with the frontal and the shape of the openings for cranial nerve I cannot be observed. The orbitosphenoid forms the anterior margins of cranial nerves III and IV, as it does in most sauropods, and completely encloses the opening for cranial nerve II. The posterior portion of that opening is visible laterally, but the anterior portion is not. The orbitosphenoid and basisphenoid contact along a suture that angles slightly ventrally as it passes anteriorly.

Comments: None.

Cranial nerves (Fig. 14)

Less than half of the foramina for cranial nerves are visible in this exemplar. The openings for cranial nerves II–VI open between or within the lateral braincase bones. Those that are exposed between the lateral and posterior braincase bones (i.e., cranial nerves IX–XI) and within posterior braincase bones (i.e., cranial nerve XII) are not visible. The opening for cranial nerve I is also not visible.

The openings for cranial nerves V, IV, II are collinear, whereas those for cranial nerves IV, III, VI form a line that is oriented approximately orthogonal to them. Cranial nerve VI exits through an opening that is completely enclosed by the basisphenoid, and cranial nerve II exits through the orbitosphenoid alone. The presence of two well marked grooves for branches of the trigeminal nerve (V_2 or V_{2-3} and V_1) on the prootic appears to be a feature restricted to Tapuiasaurus and Quaesitosaurus.

HYOMANDIBULAR ARCH ELEMENTS

Stapes

The stapes was not preserved on either side of the skull. Stapes are not yet known for any titanosaur.

Ceratobranchial (Fig. 15)

Completeness: Right and left ceratobranchial elements, most likely pertaining to ceratobranchial 2 (see below), are completely preserved and undistorted.

Contacts: The two ceratobranchial elements were the only elements of the hyoid apparatus recovered in Tapuiasaurus. They do not appear to have a bony connection to any other bony

element; indeed, no more than a single pair of hyoid elements have been recovered in association with a sauropodomorph dinosaur skull to date. It is possible though, that they contacted one another, based on comparisons to a well preserved ankylosaur hyoid apparatus (Hill et al., 2015).

Morphology: Two narrow, gently bent elements were found next to each other near the posterior end of the right mandible, which was the 'down' side of the specimen as preserved in the quarry. The two elements, which were found nearly parallel to one another with their concave sides directed anterodorsally, are clearly paired elements, even though they are bent to slightly different degrees. The two arms of the right and left ceratobranchial elements meet at 105 and 117°, respectively. Both elements have arms that are unequal in length, with the more vertically oriented arm approximately 80% as long as the anteriorly directed arm. These rod like elements appear to be slightly more flattened on the medial side than on the lateral side, and their anterior end is more expanded than is the dorsally oriented end.

Comments: The ceratobranchial in Tapuiasaurus is very similar in shape and proportions to the "hypobranchiale" preserved with Giraffatitan skull S66 (Janensch, 1935-6: fig. 54) and the "ceratohyal" element preserved with the skull of Melanorosaurus (Yates, 2007: fig. 15). All three are rod like elements that consist of arms that are slightly different in length and gently bent at an angle of approximately that is slightly tighter in Tapuiasaurus (105–115˚) and slightly more open in Giraffatitan (120˚) and Melanorosaurus (125˚). All three have one slightly more expanded end, which in Melanorosaurus is directed posteriorly and in Tapuiasaurus is oriented anteriorly (the orientation was not reported for Giraffatitan.). The ceratobranchial elements preserved in Tapuiasaurus, Giraffatitan, and Melanorosaurus contrast with the narrow, elongate, straight elements preserved between the mandibles of Abydosaurus (Chure et al., 2010: fig. 3) as well as the elongate but slightly stouter, straight bones positioned ventral to the posteroventral corner of mandibles of a subadult Camarasaurus (Gilmore, 1925: pl. 13) and the short, straight, stout elements of an adult Massospondylus (Gow, 1990: fig. 1; Sues et al., 2004: fig. 5). A juvenile specimen of Massospondylus bears a slender, gently curved ceratobranchial element with a slightly expanded anterior end that more closely resembles those of Melanorosaurus (BP/1/4376; Gow, 1990: fig. 3; Sues et al., 2004: fig. 1A). Note that Gilmore (1925: 367) reported the presence of "three rod-like bones" in the matrix beneath the lower jaws of a subadult

Camarasaurus skeleton, but it is appears that these represent three fragments pertaining to two bones rather than three separate elements.

Although no more than a single pair of hyoid elements has been preserved within any individual sauropodomorph, the shape of those elements varies considerably within the group. This variation could represent true morphological differences within a single hyoid element within sauropodomorphs, or it could indicate that different ceratobranchial elements are being preserved. That is, the slender, curved elements preserved with some sauropodomorph skulls may pertain to different hyoid elements than the straight, stout elements in others.

Recent description of a completely preserved hyoid apparatus in the ankylosaur Pinacosaurus (Hill et al., 2015) offers an opportunity to sort out the identity of hyoid elements in Tapuiasaurus and possibly other sauropodomorph dinosaurs. The elements preserved in Tapuiasaurus mostly closely resemble the ceratobranchial 2 elements of Pinacosaurus, which are slender, curved, and nearly touch each other at the midline (Hill et al., 2015: figs. 1, 3, 4). The short, stout elements preserved in Camarasaurus and some specimens of Massospondylus resemble the epibranchial elements of Pinacosaurus (Hill et al., 2015), but further investigation is required to establish that they represent homologous elements. If correct, though, differences in the shape of hyoid elements preserved with individuals of Massopondylus would be attributable to serial, rather than ontogenetic, variation.

<<Figure 15 approximately here >>

SCLERAL OSSICLES

Completeness: Scleral ossicles are preserved on the right side of the skull. They are not arranged into a sclerotic ring.

Contacts/Borders: The scleral ossicles contact one another to form a ring but they are not in direct contact with other bones – they are embedded within the eye.

Morphology: The scleral ossicles are preserved in a manner that allows discrimination of only a few of the individual plates comprising the sclerotic ring.

Comments: None.

LOWER JAW

The mandible consists of a dentigerous dentary and six postdentary bones (surangular, angular, coronoid, splenial, prearticular, articular).

Dentary (Fig. 16)

Completeness: The right and left dentaries are nearly complete. The alveolar margin of the right dentary is damaged from tooth position 3 posteriorly, but alveolar margin of the left dentary is complete and well preserved throughout its length. The right dentary is nearly complete posteriorly, lacking only the distalmost tip of its ventral process, but the left dentary is poorly preserved posteroventrally due to crushing inwards of this part of the mandible. Right and left dentaries are bowed laterally to differing degrees as preserved, with the right side more so than the left. This deformation matches that of the upper jaws. Based on the breakage visible on both upper and lower jaws, it appears that the right side preserves more of the natural curvature of the skull than does the left.

Contacts: The dentary contacts its opposite on the midline, as well as the surangular, angular, coronoid, prearticular, and splenial.

Morphology: The dentary is the longest element of the lower jaw, extending for more than 80% of its length. The dentary bears alveoli for 15 teeth, one fewer than present in the upper jaw, and these teeth are restricted to a position level with the middle of the preantorbital fenestra. The number of dentary teeth in Tapuiasaurus is the same as in Giraffatitan, Malawisaurus, and Diplodocus, but fewer than in the brachiosaurid Abydosaurus (14) and the titanosaurs Antarctosaurus (14), Brasilotitan (14), Nemegtosaurus (13), Quaesitosaurus (13), and Rapetosaurus (11). The dentaries together are U-shaped, which can be measured by the Arcade Index (AI, Boué, 1970), the ratio of the depth and breadth in the lower dental arcade. The AI of Tapuiasaurus is similar to those of the brachiosaurids Abydosaurus and Giraffatitan and the titanosaurs Rapetosaurus and Nemegtosaurus, all of which are much less than those of square-snouted forms, such as the titanosaurs Antarctosaurus, Brasilotitan, and Bonitasaura and the diplodocoids Diplodocus and Nigersaurus (Table 3).

<<Table 3 approximately here>>

The body of the dentary is shallowest at dentary tooth 5; from that point it deepens ca. 140% towards the front of the jaw and ca. 190% towards the posterior part, as measured on the better preserved left side (Table 2). The anteriormost portion of the dentary is relatively

shallow dorsoventrally compared to more basal macronarians (e.g., Camarasaurus) and diplodocoids with a "chin" (e.g., Diplodocus) but similar to those of other titanosaurs (e.g., Nemegtosaurus, Quaesitosaurus).

In dorsal and ventral views, the alveolar margin of the dentary is very slightly flared out laterally relative to its ventral margin. This gentle flaring resembles that present in Rapetosaurus, Brasilotitan, and Nemegtosaurus but is much less pronounced than in Bonitasaura and Antarctosaurus. Near the alveolar margin of the dentary are a series of foramina, some of which bear arched grooves extending towards the margin. These foramina are restricted to an area anterior and dorsal to the imaginary line connecting the last alveolus to the ventralmost part of the symphysis.

The dentary symphysis is dorsoventrally tall and anteroposteriorly narrow (4.6 x 1.5 cm). The dentaries are not fused to one another, yet they have stayed together in near-perfect articulation, despite distortion to other portions of the lower jaws (e.g., left ramus). The symphysis is oriented nearly perpendicular to the long axis of the jaw, which resembles the condition in Nemegtosaurus but differs from the more anteriorly inclined symphysis of Rapetosaurus and other sauropods (e.g., Diplodocus, Camarasaurus).

Medially, the dentary is partially covered by ovelapping postdentary elements (i.e., splenial, coronoid). The Meckelian groove extends only to the 12th or 11th dentary alveous, rather than to the symphysis as it does in certain other titanosaurs (e.g., Nemegtosaurus, Rapetosaurus). Posteriorly, Meckels' groove broadens and continues ventrally as a low shelf upon which the splenial rests. The suture between the left coronoid and dentary is visible medially in this subadult individual of Tapuiasaurus, revealing that the coronoid is a small, strap-shaped bone that does not extend for the entire length of the posterodorsal process of the dentary. The coronoid suture is visible laterally as a shallow groove extending posteriorly from a small foramen, as in Rapetosaurus. Just anteroventral to this groove on the dentary is a deeper groove emanating from a larger foramen, as best viewed on the left side (Fig. 16). Replacement foramina are visible on the medial side of the dentary. They grade from more vertically elongate, elliptical structures posteriorly to more circular structures anteriorly. Replacing teeth can be seen inside the replacement foramina in all but the first four dentary teeth on the left side.

In lateral view, the anterior portion of the dentary bears numerous neurovascular foramina that are restricted to a roughly triangular area extending from the symphysis to the coronoid. These foramina are most densely distributed anteriorly, becoming much more rare posterior to the 11th dentary tooth. There are two-to-three large foramina (ca. 4 mm

diameter) located towards the ventral margin of the dentary near tooth positions 4–6. The anteromedialmost portion of the dentary bears a well marked, vertically oriented ridge that is the breadth of one tooth position. It resembles the median ridge in the upper tooth row preserved in Nemegtosaurus and Quaesitosaurus (Wilson, 2005: fig. 5).

The posterior dentary has three posteriorly-directed processes that contact the surangular and angular. Extending dorsally from the posterior dentary is a elongate process that is overlapped laterally by the surangular. This process is transversely thick and rounded medially, forming part of the adductor fossa and the anterior portion of the coronoid process. It bears a roughened, slightly pitted texture dorsally that probably marks the insertion site for adductor musculature. Extending from the ventral portion of the posterior dentary is an elongate process that separates into two smaller processes further posteriorly. The longer and lower of these overlaps the angular and would have extended as far posteriorly as the posterior surangular foramen. The other ventral process, which is incomplete on both sides, was narrow and extended between the surangular and angular.

Comments: The dentary is bowed laterally in dorsal view, but to a lesser extent than what is present in more square-jawed titanosaurs (e.g., Antarctosaurus, Bonitasaura; Tapuiasaurus), more closely resembling taxa such as Nemegtosaurus. Like Nemegtosaurus, the dentary symphysis in Tapuiasaurus is oriented vertically relative to the axis of the jaw.
<<Figure 16 approximately here >>

Coronoid (Figs. 16, 17)

Completeness: The coronoid is completely preserved.

Contacts: The coronoid contacts the dentary.

Morphology: The coronoid is an elongate, strap-like bone positioned just behind the dentary tooth row. It forms a narrow triangle in cross-section, with a base that is 4 mm that tapers to a sharp apex that is less than 1 mm. Although the coronoid fuses to the dentary in those adult titanosaurs that possess this bone (e.g., Nemegtosaurus, Quaesitosaurus, Rapetosaurus), in Tapuiasaurus a clear suture line is visible separating the two elements.

Comments: The coronoid element (= ‘intercoronoid;’ = ‘complementare’) of sauropodomorphs probably corresponds to the middle coronoid of basal tetrapods (for

discussion see Wilson, 2005). In basal sauropodomorphs (Plateosaurus), basal sauropods (Omeisaurus, Mamenchisaurus), and non-titanosaur macronarians (Camarasaurus, Giraffatitan), the coronoid lies along the medial surface of the posterior dentary teeth. In all titanosaurs for which suffient cranial remains are preserved, the coronoid is restricted to postdentigerous dentary, to which it is partially fused in adults (i.e., Bonitasaura, Brasilotitan, Malawisaurus, Karongasaurus, Nemegtosaurus, Quaesitosaurus, Rapetosaurus).

This portion of the lower jaw was suggested to function as a 'guillotine' in the titanosaur Bonitasaura (Apesteguía, 2004; Gallina & Apesteguía, 2011), who identified it to be part of the dentary rather than an independent ossification.

<<Figure 17 approximately here >>

Surangular (Figs. 16, 18)

Completeness: Both right and left surangulars lack part of their ventral margin in the region near its contact with the dentary. This extremely thin pane of the surangular is broken away in several otherwise intact titanosauriform lower jaws, including those of Euhelopus, Nemegtosaurus, and Quaesitosaurus.

Contacts: The surangular contacts the dentary, angular, prearticular, and articular.

Morphology: The surangular is a flat, elongate bone that extends for half the length of the lower jaw and forms the coronoid process and the lateral wall of the adductor fossa. The surangular bears a tranvsersely thickened dorsal margin that is pierced by three relatively large foramina. A conspicuous posterior surangular foramen (ca. 4 mm diameter) opens posteriorly from a position near the anterior margin of the articular; the opening is directed posteriorly. The dorsal margin of a large anterior surangular foramen is preserved on both surangular bones, but most of the margin has been broken away during the process of preparation (compare Figs. 1B and 16). It may have been associated with a small fossa, which is still preserved just anterior to the coronoid eminence. A small foramen (< 2 mm diameter) is present just posterior to the summit of the coronoid process; the opening is directed anteriorly.

The dorsal margin of the surangular is for the most part convex, but with localized steep breaks in slope just posterior to the posterior surangular foramen and anterior to the summit of the coronoid eminence. The surangular is thickest tranversely between these two

landmarks. The ventral margin of the surangular bears a sharp dorsal embayment just ventral to the posterior surangular foramen. This embayment receives a similarly shaped dorsal project of the angular bone, which would have acted to limit anteroposterior displacement of these two bones. The surangular is deepest at the level of the summit of the coronoid eminence, where it is approximately 125% the height of the angular.

The surangular does not quite extend to the posterior margin of the mandible. In lateral view, the articular can be seen extending a few millimeters beyond both the surangular and angular bones. The articular and surangular meet over a relatively small area of approximately 3.5 x 1.5 cm.

Comments: Nemegtosaurus, Rapetosaurus, and Tapuiasaurus all possess an enlarged anterior surangular foramen. Rapetosaurus appears to share with Tapuiasaurus the presence of a ventral embayment in the posterior surangular and the corresponding angular prominence (see Curry Rogers & Forster, 2004: figs. 30, 31), but Nemegtosaurus apparently does not (Wilson, 2005: fig. 13).

<<Figure 18 approximately here >>

Angular (Figs. 16, 18)

Completeness: The angular is completely preserved on the right side but slightly damaged in its middle third, where a break has offset anterior and posterior portions of the bone. The left angular is badly damaged, especially in the anterior two-thirds of its lateral surface, but it provides useful information about the anterior extent of the bone ventrally.

Contacts: The angular contacts the dentary, splenial, surangular, prearticular, and articular.

Morphology: The angular is a low, elongate bone that forms the posteroventral portion of the lower jaw. It borders the surangular dorsally and is overlapped by the dentary laterally and by the splenial medially. Together with the surangular laterally and the prearticular medially, the angular clasps the articular.

The angular bears a gently undulating ventral margin that is deepest and most convex below the coronoid process, becoming concave anterior and posterior to that point. A prominent projection in the dorsal margin of the posterior angular keys into a complementary concavity on the surangular. An elongate, shallow fossa is present on the lateral surface of the projection. The angular has a long, overlapping contact with the dentary that is delimited by a

horizontal ridge laterally. Medially, the posterior portion of the angular forms a shelf upon which rests the prearticular. The anterior extent of the angular is not visible externally in the well-preserved right lower jaw. The left lower jaw, in contrast, has been distorted such that the lower jaw bones are open ventrally, and the anterior extent of the angular can be estimated. The angular extends anteriorly to the distal portion of the tooth row, resting on the same ventromedial ridge of the dentary as does the splenial.

Comments: As mentioned above, the dorsal keying of the posterior portions of the angular and surangular appears to be present in Rapetosaurus but not Nemegtosaurus.

Splenial (Fig. 18)

Completeness: The splenial is incomplete on both sides of the skull, lacking the processes that extend anteriorly and posteriorly from it.

Contacts: The splenial contacts the dentary, angular, and prearticular.

Morphology: The splenial is a arrow-shaped bone that forms part of inner margin of the lower jaw. Its anterodorsal and ventral margins rest in the triangular Meckelian groove of the dentary, which is open posteriorly. Major processes extend from the three vertices of the splenial, none of which is completely preserved. These are directed anteriorly, posterodorsally, and posteroventrally. The paths of all three processes can be estimated based on the shapes of the bones they articulate with. The anterior process of the splenial is sharply tapering and extends to the tenth dentary alveolus, based on the shape of the anterior Meckelian groove. The posterodorsal process of the splenial probably tapers distally, following the underside of the posterodorsal process of the dentary, which forms part of the coronoid region of the lower jaw. The posteroventral process of the coronoid extends posteriorly to cover the angular medially. Its shape is not known, but in other titanosaurs it is tongue-shaped (e.g., Nemegtosaurus).

The splenial foramen is present near the geometric center of the bone. Two other foramina are also present, one on the posteroventral process and one just anterodorsal to the splenial foramen.

Comments: None.

Prearticular (Fig. 18)

Completeness: The prearticular is complete on the right side but badly damaged anteriorly on the left side.

Contacts: The prearticular contacts the articular, surangular, angular, and splenial.

Morphology: The prearticular is a strap-like element that forms the inner wall of the posterior lower jaw. Its dorsal margin is bent slightly medially to form the inner margin of a cup that supports the articular ventrally and medially. It has a concave dorsal margin that is visible laterally through the broken pane of the surangular. Ventrally, the prearticular rests atop a shelf of the angular along a fairly straight suture. Anteriorly it is overlapped medially by the splenial, which together with the dentary obscures the prearticular anteriorly.

Comments: None.

Articular (Figs. 16, 18, 19)

Completeness: The articular is complete on both sides of the skull.

Contacts: The articular contacts the angular, prearticular, and surangular; it articulates with the quadrate of the upper jaw.

Morphology: The articular is just visible laterally at the posterior edge of the mandible (Fig. 16). Its dorsal surface is visible medially, dorsally, and posteriorly. The dorsal surface of the articular, which forms the jaw joint, teardrop-shaped. It is more than two and a half times as long anteroposteriorly as it is broad transversely (ca. 4.1 cm x 1.6 cm). The dorsal surface is more or less flat, and there are no obvious restrictions to movement across this surface apart from the presence of an anterolaterally-positioned wall formed by the surangular.

Comments: The articular is rarely preserved in titanosaurs, even in intact jaws (e.g., Nemegtosaurus, Quaesitosaurus).

<<Figure 19 approximately here >>

TEETH

The dentition is restricted anteriorly in Tapuiasaurus and other sauropods compared to their basal sauropodomorph outgroups, in which upper teeth extend all the way to the orbit (Wilson 2002: character 66). The anterior restriction of dentition is partly accomplished by the dramatic reduction of the number of alveoli in the tooth row, but in certain forms the teeth are further restricted by narrowing of crown breadth. Narrow crowns first appeared during the Late Jurassic in diplodocoid sauropods, which persisted until the end of the Early Cretaceous alongside broad-crowned forms. By the Late Cretaceous, however, sauropod tooth morphospace was restricted to only narrow-crowned forms, and represented by titanosaurs (Chure et al., 2010). Tapuiasaurus possesses the narrowest crowns of any Early Cretaceous macronarian and represents their only excursion into diplodocoid tooth morphospace. Narrow crowns are associated with increased packing of teeth in jaws (Chure et al., 2010) and increased rates of replacement (D'Emic et al., 2013).

Tapuiasaurus contains 16 alveoli in each upper jaw but only 15 in each lower jaw. In addition to differences in the absolute number of teeth, as discussed below upper and lower teeth also differ in size, shape, curvature, and wear patterns (see Tables 4, 5).

<<Tables 4,5 approximately here>>

Upper teeth (Fig. 20)

There are 16 tooth positions in each upper jaw; 4 in the premaxilla, and 12 in the maxilla. Owing to the presence of an additional tooth position and the relatively larger size and spacing between teeth, the upper tooth row is approximately 130% the length of the lower tooth row (Table 2).

The average slenderness of the upper tooth crowns, which is a measure of apicobasal length vesus mesiodistal width, is 4.2–4.7, which is considerably more than teeth of the lower jaw, which are shorter (see Table 4). The upper crowns are elliptical, with their mesiodistal breadth (B) exceeding their labiolingual depth (D) in teeth that can be measured (B/D = 1.3–1.6). The apicobasal axis of the upper crowns is gently curved lingually. The apparent curvature of the tooth is accentuated by the dramatic reduction of the depth of the labial portion of the crown (i.e., part labial to the carina) towards the apex of the tooth. The mesial teeth of the upper jaw are oriented nearly perpendicular to the alveolar margin, but those of the distal portion are slightly procumbent, angling approximately 15˚ from perpendicular. This orientation of the distal teeth effectively shortens to upper tooth row apically, making it closer in length to that of the lower jaw. Distal teeth are also peculiar in the twisting of the

crown relative to the root. These tend to be twisted such that the distal carina is shifted labially, and the mesial carina is shifted lingually.

The complete mesial crowns (e.g., right premaxillary teeth 1 and 3) are symmetrical in labial view. The mesial and distal edges taper at the same rate and starting from the same point. In contrast, the more distally positioned teeth (e.g., right maxillary teeth 4 and 5) are more asymmetrical in labial view, with the distal edge appearing more straight and the mesial edge tapering more dramatically and farther from the tooth apex. It also appears that the distal crowns are asymmetrical in cross-section, with more of their labiolingual depth on the mesial side of the tooth.

The gaps between teeth vary along the upper tooth row (Table 5). The two front teeth are separated by a 1.0 mm gap, which is the tightest spacing between any two upper teeth. Most other teeth are separated by a gap of at least 2 mm, and tooth spacing peaks between the 5th and 8th upper teeth, where it reaches 4–5 mm. The size and distribution of gaps between upper teeth differ from those of lower teeth, which tend to increase along the tooth row to a maximum of nearly 7 mm at the distal end of the tooth row.

Upper teeth show signs of lingual wear, lingual and labial wear, mesial and distal wear, and apical wear. This broad range of wear patterning constrasts with the much more stereotyped labial wear in lower teeth (see below). From the sample of upper teeth preserved, it is possible to reconstruct a wear sequence. Apical wear is the most areally restricted and is included in both lingual and mesial-distal wear patterning, so it must have appeared first (e.g., left premaxillary tooth 2, right premaxillary tooth 3). Slightly more worn teeth bear elliptical wear facets on their lingual surface; at later stages, lingual wear can occupy more of the apex to create a blunt-ended tooth. Several of the upper teeth have both labial and lingual wear facets (right premaxillary teeth 2, 4, right maxillary teeth 2, 3). The presence of teeth with lingual but not labial wear but not the converse pattern of wear (i.e., labial but not lingual wear) suggests that labial wear occurs later in the wear cycle than the lingual wear. This inference is supported by the fact that all four teeth with this type of wear were in the process of replacing when the individual died. The lower teeth opposing the double-faceted upper teeth all either fresh or heavily labially worn, which suggests that these lower teeth replaced at a similar time or slightly earlier. In no case is there lingual wear on lower teeth, indicating that labial wear on the upper teeth was not produced by the lower jaw sliding forward and 'underbiting' the uppers. Double wear facets have been reported in isolated teeth from the Upper Cretaceous Bauru Group of Brazil (Kellner, 1996: fig. 7), titanosaur teeth from the Upper Cretaceous of Uzbekistan (Sues et al., 2015: fig. 5G–I), and in teeth of

Nigersaurus from Lower Cretaceous beds of Niger (Sereno & Wilson 2005; Sereno et al., 2007). It is likely that these all represent upper teeth. Sereno & Wilson (2005: 170) suggested that the isolated teeth from the Bauru Group could represent a late-surviving rebbachisaurid allied to Nigersaurus, but the presence of similar facets in Tapuiasaurus and the central Asian titanosaur indicates that those teeth could pertain to a titanosaur, as originally suggested.

<<Figure 20 approximately here >>

Lower teeth (Fig. 21)

There are 15 teeth in each dentary, which is one fewer than the number of upper teeth. In addition, the average SI (crown length/width) of the dentary teeth is considerably lower than that of the upper teeth (3.7–3.8 vs. 4.2–4.7). This difference in SI is a product of tooth length, not tooth breadth. Whereas upper teeth are typically longer than lower teeth (relative length = 1.2–2.2), they are approximately the same breadth or slightly broader (relative breadth = 0.9–1.3).

As in the upper teeth, the mesiodistal breadth of dentary teeth always exceeds their labiolingual depth (B/D = 1.3–1.5). In cross-section, the crowns are gently hexagonal, with slightly flattened labial and lingual faces that angle towards well developed mesial and distal carinae. These carinae only extend approximately 0.4 mm from the main tooth body, and they are made only from enamel and thus are translucent. The dentary teeth are relatively 'high-shouldered,' meaning that mesiodistal width tapers near the crown apex (ca. 80% of crown length). In labial or lingual view, the dentary crowns are nearly symmetrical, with the mesial and distal 'shoulders' at approximately the same height.

Spacing of the dentary teeth increases along the lower jaw (Table 5). There is a 1.5 mm gap separating the right and left 1st dentary teeth, and this doubles to more than 3 mm between the 9th-10th on the right side and 10th-11th dentary teeth on the left side. As observed on the left side, dentary tooth spacing more than doubles a second time between the penultimate and last dentary teeth. The total length of the dentary tooth row is approxately 11 cm, which is considerably shorter than the approximately 15 cm upper tooth row (Table 2).

The apicodistal axis of the dentary teeth ranges from straight to gentle labial curvature. The variation in curvature does not appear to relate to position in the tooth row; the antepenultimate left dentary tooth is markedly labially curved but its opposite on the right side appears to have a straight apicodistal axis. Similarly, some of the mesial dentary teeth bear a gentle labial curvature whereas others are straight (e.g., right dentary teeth 1 and 3).

Because the curvature tends to be most pronounced apically in more mesially-positioned dentary teeth, these teeth become straighter as they are worn (e.g., right dentary teeth 1 and 2). The dentary teeth are oriented nearly perpendicular to the jaw axis, rather than slightly procumbent as they are in certain other titanosauriforms (e.g., Euhelopus, Giraffatitan).

Lower teeth show a more restricted range of wear than do upper teeth. Tooth wear is present on 7 of the 11 dentary crowns that are sufficiently well preserved to observe it, and in all but one case, wear is present only on the labial surface of the crown (Table 4). In the one exception, apicodistal wear was observed (penultimate left dentary tooth; Table 4); in no case did wear extend onto the lingual surface of the tooth, and no apex-only wear was observed. Owing to the absence of lingual facets on the lower teeth, the labial facets on upper teeth could not have been created by action of the lower teeth. Labial wear on upper teeth must have been created by some other resistant structure or by substrate.

<<Figure 21 approximately here >>

RECONSTRUCTION

A reconstruction of the skull of Tapuiasaurus macedoi is presented in Figure 22. The reconstruction has removed some of the preservational distortion that the skull experienced (see above, "General") and reconstructed parts of the skull that were not completely preserved (e.g., narial region).

<<Figure 22 approximately here >>

REVISED DIAGNOSIS OF TAPUIASAURUS MACEDOI

Zaher et al. (2011: 4) identified 3 autapomorphies of Tapuiasaurus macedoi: (1) hook-shaped posteroventral process of the quadratojugal; (2) anterior process of the jugal tapering and forming most of the ventral margin of the antorbital fenestra; (3) anterolateral tip of the pterygoid contacts the medial surface of the ectopterygoid. Based on our analysis of the holotypic and only specimen of Tapuiasaurus macedoi, which has undergone additional preparation, we can add seven additional diagnostic features of the species: (4) maxilla with a tapering post-dentigerous process of the maxilla that is elevated above the alveolar margin; (5) jugal with an elongate lacrimal process forming much of the posteroventral border of the antorbital fenestra; (6) lateral temporal fenestra divided by a second squamosal-postorbital contact, forming a small posterodorsal and elongate anteroventral openings; (7) quadrate and

quadratojugal with a narrow (ca. 2 mm), end-on articulation; (8) maxillary teeth with labial wear; (9) absence of a posttemporal foramen; (10) flat overlapping articulation between squamosal and quadratojugal; (11) basisphenoid with median ridge extending from contact with basioccipital onto ventral surface.

PHYLOGENETIC POSITION OF TAPUIASAURUS MACEDOI

Below we discuss the evolutionary relationships of Tapuiasaurus macedoi based on a revised phylogenetic analysis of rescored character data from new observations and additional preparation. We then examine the role of missing data and the implications of the missing occurrences within particular strata in the original and revised results.

ZAHER ET AL. (2011) ANALYSIS

In their initial description of Tapuiasaurus macedoi, Zaher et al. (2011) performed a phylogenetic analysis that recovered Tapuiasaurus as a member of Nemegtosauridae, which also includes Rapetosaurus and Nemegtosaurus. This clade was positioned within Lithostrotia with moderate support, being the sister group of the clade formed by Isisaurus, Diamantinasaurus, and Saltasauridae. Within Nemegtosauridae, Tapuiasaurus was hypothesized to be more closely related to Rapetosaurus than to Nemegtosaurus, a result that was considerably shorter than alternative arrangements, including one that placed it outside the two Late Cretaceous species (see Zaher et al. 2011: fig. 7).

Zaher et al. (2011) used a modified version of the Wilson (2002) matrix, which scored 27 terminal taxa for 234 characters. To this they added 12 cranial characters, some new and some from Curry Rogers (2005), as well as 4 terminal taxa (viz. Phuwiangosaurus, Tangvayosaurus, Diamantinasaurus, Tapuiasaurus). Revised scorings for Euhelopus were used (Wilson & Upchurch, 2009: table 6), as were previous scorings for Phuwiangosaurus and Tangvayosaurus (Suteethorn et al., 2009) and Diamantinasaurus (Hocknull et al., 2009). Of the resultant 246 characters used by Zaher et al. (2011), there are 88 cranial characters (35.8%), 72 axial characters (29.3%), 85 appendicular characters (34.6%), and 1 dermal character (0.4%). Of the 31 resulting terminal taxa, 12 (39%) are titanosaurs.

The taxonomic scope of the Wilson (2002) matrix was Sauropoda, which ranges from the Late Triassic to the latest Cretaceous. Zaher et al. (2011) repurposed that matrix to focus on a much narrower taxonomic scope, Titanosauria, which is restricted to the Cretaceous

(D'Emic, 2012). Wilson (2002) included 8 titanosaurs in his analysis, and although this represents 30% of the terminal taxa, it accounts for only a small percentage of the 70+ species currently recognized to comprise that clade (J.A. Wilson & M.D. D'Emic, unpubl. data). Although there was good character support for two of the seven nodes within Titanosauria (decay index = 4) and moderate support for another (decay index = 2), three nodes had a decay index of 1 (Wilson, 2002: table 12). With the addition of four more titanosaur terminal taxa in the Zaher et al. (2011) analysis, the original character budget was stretched across 50% more nodes. Even with the addition of 12 new characters by Zaher et al. (2011), we might expect reduced levels of support within Titanosauria (see Whitlock et al., 2011 for discussion of 'diluent' taxa).

The phylogenetic position of Tapuiasaurus within a clade formed by the latest Cretaceous Rapetosaurus and Nemegtosaurus was not robustly supported (decay index = 1) by the data assembled by Zaher et al. (2011). Other relationships within Titanosauria had better support, with decay indices of 2 and 3. Phylogenetic tests using constraint trees demonstrated that the published topology was significantly shorter than alternative arrangements placing Tapuiasaurus in a more basally diverging position.

RE-ANALYSIS

Owing to the low level of support for the monophyly of Nemegtosauridae in the original analysis, combined with broad taxonomic scope of the Wilson (2002) matrix, extensive missing data, and lengthy implied ghost lineages (see below), we direct the new morphological data described here for Tapuiasaurus towards a re-analysis of its phylogenetic position.

Our modifications to the Zaher et al. (2011) matrix were restricted to rescoring the cranial and postcranial data for Tapuiasaurus and scoring cranial data for Isisaurus. No other matrix cells were changed (Table 6). The revised Tapuiasaurus scoring contains substantially fewer missing entries than the original analysis (Table 7). Most of the disambiguations (i.e., replacing a "?" with a positive score) were localized within the skull, for which Tapuiasaurus now has the lowest missing data score for any terminal taxon (4.5% missing cranial data). Although there were several disambiguations in other parts of the skeleton, Tapuiasaurus still remains very incompletely scored postcranially, second only to Nemegtosaurus (100% incomplete) in postcranial missing data.

In addition to the new scorings for Tapuiasaurus, we added scorings for a braincase and skull roof of Isisaurus, based on relatively new links between these elements and the

holotypic postcranial skeleton (Wilson et al., 2005, 2009). Only 10 additional data cells were filled for Isisaurus.

<< Tables 6,7 approximately here >>

The rescored phylogenetic dataset of 27 terminal taxa for 246 characters was analyzed under equally weighted parsimony using TNT v.1.1 (Goloboff et al., 2008a, b). A traditional heuristic tree search was conducted in which 1,000 replicates of Wagner trees were created using random addition sequences of taxa, followed by tree bisection-reconnection (TBR) branch swapping. A final round of TBR was applied to the most parsimonious trees (MPTs) found in the replicates. Thirty-four MPTs were found after this heuristic tree search of 462 steps (CI = 0.593, RI = 0.770). The strict consensus of these 34 MPTs shows a large polytomy involving all titanosaurs. Evaluation of the topological variation among the 34 MPTs using iterPCR (Pol & Escapa, 2009) identified Nemegtosaurus and Tapuiasaurus as the two unstable taxa that caused the large polytomy among titanosaurs. A reduced strict consensus showing the six alternative positions of Nemegtosaurus and the three alternative positions of Tapuiasaurus within an otherwise completely resolved topology for Titanosauria is shown in Figure 23.

<< Figure 23 approximately here >>

In contrast to the original analysis, the rescored analysis does not unequivocally resolve Tapuiasaurus, Rapetosaurus, and Nemegtosaurus as a monophyletic group. Although this topology is retrieved in two of the 34 MPTs (Fig. 23, letters c and d), all other most parsimonious topologies depict Tapuiasaurus more basally than in the original analysis: either as the sister group of Lithostrotia or Tangvayosaurus + Lithostrotia (Fig. 23, letters a and b). The alternative positions of Nemegtosaurus, in contrast, are within or adjacent Saltasauridae (Fig. 23, letters e–m). Rapetosaurus is placed in an equivalent position to that of the original analysis (within Lithostrotia and basal to Isisaurus and saltasaurids). The affinities of Tapuiasaurus with Lithostrotia are based on character data present in the original analysis, such as the posterolaterally oriented quadrate fossa (char. 35.1), basisphenoid-quadrate contact (char. 52.1), and reduced cervical neural arch lamination (char. 81.1). The key difference with respect to the previous result is that Tapuiasaurus is placed some of the MPTs outside Lithostrotia, a basal position supported in those trees by the absence of derived characters shared by Malawisaurus and/or Rapetosaurus and more derived titanosaurs: presence of osteoderms (char. 234.1), simple undivided cervical pneumatopores (char. 83.0), mid-posterior dorsal neural spines oriented posteriorly (char. 104.1), cylindrical tooth crowns

(char. 70.2), coracoid proximodistal length twice that of the scapular articulation (char. 155.1), and distal radius breadth about twice as the radial midshaft (char. 170.1).

The support values for most nodes within Titanosauria are extremely low (e.g., decay index = 0, bootstrap/jackknife frequencies below 50%). If we ignore the alternative positions of the unstable Nemegtosaurus and Tapuiasaurus among suboptimal trees (for decay index) or trees found in the bootstrap/jackknife pseudoreplicates, then support values are markedly higher for basal nodes of Titanosauria (decay indices = 3–5, bootstrap/jackknife frequencies = 63–80%). This indicates two important facts. First, the phylogenetic position of two taxa known primarily from skull anatomy (Tapuiasaurus and Nemegtosaurus) must be regarded as highly labile. Second, the addition of new information on Tapuiasaurus and Isisaurus reveals character conflict, previously hidden by missing data, that makes Tapuiasaurus and Nemegtosaurus unstable in the revised dataset.

MISSING DATA AND ITS EFFECTS ON TOPOLOGY

Missing data in the titanosaurs scored in the original Zaher et al. (2011) analysis ranged from 40–68% (Table 7). Tapuiasaurus, which could not be scored for 56% of the 246 characters in that analysis, is close to the average value of 57% for all titanosaur terminal taxa. Cranial data contribute most of the missing data in titanosaurs, with an average of 73% and a range from 11–100%. Postcranial anatomy was scored much more completely, with an average of 52% and a range from 29–100%. Missing data scores across the entire Wilson (2002) Sauropoda-wide matrix are lower, with an average of 21% total missing data, 56.7% cranial missing data, and 35.8% postcranial missing data. The revised data matrix included new Tapuiasaurus scorings that moderately lowered its total missing data from 56% to 46%. The new cranial scorings of Isisaurus only marginally reduced the overall missing data for this taxon, from 67% to 62%. This relatively small difference in missing data, affecting only two taxa, had a substantial impact on the topology as well as in the support values.

As noted above, the changes in the revised version of the dataset included resolution of missing entries in Isisaurus and Tapuiasaurus (i.e., replacement of a "?" with a definitive score) and rescoring of some character cells in Tapuiasaurus with a different character state based on the new information and/or interpretation. We can assess the overall similarity between the original and revised matrices using the Character State Similarity Index (CSSI; Sereno 2009), which ranges from 0 (complete dissimilarity) to 1 (identity). The CSSI compares the total number of character state conflicts (csc, changes between any two unambiguous states) and character state resolutions (csr, changes from an ambiguous state to

any unambiguous state) relative to the total number of character states (tcs), such that CSSI = (tcs – [csc + 0.5csr]) / tcs. The CSSI between the original and rescored matrix was 0.86.

The missing data content and information content (as measured by the CSSI) are very similar in the original and revised matrices, yet the changes introduced in the revised version yielded an important effect on the topological results and support values among titanosaurs. This reinforces the notion that application of bulk statistics, such as the CSSI or % missing data, to a matrix or matrices may not reliably predict or explain topological differences, nor may they reliably identify problematic taxa.

Given that scoring changes in the revised matrix are exclusively focused on two taxa (Isisaurus and Tapuiasaurus), we explored the impact of these changes by running analyses in which we evaluated the resultant topology when only one set of changes was introduced. We present the results as a Punnett square in Figure 24. As noted above, the original data matrix supported the monophyly of a group formed by Rapetosaurus, Tapuiasaurus and Nemegtosaurus (Nemegtosauridae is marked with an asterisk in the upper left square in Fig. 24). Nemegtosaurid monophyly is also supported when the data matrix is analyzed using the original scorings for Isisaurus but the revised scorings for Tapuiasaurus, which comprise 51 out of the 61 scoring changes introduced (lower left square in Fig. 24). Accordingly, the CSSI for Isisaurus (original) x Tapuiasaurus (rescored) compared to the original data matrix (0.86) is very close to the CSSI between the original and fully rescored data matrices (0.88). Conversely, although the data matrix with the original scorings for Tapuiasaurus but the revised scorings for Isisaurus is almost identical to the original data matrix in terms of their information content (including 10 out of the 61 scoring changes; CSSI = 0.98), its yields a distinct topological result in which Tapuiasaurus and Rapetosaurus as sister taxa but Nemegtosaurus is unstable, taking two alternative positions among the most parsimonious trees ('N' in upper right square in Fig. 24). Interestingly, it is the combined effect of the changes introduced for both Tapuiasaurus and Isisaurus that produces the break up of the clade Nemegtosauridae in many of the MPTs of the revised analysis, in which Tapuiasaurus moves stemwards to a position outside Malawisaurus and Nemegtosaurus moves tipwards towards Saltasauridae ('N' and 'T' in lower right square in Fig. 24). Neither set of changes is sufficient to effect these topological changes independently.

<<Figure 24 approximately here >>

A revealing fact of the exploratory analyses performed above is that important topological effects were introduced with changes to only a few cells of this data matrix—i.e., in a revised matrix that has nearly identical information content as the original (CSSI = 0.98).

We therefore explored which of the new scorings were the most influential for the topological changes of the revised phylogenetic analysis. The result of this exploration indicates that changing a minimum of five scorings is required for obtaining the topologies of the revised analysis, many of which reject the monophyly of Nemegtosauridae. The five key changes are in the scorings of Tapuiasaurus and include two disambiguations (characters 83, 234) and three rescored cells (characters 70, 155, 170). As noted above, the basal position of Tapuiasaurus (outside Lithostrotia) is supported in most of the MPTs of the revised analysis by the absence of six derived characters shared by Malawisaurus and/or Rapetosaurus. Five of these six characters are the ones identified as bearing key changes in the scorings of Tapuiasaurus. These include four characters on different regions of the postcranium (cervical vertebra [character 83], coracoid [character 155], radius [character 170], osteoderms [character 234]), and one character on the shape of teeth (character 70).

These exploratory analyses and evaluation of influential characters and scorings reveal an important outcome: the positions of both Nemegtosaurus and Tapuiasaurus are highly labile, and despite the relatively high nodal support in the original analysis they are sensitive to minor alterations of the data matrix. The levels of missing data for these taxa are somewhat high, but the distribution of these missing entries is remarkable. Tapuiasaurus has very few missing entries in the cranial data but a high level of missing data within the postcranial skeleton (original: 23.9%, 80%; rescored: 4.5%, 74.5%). The pattern is even more striking in Nemegtosaurus, which has low cranial missing data (11.4%) but completely lacks postcranial data (100%). Rapetosaurus, in contrast, is more stable in these analyses and has more missing entries in the cranial characters (19.3%) but comparatively fewer missing entries in the postcranial characters (58.6%). The correlation of instability and high amount of missing entries in the postcranial characters probably has more to do with the particular distribution of missing entries among titanosaurs rather than with the phylogenetic informativeness of cranial versus postcranial characters in this group. The other (nine) titanosaurs included in the data matrix have the converse pattern of missing data (Table 7). Five of the taxa have no cranial remains known (Tangvayosaurus, Diamantinasaurus, Opisthocoelicaudia, Alamosaurus, Neuquensaurus). Cranial data for Isisaurus were not scored in the original analysis, but we could score 10 cranial characters (now 87.5% missing). The remaining three taxa could be scored for certain cranial characters, but cranial missing data scores were nonetheless quite high (Saltasaurus [79.5%], Malawisaurus [81.8%], Phuwiangosaurus [63.6%]). Postcranial characters were much more densely sampled among

these nine titanosaurs, with missing data ranging from 11.0% to 66.9% (with an average value of 45% missing data).

Thus there is an uneven distribution of missing data among titanosaurs, with a few that mostly or exclusively known from cranial remains (viz. Nemegtosaurus, Tapuiasaurus), and the rest known predominantly from postcranial remains. Under these conditions, the taxa with high missing data scores are highly unstable. This indicates that caution should be taken when interpreting results based on the phylogenetic position of taxa that are mostly scored for characters that cannot be scored in other taxa. These issues are not measured or evaluated by commonly used measures of nodal support (e.g., decay index, bootstrap, jackknife), which are focused on stability of clades rather than specific terminal taxa. Missing entries cannot create or provide support for specific topological results, which must be based on positive (i.e., non-"?") scores, but they can nonetheless affect results in two important ways. First, they can influence the stability of certain taxa, especially when the distribution missing data is highly uneven as it is in titanosaurs. Second, certain configurations of missing data can conspire to render less likely certain sister-taxon relationships. For example, the Late Cretaceous Mongolian titanosaurs Nemegtosaurus and Opisthocoelicaudia cannot both be scored for any one character, and so there can be no unambiguous synapomorphies that can link them. This is also true for the other four titanosaurs with 100% missing cranial data. Thus, sister-taxon relationships between pairs or clusters of taxa that have no overlapping scores are less likely to be recovered, or if they are they are likely to be unstable.

MISSING LINEAGES

The topological arrangement of terminal taxa in a calibrated phylogeny typically contains temporal gaps between sister taxa due to disjunct stratigraphic distributions. These ghost lineages (Norell, 1992) or minimum implied gaps (MIGs; Storrs, 1993) have been implemented in various ways to correct taxonomic ranges (Norell, 1992, 1993), improve diversity estimates (e.g., Barrett & Upchurch, 2005; Upchurch & Barrett, 2005), and estimate phylogenetic relationships (Fisher, 1992). Cladistic and stratocladistic approaches use ghost lineages in different ways, with the former evaluating them post-analysis and the latter treating them as ad hoc hypotheses that contribute to treelength the same way as ad hoc hypotheses of homoplasy (see Fisher, 1992). Although we will not undertake a stratocladistic analysis here, we nonetheless consider ghost lineages as arguments of non-occurrence in the fossil record that invite exploration of potential causes. In the following discussion we compare the stratigraphic fit of different topologies using the same taxon sampling (i.e., with

the same choices about included taxa, inclusion of higher-level taxa, stratigraphic uncertainty) focusing on interrelationships within Titanosauria by fixing non-titanosaur topology to one of the most parsimonious solutions.

The topology of Zaher et al. (2011: fig. 7) contains three lengthy ghost lineages within Titanosauria that result from nesting the Early Cretaceous Tapuiasaurus within a clade of predominantly latest Cretaceous taxa. Recall that this topology was one of the equally parsimonious topologies retrieved in our revised analysis (see above). In this topology, the longest implied gaps extend by 55 million years the lineages leading to the nemegtosaurids Nemegtosaurus and Rapetosaurus. A third extensive ghost lineage also implied by this topology, approximately 20 million years long, precedes the appearance of the clade uniting Diamantisaurus, Isisaurus, and Saltasauridae. The total MIG in the most parsimonious trees that reproduce the results of Zaher et al. (2011) is 388 million years (MSM* = 0.39). However, most of the most parsimonious trees of the revised analysis reject the monophyly of Nemegtosauridae by placing Tapuiasaurus more stemward and Nemegtosaurus more tipward (Figs. 23, 24). These most parsimonious trees imply shorter MIGs that are either 308 million years (MSM* = 0.45) or 338 million years (MSM* = 0.50), because the ghost lineages associated with Nemegtosaurus and Rapetosaurus are not as long as they are in topologies clustering them with the Aptian Tapuiasaurus. The ghost lineages within Titanosauria in the more stratigraphically-consistent topologies are caused by the position of the Early Cretaceous (late Albian) Diamantisaurus nested within Late Cretaceous-aged taxa (see Fig. 23).

What does it mean to have a range of MIGs from 308–388 million years associated with the results of our revised dataset? We attempt to contextualize these results by comparing them to MIGs implied by two alternative sets of trees derived from the same dataset. First, we calculated the MIGs for up to 10,000 trees that were 2, 5, and 9 steps longer than our most parsimonious trees for the rescored analysis, representing a 0.4–2% increase in treelength. These suboptimal trees were obtained by branch swapping of optimal trees and therefore inhabit regions of the treespace neighboring the most parsimonious solutions. Second, we calculated MIGs for 10,000 trees with randomly-generated topologies within Titanosauria. Figure 25 summarizes the results. Randomly generated trees are shown in blue, and suboptimal trees drawn from the rescored dataset in orange. MIGs for the most parsimonious trees generated from the original and rescored datasets are represented along the x-axis by bars placed above the curves.

<<Figure 25 approximately here >>

MIGs for the 10,000 randomly generated trees range from 243–603 million years. These obtain a left-skewed distribution, in which few trees imply short missing intervals, and increasingly large numbers of trees imply ever longer missing intervals. Nearly half of the 10,000 randomly generated trees are in the right-most bin, representing MIGs of 603 million years. The MIGs for the most parsimonious trees recovered by the original and rescored datasets are on the long left tail of the distribution of randomly generated trees (both the MPTs that recover Tapuiasaurus within Nemegtosauridae and those positioning it more basally; see horizontal bars in Fig. 25). Nevertheless there are 29 randomly generated trees that imply significantly smaller MIGs—in three cases 80 million years shorter than the most parsimonious solutions to the rescored dataset.

The three sets of suboptimal trees generated from the rescored dataset have much more symmetrical profiles than do the randomly generated trees, and their distribution is slightly skewed rightward and centered around MIGs similar to those of the most parsimonious trees (323–383 million years; Fig. 25). MIGs for the suboptimal trees of 2, 5, and 9 extra steps differ in both frequency and rightward excursion (MIG duration). There are only 174 trees up to two steps longer than the most parsimonious tree, and their MIGs range from 278–418 million years. There are 69 solutions that imply slightly less stratigraphic inconsistency for a small relaxation in morphological consistency. There are more than 4,000 trees up to five steps longer than the most parsimonious tree, and these cover a broader range of MIGs (263–603 million years) including 856 that offer a better fit with the observed stratigraphic distribution of taxa. We were able to save 10,000 suboptimal trees up to 9 steps longer than the most parsimonious trees. The MIGs associated with these trees match the range for the randomly-generated trees (243–603 million years) but their distribution is completely different. The +9 suboptimal trees have a modal value at 343 million years and a right tail that includes relatively few trees. There were 1,814 trees offering improved stratigraphic consistency for a 2% increase in treelength.

The most parsimonious solutions generated by the original and rescored datasets are clearly on the left tail of the distribution of MIGs implied by the randomly-generated trees, regardless of the phylogenetic position of Tapuiasaurus. That is, they represent the most parsimonious morphological solution, and they are significantly more concordant with the stratigraphic distribution of taxa than a random distribution of taxa. When compared to the MIGs of suboptimal trees, however, the most parsimonious solutions are positioned closer to the center of that distribution. That is, compared to trees occupying adjacent regions of treespace, in this case within 9 evolutionary steps (2% treelength), the most parsimonious

trees have only an average correspondence with the stratigraphic record. There are hundreds of slightly less parsimonious topologies that imply significantly shorter missing lineages—with MIGs that are up to 80 million years shorter than those of the most parsimonious trees.

The variation in MIGs among near-optimal topologies is governed by the position of two Early Cretaceous taxa: Tapuiasaurus and Diamantinasaurus. Any topology nesting either of these among Late Cretaceous taxa will imply an early diversification of that clade, with long ghost lineages extending back to the Early Cretaceous. As noted above, Tapuiasaurus varies in position among the most parsimonious trees and creates lengthy ghost lineages when positioned close to Late Cretaceous taxa (as originally obtained by Zaher et al., 2011). The late Early Cretaceous Diamantinasaurus is invariably placed as more derived than the latest Cretaceous Isisaurus and Rapetosaurus in the most parsimonious trees, implying ghost lineages spanning most of the Late Cretaceous leading to these two taxa (Fig. 23). The more stratigraphically consistent topologies that place Diamantinasaurus basal to Isisaurus and Rapetosaurus—by resolving all Early Cretaceous titanosaurs basal to a clade of Late Cretaceous titanosaurs—imply two (Diamantinasaurus basal to Isisaurus) or five (Diamantinasaurus basal to Rapetosaurus) extra steps for the morphological matrix. Thus there is a tradeoff between morphological and stratigraphic concordance that is difficult to resolve. What is clear is that Tapuiasaurus and Diamantinasaurus are relatively early-appearing taxa that possess derived features suggesting affinities with later-appearing taxa. Achieving a robust understanding of their phylogenetic position is essential for understanding the evolutionary dynamics and the timing of cladogenetic events in the history of Titanosauria.

CONCLUSIONS

Our redescription of the complete, well preserved skull of the Early Cretaceous Brazilian titanosaur Tapuiasaurus macedoi provides detailed morphological information on South America's first titanosaur skull. Several new autapomorphies have been identified, and a much more complete scoring of the cladistic character dataset has led to a revised interpretation of its phylogenetic position. Tapuiasaurus is now resolved in most of the most parsimonious trees as a basal titanosaur positioned adjacent other Early Cretaceous forms, such as Phuwiangosaurus, Tangvayosaurus, and Malawisaurus. This result contrasts with previous results that positioned Tapuiasaurus within Nemegtosauridae as sister-taxon to the

only other titanosaurs with well preserved skulls, the Late Cretaceous Malagasy and Mongolian forms Rapetosaurus and Nemegtosaurus. A key implication of this previous Tapauisaurus-as-nemegtosaurid hypothesis is that the 'classic' titanosaur skull morphology was viewed restricted to a subgroup of titanosaurs that is geographically widespread (South America, Madagascar, Asia) and long lived (Aptian–Maastrichtian) but apparently not diverse. Our revised hypothesis, which posits that Tapuiasaurus is a basal titanosaur, implies that the 'classic' titanosaur morphology is more widespread, elements of which can be expected to be present in a broad array of titanosaurs, for which cranial remains are poorly known or completely unknown.

Further exploration into the effects on resultant topology of missing data in our character-taxon matrix led to two important conclusions. First, in datasets that contain large amounts of missing data, particularly when restricted to a particular anatomical region, resolution of even small amounts of that missing data can have dramatic effects on topology. In our analysis, resolution of 10 data cells (out of 246) for Isisaurus destabilized relationships within Nemegtosauridae. Second, taxa that are mostly scored for characters that cannot be scored in other taxa may be topologically unstable. In our dataset, it was the two taxa known predominantly (Tapuiasaurus) or exclusively (Nemegtosaurus) from cranial data, that assumed variable positions in an otherwise relatively stable topology.

We also contextualized the duration of missing lineages implied by our most parsimonious topologies by comparing it to those generated by suboptimal trees (up to 2% increase in treelength) and randomly generated topologies. There were both suboptimal and random trees that had a better fit to the stratigraphic record. In the case of random trees, although most implied much longer missing stratigraphic ranges that the most parsimonious solutions to the rescored dataset, a few random trees were significantly shorter. There were numerous suboptimal trees that greatly improved stratigraphic fit with relatively little compromise in terms of treelength.

Preparation of the remainder of the holotype of Tapuiasaurus macedoi, which includes elements of the axial skeleton (e.g., articulated anterior neck) and appendicular skeleton (e.g., nearly complete pes), is underway. We plan to finish preparation on and study of the complete holotype, which we can then incorporate into a new data matrix that samples cranial bones that are widely preserved (braincase, teeth) in addition to other elements.

ACKNOWLEDGEMENTS

We are grateful to I. Ferreira, who allowed access to the site, and to L. Lobo, M. G. Soler, M. A. Obeid, N. Brilhante, M. Padilha, B. Augusta, N. Mezzacappa, and W. Pinto, who helped in the field. The Departmento Nacional de Produção Mineral (DNPM) provided authorization for excavation and transportation of the specimen to the Museu de Zoologia of the Universidade de São Paulo. The phylogenetic analysis was performed with TNT, which is freely available (http://www.lillo.org.ar/phylogeny/tnt/) thanks to support from the Willi Hennig Society. Collections work was facilitated by D. de Almeida Campos (Museu de Ciências da Terra, Rio de Janeiro), S. A. K. de Azevedo and A. Kellner (Museu Nacional do Rio de Janeiro), S. Apesteguía (Universidad Maimónides, Buenos Aires), H. Osmólska (Polska Academia, Nauk, Warszawa), and V.Alifanov (Russian Academy of Sciences, Moscow). B. Miljour adjusted levels and cropped photographs in all figures; C. Abraczinskas labeled and added stippled/hatched overlays to all anatomical photographs (Figs. 1–21), collaborated on the reconstruction in Figure 22, and helped develop color scheme and arrangement for Figures 23–25. H. Rane assisted with proofing the manuscript. This manuscript was improved by comments from L. Salgado and an anonymous reviewer. JAW and DP gratefully acknowledge FAPESP for support of their research at Universidade de São Paulo. This research was supported by a BIOTA/FAPESP grant (11/50206-9) and two Visiting Researcher's grants (2011/51167-7; 2010/50008-00) from the Fundação de Amparo à Pesquisa do Estado de São Paulo to HZ.

REFERENCES

Ameghino F. 1898. Sinopsis geológico-paleontológica. Supplemento. Adiciones y correcciones. Universidad de La Plata: La Plata.

Apesteguía S. 2004. Bonitasaura salgadoi gen. et sp. nov.: a beaked sauropod from the Late Cretaceous of Patagonia. Naturwissenschaften **91:** 493–497.

Barrett PM, Upchurch P. 2005. Sauropodomorph diversity through time: macroevolutionary and paleoecological implications. In: Curry Rogers KA and Wilson JA, eds. The Sauropods: Evolution and Paleobiology. Berkeley: University of California Press. 125–156.

Boué C. 1970. Morphologie fonctionnelle des dents labiales chez les ruminants. Mammalia **34:** 696–711.

Calvo JO, Salgado L. 1995. Rebbachisaurus tessonei sp. nov. a new Sauropoda from the Albian-Cenomanian of Argentina; new evidence on the origin of the Diplodocidae. Gaia **11:** 13–33.

Calvo JO, Coria RA, Salgado L. 1997. One of the most complete titanosaurids (Dinosauria - Sauropoda) recorded in the world. Ameghiniana **34:** 534.

Chure DJ, Britt BB, Whitlock JA, Wilson JA. 2010. First complete sauropod dinosaur skull from the Cretaceous of the Americas and the evolution of sauropod dentition. Naturwissenschaften **97:** 379–391.

Cohen KM, Finney SC, Gibbard PL, Fan J-X. 2013; updated. The ICS International Chronostratigraphic Chart. Episodes **36**: 199–204.

Curry Rogers K. 2005. Titanosauria. In: Curry Rogers KA and Wilson JA, eds. The Sauropods: Evolution and Paleobiology. Berkeley: University of California Press. 50–103.

Curry Rogers K, Forster CA. 2001. The last of the dinosaur titans: a new sauropod from Madagascar. Nature **412:** 530–534.

Curry Rogers K, Forster CA. 2004. The skull of Rapetosaurus krausei (Sauropoda, Titanosauria) from the Late Cretaceous of Madagascar. Journal of Vertebrate Paleontology **24:** 121–144.

Curry Rogers K, Wilson JA. 2014. Vahiny depereti, gen. et sp. nov., a new titanosaur (Dinosauria, Sauropoda) from the Upper Cretaceous Maevarano Formation, Madagascar. Journal of Vertebrate Paleontology **34:** 606–617.

D'Emic MD. 2012. The early evolution of titanosauriform sauropod dinosaurs. Zoological Journal of the Linnean Society **166:** 624–671.

D'Emic MD, Whitlock JA, Smith KM, Fisher DC, Wilson JA. 2013. Evolution of high tooth replacement rates in sauropod dinosaurs. PLoS One **8:** e69235.

Filippi LS, Canudo JI, Salgado JL, Garrido A, Cerda IA, Otero A. 2011. A new sauropod titanosaur from the Plottier Formation (Upper Cretaceous) of Patagonia (Argentina). Geologica Acta **9:** 1–23.

Fisher DC. 1992. Stratigraphic parsimony. In: Maddison WP and Maddison DR, eds. MacClade: Analysis of Phylogeny and Character Evolution (ed. W. P. Maddison and D. R. Maddison). Sunderland, Massachussets: Sinauer Associates. 124–129.

Gallina PA, Apesteguía S. 2011. Cranial anatomy and phylogenetic position of the titanosaurian sauropod Bonitasaura salgadoi. Acta Palaeontologica Polonica **56:** 45–60.

Garcia RA, Paulina-Carabajal A, Salgado L. 2008. Un nuevo basicráneo de titanosaurio de la Formación Allen (Campaniano–Maastrichtiano), Provincia de Río Negro, Patagonia, Argentina. Geobios **4:** 625–633.

Gilmore CW. 1925. A nearly complete articulated skeleton of Camarasaurus, a Saurischian dinosaur from the Dinosaur National Monument, Utah. Memoirs of the Carnegie Museum **10:** 347–384.

Goloboff PA, Farris JS, Nixon KC. 2008. TNT, a free program for phylogenetic analysis. Cladistics **24:** 774–786.

Goloboff PA, Farris S, Nixon K. 2008b. TNT: Tree analysis using New Technology, version 1.1 (Willi Henning Society Edition). Updated at http://www.lillo.org.ar/phylogeny/tnt/. Accessed March 3, 2012.

Gow CE. 1990. Morphology and growth of the Massospondylus braincase (Dinosauria Prosauropoda). Palaeontologia Africana **27:** 59–75.

Harris JD. 2004. Confusing dinosaurs with mammals: tetrapod phylogenetics and anatomical terminology in the world of homology. The Anatomical Record **281A:** 1240–1246.

Hill RV, D'Emic MD, Bever GS, Norell MA. 2015. A complex hyobranchial apparatus in a Cretaceous dinosaur and the antiquity of avian paraglossalia. Zoological Journal of the Linnean Society **175:** 892–909.

Hocknull SA, White MA, Tischler TR, Cook AG, Calleja ND, Sloan T, Elliot DA. 2009. New Mid-Cretaceous (Latest Albian) Dinosaurs from Winton, Queensland, Australia. PLoS One **4:** e6190. doi:6110.1371/journal.pone.0006190.

Holland WJ. 1924. The skull of Diplodocus. Memoirs of the Carnegie Museum **9:** 379–403.

Janensch W. 1935-6. Die Schädel der Sauropoden Brachiosaurus, Barosaurus, und Dicraeosaurus. Palaeontographica **2 (Supplement 7):** 147–298.

Kellner AWA. 1996. Remarks on Brazilian dinosaurs. Memoirs of the Queensland Museum **39:** 611–626.

Kurzanov SM, Bannikov AF. 1983. A new sauropod from the Upper Cretaceous of Mongolia. Paleontological Journal **2:** 90–96.

Lydekker R. 1893. The dinosaurs of Patagonia. Anales del Museo de la Plata **2:** 1–14.

Madsen Jr. JH, McIntosh JS, Berman DS. 1995. Skull and atlas-axis complex of the Upper Jurassic sauropod Camarasaurus Cope (Reptilia: Saurischia). Bulletin of Carnegie Museum of Natural History **31:** 1–115.

Martinelli AG, da Silva Marinho T, Filippi LS, Ribeiro LCB, da Fonseca Ferraz ML, Cavellani CL, de Paula Antunes Teixeira V. 2015 in press. Cranial bones and atlas of titanosaurs (Dinosauria, Sauropoda) from Late Cretaceous (Bauru Group) of Uberaba, Minas Gerais State, Brazil. **Journal of South American Earth Sciences.** doi: 10.1016/j.jsames.2015.02.009.

Martinez R. 1998. An articulated skull and neck of sauropoda (Dinosauria: Saurischia) from the Upper Cretaceous of Central Patagonia, Argentina. Journal of Vertebrate Paleontology **18:** 61A.

Norell MA. 1992. Taxic origin and temporal diversity: the effect of phylogeny. In: Novacek MJ and Wheeler QD, eds. Extinction and Phylogeny. New York: Columbia University Press. 89–118.

Norell MA. 1993. Tree-based approaches to understanding history: comments on ranks, rules, and the quality of the fossil record. American Journal of Science **293-A:** 407–417.

Nowinski A. 1971. Nemegtosaurus mongoliensis n. gen., n. sp. (Sauropoda) from the Uppermost Cretaceous of Mongolia. Palaeontologia Polonica **25:** 57–81.

Osborn HF. 1924. Sauropoda and theropoda of the Lower Cretaceous of Mongolia. American Museum Novitates **128:** 1–7.

Paulina Carabajal A. 2012. Neuroanatomy of titanosaurid dinosaurs from the Upper Cretaceous of Patagonia, with comments on endocranial variability within Sauropoda. The Anatomical Record **295:** 2141–2156.

Pol D, Escapa IH. 2009. Unstable taxa in cladistic analysis: identification and the assessment of relevant characters. Cladistics **25:** 515–527**.**

Salgado L, Calvo JO. 1992. Cranial osteology of Amargasaurus cazaui Salgado & Bonaparte (Sauropoda, Dicraeosauridae) from the Neocomian of Patagonia. Ameghiniana **29:** 337–346.

Sereno PC. 2009. Comparative cladistics. Cladistics **25:**624–659.

Sereno PC, Wilson JA. 2005. Structure and evolution of a sauropod tooth battery. In: Curry Rogers KA and Wilson JA, eds. The Sauropods: Evolution and Paleobiology. Berkeley, California: University of California Press. 157–177.

Sereno PC, Wilson JA, Witmer LM, Whitlock JA, Maga A, Ide O, Rowe TA. 2007. Structural extremes in a Cretaceous dinosaur. PLoS One **2:** e1230.

Sereno PC, Martínez R, Alcober OA. 2013. Osteology of Eoraptor lunensis (Dinosauria, Sauropodomorpha). Society of Vertebrate Paleontology Memoir **12:** 83–179.

Storrs GW. 1993. The quality of the Triassic sauropterygian fossil record. Revue de Paléobiologie (Vol. spéc.) **7:** 217–228.

Sues H-D, Reisz RR, Hinic SJ, Raath MA. 2004. On the skull of Massospondylus carinatus Owen, 1854 (Dinosauria: Sauropodomorpha) from the Elliot and Clarens Formations (Lower Jurassic) of South Africa. Annals of the Carnegie Museum **73:** 239–257.

Sues, H-D, Averianov A, Ridgeley RC, Witmer LM. 2015. Titanosauria (Dinosauria: Sauropoda) from the Upper Cretaceous (Turonian) Bissekety Formation of Uzbekistan. Journal of Vertebrate Paleontology. e889145.

Suteethorn S, Le Loeuff J, Buffetaut E, Suteethorn V, Taubmook C, Chonglakmani C. 2009. A new skeleton of Phuwiangosaurus sirindhornae (Dinosauria, Sauropoda) from NE Thailand. In: Buffetaut E, Cuny G, Le Loeuff J and Suteethorn V, eds. Late Palaeozoic and Mesozoic Ecosystems in SE Asia. London: Geological Society of London. 189–215.

Upchurch P, Barrett PM. 2005. Phylogenetic and taxic perspectives on sauropod diversity. In: Curry Rogers KA and Wilson JA, eds. The Sauropods: Evolution and Paleobiology. Berkeley: University of California Press. 104–124.

Whitlock JA, D'Emic MD, Wilson JA. 2011. Cretaceous diplodocids in Asia? Re-evaluating the phylogenetic affinities of a fragmentary specimen. Palaeontology **54:** 351–364.

Wilson JA. 2002. Sauropod dinosaur phylogeny: critique and cladistic analysis. Zoological Journal of the Linnean Society **136:** 217–276.

Wilson JA. 2005. Redescription of the Mongolian sauropod Nemegtosaurus mongoliensis Nowinski (Dinosauria: Saurischia) and comments on Late Cretaceous sauropod diversity. Journal of Systematic Palaeontology **3:** 283–318.

Wilson JA. 2006. Anatomical nomenclature of fossil vertebrates: standardized terms or lingua franca? Journal of Vertebrate Paleontology **26:** 511–518.

Wilson JA, D'Emic MD, Curry Rogers KA, Mohabey DM, Sen S. 2009. Reassessment of the sauropod dinosaur Jainosaurus (="Antarctosaurus") septentrionalis from the Upper Cretaceous of India. Contributions from the Museum of Paleontology the University of Michigan **32:** 17–40.

Wilson JA, Malkani MS, Gingerich PD. 2005. A sauropod braincase from the Pab Formation (Upper Cretaceous, Maastrichtian) of Balochistan, Pakistan. Gondwana Geological Magazine **8:** 101–109.

Wilson JA, Sereno PC. 1998. Early evolution and higher-level phylogeny of sauropod dinosaurs. Society of Vertebrate Paleontology Memoir **5:** 1–68.

Wilson JA, Upchurch P. 2009. Redescription and reassessment of the phylogenetic affinities of Euhelopus zdanskyi (Dinosauria: Sauropoda) from the Early Cretaceous of China. Journal of Systematic Palaeontology **7:** 1–41.

Yates A. 2007. The first complete skull of the Triassic dinosaur Melanorosaurus haughton (Sauropodomorpha: Anchisauria). Special Papers in Paleontology **77:** 9–55.

Zaher H, Pol D, Carvalho AB, Nascimento PM, Roccomini C, Larson P, Juarez-Valieri R, Pires-Domingues R, da Silva NJ, Campos DA. 2011. A complete skull of an Early Cretaceous sauropod and the evolution of advanced titanosaurians. PLoS One **6:** e16663.

Submitted XXXXXX 2015

FIGURE LEGENDS

Figure 1. Tapuiasaurus macedoi (MZSP-Pv 807). **A**, skull in quarry, with left side exposed and showing the position of the lower jaws, and ceratobranchials. In addition, the anteriormost cervical ribs are positioned just posterior to the ceratobranchials (parallel, nearly vertical splint-like elements); they most likely pertain to the axial vertebra. **B**, skull in early stages of preparation, with right side exposed. Note that a small portion of the surangular was been damaged in the initial stages of preparation; more of this region of extremely thin bone was lost during subsequent preparation (compare to Fig. 16).

Figure 2. Tapuiasaurus macedoi (MZSP-Pv 807). Cranium in right lateral (**A**) and left lateral (**B**) views.

Figure 3. Tapuiasaurus macedoi (MZSP-Pv 807). Right premaxilla and maxilla in lateral view. Adjacent bones and openings have been shaded to deemphasize them. Dashed lines indicate a missing margin; hatching indicates a broken surface; dot pattern indicates matrix. Abbreviations: **amfo**, anterior maxillary foramen; **aofe**, antorbital fenestra; **ect**, ectopterygoid; **f**, foramen; **fo**, fossa; **j**, jugal; **l**, left; **la**, lacrimal; **ltf**; lateral temporal fenestra; **m**, maxilla or maxillary; **na**, narial; **or**, orbit; **pal**, palatine; **paofe**, preantorbital fenestra; **pm**, premaxilla; **pr**, process; **pt**, pterygoid; **q**, quadrate;

qj, quadratojugal; **r**, right; **snf**, subnarial foramen; **tab**, tab; Arabic numerals indicate tooth positions.

Figure 4. Tapuiasaurus macedoi (MZSP-Pv 807). Anterior snout in ventral view (stereopairs). Dot pattern indicates matrix. Abbreviations: **add ch**, adductor chamber; **ect**, ectopterygoid; **f**, foramen; **fl**, flange; **m**, maxilla or maxillary; **pal**, palatine; **pa sh**; palatal shelf; **pm**, premaxilla; **p-m pr**, posteromedial process of the premaxilla; **ppf**, postpalatine fenestra; **pt**, pterygoid; **rep f**, replacement foramen; **tab**, tab; **v**, vomer; Arabic numerals indicate tooth positions.

Figure 5. Tapuiasaurus macedoi (MZSP-Pv 807). Detail of right maxillary region showing series of openings between preantorbital fenestra and anterior maxillary fenestra (stereopairs). Note difference in bone texture on body of maxilla (lower right) versus base of ascending process and jugal process (upper left). Dotted line indicates pm-m suture. Abbreviations: **amfo**, anterior maxillary foramen; **aofe**, antorbital fenestra; **f**, foramen; **m**, maxilla; **paofe**, preantorbital fenestra; **pm**, premaxilla.

Figure 6. Tapuiasaurus macedoi (MZSP-Pv 807). Computed Tomography (CT) coronal slice though the snout showing replacement premaxillary and maxillary teeth. Abbreviations: **l**, left; **m**, maxilla; **pm**, premaxilla; **r**, right; Arabic numerals refer to numbered tooth positions; lower case Roman numerals indicate position in the tooth file.

Figure 7. Tapuiasaurus macedoi (MZSP-Pv 807). Skull roof in anterodorsal view. Dashed lines indicate a missing margin; dot pattern indicates matrix. Abbreviations: **aofe**, antorbital fenestra; **en**, external naris; f, foramen; **fo**, fossa; **fr**, frontal; **j**, jugal; **l**, left; **la**, lacrimal; **m**, maxilla; **na**, nasal or narial; **p**, parietal; **pm**, premaxilla; **po**, postorbital; **prf**, prefrontal; **q**, quadrate; **r**, right; **stf**, supratemporal fenestra.

Figure 8. Tapuiasaurus macedoi (MZSP-Pv 807). Skull roof in posterodorsal view. Adjacent bones have been shaded to deemphasize them. Dashed lines indicate a missing margin; hatching indicates a broken surface. Abbreviations: **fm**, foramen magnum; **fr**, frontal; **m**, maxilla; **na**, nasal; **oc ri**; occipital ridge; **pa**, parietal; **po**, postorbital; **prf**, prefrontal; **so**, supraoccipital; **sq**, squamosal; **stf**, supratemporal fenestra; **su**, suture.

Figure 9. Tapuiasaurus macedoi (MZSP-Pv 807). Braincase and skull roof in posterior view. Dashed lines indicate a missing margin; hatching indicates a broken surface; dot pattern indicates matrix. Abbreviations: **aofe**, antorbital fenestra; **bpt**, basipterygoid process; **bt**, basal tubera; **eo-op**, exoccipital-opisthotic; **fa**, facet; **fr**, frontal; **ft**, fragment; **j**, jugal; **ltf**, lateral temporal fenestra; **m**, maxilla; **oc**, occipital condyle; **p**,

parietal; **pal**, palatine; **pm**, premaxilla; **po**, postorbital; **pop**, paroccipital process; **prf**, prefrontal; **pro**, proatlas; **pt**, pterygoid; **q**, quadrate; **q-bt**, quadrate-basal tuber contact; **q fo**, quadrate fossa; **qj**, quadratojugal; **ri**, ridge; **so**, supraoccipital; **sq**, squamosal.

Figure 10. Tapuiasaurus macedoi (MZSP-Pv 807). Right postorbital in lateral view. Adjacent bones and openings have been shaded to deemphasize them. Dashed lines indicate a missing margin; hatching indicates a broken surface; dot pattern indicates matrix. Abbreviations: **fr**, frontal; **fr pr**, frontal process of the postorbital; **j**, jugal; **j pr**, jugal process of the postorbital; **la**, lacrimal; **ltf**, lateral temporal fenestra; **or**, orbit; **orn**, ornamentation; **p**, parietal; **prf**, prefrontal; **sq**, squamosal; **sq pr**, squamosal process of the postorbital; **stf**, supratemporal fenestra.

Figure 11. Tapuiasaurus macedoi (MZSP-Pv 807). **A**, **B** right and left lacrimals in lateral view. Adjacent bones and openings have been shaded to deemphasize them. Abbreviations: **aofe**, antorbital fenestra; **fr**, frontal; **j**, jugal; **la ap**, lacrimal anterior process; **la fo**, lacrimal foramen; **ltf**, lateral temporal fenestra; **m**, maxilla; **or**, orbit; **pm**, premaxilla; **po**, postorbital; **prf**, prefrontal; **qj**, quadratojugal; **sq**, squamosal.

Figure 12. Tapuiasaurus macedoi (MZSP-Pv 807). Right jugal in lateral view. Adjacent bones and openings have been shaded to deemphasize them. Dashed lines indicate a missing margin; hatching indicates a broken surface; dot pattern indicates matrix. Abbreviations: **bs**, basisphenoid; **ect**, ectopterygoid; **la**, lacrimal; **la pr**, lacrimal process of the jugal; **j**, jugal; **m**, maxilla**; m pr**, maxillary process of the jugal; **pal**, palatine; **po**, postorbital; **po pr**, postorbital process of the jugal; **pt**, pterygoid; **q**, quadrate, **qj**, quadratojugal; **qj pr**, quadratojugal process of the jugal.

Figure 13. Tapuiasaurus macedoi (MZSP-Pv 807). Right squamosal and quadratojugal in lateral view. Adjacent bones and openings have been shaded to deemphasize them. Dotted black line indicates sq-qj suture. Dashed lines indicate a missing margin; hatching indicates a broken surface; dot pattern indicates matrix. Abbreviations: **aofe**, antorbital fenestra; **em**, embayment; **en**, external naris; **ho**, hook; **j**, jugal; **la**, lacrimal; **ltf**, lateral temporal fenestra; **m**, maxilla; **or**, orbit; **p**, parietal; **po**, postorbital; **qj**, quadratojugal; **sq**, squamosal; **sq-qj**, squamosal-quatrojugal suture; **stf**, supratemporal fenestra.

Figure 14. Tapuiasaurus macedoi (MZSP-Pv 807). Braincase in right lateral view, as exposed within the orbit (stereopairs). Dotted lines indicate sutures. Abbreviations:

bs, basisphenoid; **f**, foramen; **ls**, laterosphenoid; **os**, orbitosphenoid; **pro**, prootic; **sc**, scleral ossicles; Roman numerals indicate cranial nerve openings.

Figure 15. Tapuiasaurus macedoi (MZSP-Pv 807). Right (**A**, **B**) and left (**C**, **D**) ceratobranchials in lateral (**A**, **D**) and medial (**B**, **C**) views. Images are oriented as preserved; the more narrow end of each element points dorsally, and the more expanded end points anteriorly. **A** and **C** represent the view from the right side of the skull (right ceratobranchial in lateral view, left ceratobranchial in medial view); **B** and **D** represent the view from the left side of the skull. See Figure 1A for a view of these elements in situ.

Figure 16. Tapuiasaurus macedoi (MZSP-Pv 807). **A**, left and **B**, right mandibles in lateral view. Adjacent bones have been shaded to deemphasize them. Dashed lines indicate a missing margin; hatching indicates a broken surface; dot pattern indicates matrix. Abbreviations: **ang**, angular; **art**, articular; **asaf**, anterior surangular foramen; **cor**, coronoid; **d**, dentary; **d15**, dentary tooth 15; **psaf**, posterior surangular foramen; **sang**, surangular.

Figure 17. Tapuiasaurus macedoi (MZSP-Pv 807). Left coronoid in medial view. Adjacent bones have been shaded to deemphasize them. Dot pattern indicates matrix. Abbreviations: **cor**, coronoid; **d**, dentary; **d15**, dentary tooth 15; **spl**, splenial.

Figure 18. Tapuiasaurus macedoi (MZSP-Pv 807). Posterior portion of right mandible in medial view. Dashed lines indicate a missing margin; hatching indicates a broken surface; dot pattern indicates matrix. Abbreviations: **ang**, angular; **art**, articular; **d**, dentary; **f**, foramen; **part**; prearticular; **sang**, surangular; **spl**, splenial.

Figure 19. Tapuiasaurus macedoi (MZSP-Pv 807). **A**, left and **B**, right posterior mandibles in dorsal view. Dot pattern indicates matrix. Abbreviations: **ang**, angular; **art**, articular; **part**, prearticular; **sang**, surangular.

Figure 20. Tapuiasaurus macedoi (MZSP-Pv 807). Upper teeth, wear pattern. **A**, right premaxilla and maxilla in oblique anterolateral view, with blown up images of maxillary tooth 3 and 4 showing labial wear facets. **B**, right premaxilla and maxilla in oblique ventromedial view with blown up image of maxillary teeth 4 and 5 showing lingual wear facets. Both labial and lingual facets are present on right premaxillary tooth 3 and right maxillary teeth 1, 3, and 4. Note that **A** and **B** were photographed at different stages of preparation; **A** was shot before matrix on the lingual faces of teeth was removed. The triangular piece of bone missing from just behind the tooth row in

A represents a sample removed for analysis. Scale bars are for images of the premaxilla and maxilla; teeth are not to scale.

Figure 21. Tapuiasaurus macedoi (MZSP-Pv 807). Lower teeth, wear pattern. **A**, conjoined mandibles in oblique right dorsolateral view showing the first 13 right dentary teeth. **B** and **C** are close-up photographs of the first four dentary teeth in lingual and labial views, respectively. Abbreviations: **d1–11**, dentary tooth positions; **d**, dentary; **wf**, wear facet.

Figure 22. Reconstruction of the skull of Tapuiasaurus macedoi in right lateral view. Abbreviations: **ang**, angular; **aofe**, antorbital fenestra; **art**, articular; **asaf**, anterior surangular foramen; **bs**, basisphenoid; **cor**, coronoid; **d**, dentary; **ect**, ectopterygoid; **f**, foramen; **fr**, frontal; **j**, jugal; **la**, lacrimal; **ls**, laterosphenoid; **ltf**, lateral temporal fenestra; **m**, maxilla or maxillary; **na**, nasal; **os**, orbitosphenoid; **p**, parietal; **pal**, palatine; **paofe**, preantorbital fenestra; **pm**, premaxilla or premaxillary; **po**, postorbital; **pr**, prootic; **prf**, prefrontal; **psaf**, posterior surangular foramen; **pt**, pterygoid; **q**, quadrate, **qj**, quadratojugal; **sang**, surangular; **scl**, sclerotic ring; **sq**, squamosal; **snf**, subnarial foramen; **stf**, supratemporal fenestra; **tab**, tab. Arabic numerals refer to tooth positions.

Figure 23. Temporally-calibrated cladogram representing a reduced consensus of 34 most parsimonious trees generated in a cladistic analysis of 31 taxa and 246 characters (see text for details). The reduced consensus was generated using the iterPCR script in TNT (see Pol & Escapa 2009), which identified Tapuiasaurus and Nemegtosaurus as wildcard taxa that linked with 13 different lithostrotian taxa in the most parsimonious trees (labeled **a**–**c** and **d**–**m**, respectively). The italicized numbers at nodes within Titanosauria represent decay indices greater than 1. The colored bars represent the temporal distribution of diplodocoid (brown) and macronarian (blue) taxa; in all cases their vertical extent reflects stratigraphic uncertainty rather than a true range. Dates at epoch and stage boundaries are based on Cohen et al. (2013). Coloration of chronostratigraphic units follows the Commission for the Geological Map of the World (http://www.ccgm.org).

Figure 24. Punnett square showing the topological results within Titanosauria after re-analysis of the original Zaher et al. (2011) data matrix with and without rescored data for Tapuiasaurus and Isisaurus. Tapuiasaurus was fully rescored based on the present study; in addition, cranial data for Isisaurus were added, based on previous study of original materials (see Wilson et al. 2005). Re-analysis including only the rescored

Tapuiasaurus data (lower left) yields the same topology as the original matrix, which includes an intact Nemegtosauridae (*****; upper left). Re-analysis adding only the new Isisaurus data (upper right) supports the grouping of Tapuiasaurus + Rapetosaurus but does not unequivocally support the monophyly of the three nemegtosaurid taxa (in bold-face type) because Nemegtosaurus (**N**) is alternatively placed as the sister group of the Tapuiasaurus + Rapetosaurus clade or Isisaurus. Re-analysis using both new Isisaurus data and rescored Tapuiasaurus data (lower right) disbands the three nemegtosaurid taxa, with Nemegtosaurus (**N**) positioned more tipward and Tapuiasaurus (**T**) positioned more stemward. CSSI is the Character State Similarity Index (Sereno 2009), which measures similarity between matrices that score the same characters (see text for explanation). Abbreviations: **Nemegto.**, Nemegtosaurus; **Tapuia.**, Tapuiasaurus.

Figure 25. Stratigraphic consistency in suboptimal and randomly generated trees. Histogram shows the Minimum Implied Gap (**MIG**) implied by different topological rearrangements within Titanosauria; non-titanosaur relationships were fixed (see upper right inset). The MIGs for most parsimonious trees from the original analysis ($\mathbf{MPT_{Or}}$; 383 million years) and rescored analysis ($\mathbf{MPT_{Re}}$; 323–343 million years) are indicated by the horizontal spans above the histogram. Note that the fixed topology for non-titanosaurs used the more stratigraphically consistent of two sets of relationships among basal sauropods. Orange bars represent MIGs for up to 10,000 suboptimal trees 2, 5, and 9 steps longer than the most parsimonious tree(s) generated by the rescored Tapuiasaurus matrix. Blue bars represent MIGs for 10,000 randomly selected trees of any length. MIGs for the most parsimonious trees are on the left tail of the distribution for random trees, but they fall closer to the center of the distribution for suboptimal trees.

Table 1. Completeness of cranial remains associated with 27 Cretaceous titanosauriform genera. Genera are listed alphabetically by region. Unnamed specimens (e.g., MML-194; García et al., 2008) and indeterminate taxa (e.g., Asiatosaurus mongoliensis; Osborn, 1924) are not listed. Solid black dots indicate cranial remains are known for a given region, and open circles indicate they are partially known for a region. Parentheses indicate uncertain association. Early Cretaceous titanosauriform genera with cranial remains are known from Africa (Malawisaurus, Karongasaurus), the Americas (Abydosaurus, Ligabuesaurus, Tapuiasaurus), and Asia (Euhelopus, Mongolosaurus, Phuwiangosaurus).

	braincase	skull roof	cheek/orbit series	upper jaw	palate	lower jaw	teeth
AFRICA							
Malawisaurus dixeyi	●	○	○	○	○	●	●
Karongasaurus gittelmani						●	●
AMERICAS							
Abydosaurus mcintoshi	●	●	●	●	●	●	●
Alamosaurus sanjuanensis							(○)
Antarctosaurus wichmannianus	●	●	○			●	●
Auca Mahuevo embryo	○	○	○	○	○	○	○
Bonatitan reigi	●	●					
Bonitasaura salgadoi		○	○			●	●
Brasilotitan nemophagus						●	

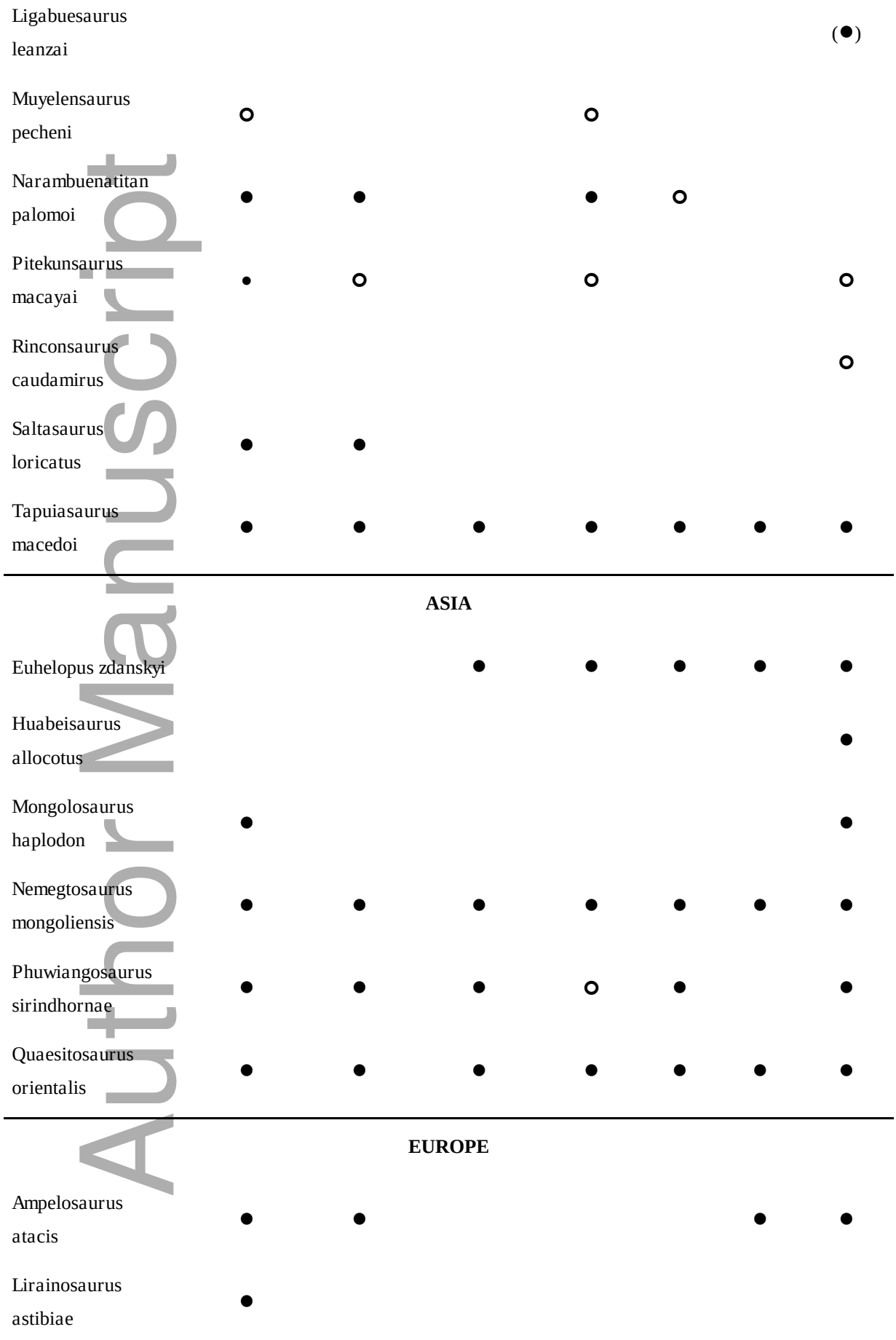

Magyarosaurus dacus	●	●					
INDIA							
Isisaurus colberti	●						
Jainosaurus septentrionalis	●	●					
MADAGASCAR							
Rapetosaurus krausei	●	●	●	●	●	●	●
Vahiny depereti	●						

Table 2. Measurements (cm) of the skull and lower jaws of Tapuiasaurus macedoi (MZSP-PV 807). See Figure 2 for location of landmarks used in measurements. An "i" indicates an incomplete measurement.

Measurement	**Right**	**Left**
Skull, length parallel to tooth row	44.1	39.8
Quadrate → premaxilla, length	33.4	28.9
Quadrate → squamosal, length	16.8	13.6
Squamosal → nasal, length	13.1	12.7
Nasal → premaxilla, length	37.8	36.1
Squamosal → premaxilla, length	43.5	38.1
Dentigerous upper jaw, length along curve	15.3	13.1
Orbit, greatest diameter	14.9	12.6
Orbit, least diameter	8.2	5.9
Antorbital fenestra, greatest diameter	12.0	13.0
Antorbital fenestra, least diameter	5.6	3.8
Lateral temporal fenestra, greatest diameter	12.7	10.2
Lateral temporal fenestra, least diameter	1.9	1.1
Preantorbital fenestra, greatest diameter	5.7	5.8
Articular → dentary, length	32.2	27.5
Dentary symphysis, greatest depth	4.4	4.6
Dentary, least depth	3.7	3.3
Dentary, greatest posterior depth	6.3	6.2
Surangular-angular, greatest depth	7.0	5.9

Measurement	Right	Left
Dentigerous lower jaw, length along curve	11.9	12.2

Table 3. Arcade Index (AI) for the dentaries of selected neosauropods. AI is the ratio of the transverse breadth and anteroposterior length of the dentigerous portion of the dentary. Genera are listed by ascending AI score. Note that AI is not correlated with phylogeny, age, or number of teeth. An asterisk (*) indicates that the upper AI (Whitlock, 2011) is reported because dentary was either not available or not suitable for measurement. AIs for diplodocoids, Giraffatitan, and Camarasaurus were taken from Whitlock (2011: table 2).

Genus	**Higher-level group**	**Age**	**# Teeth**	**AI**
Camarasaurus	basal Macronaria	Late Jurassic	13	0.4
Dicraeosaurus	Diplodocoidea	Late Jurassic	16	0.6
Giraffatitan	Titanosauriformes	Late Jurassic	15	0.6
Abydosaurus	Titanosauriformes	Early Cretaceous	14	0.6*
Tapuiasaurus	**Titanosauria**	**Early Cretaceous**	**15**	**0.8**
Rapetosaurus	Titanosauria	Late Cretaceous	11	0.8
Nemegtosaurus	Titanosauria	Late Cretaceous	13	0.9
Diplodocus	Diplodocoidea	Late Jurassic	15	1.2
Apatosaurus	Diplodocoidea	Late Jurassic	10–11	1.5
Bonitasaura	Titanosauria	Late Cretaceous	>10	>1.5
Brasilotitan	Titanosauria	Late Cretaceous	14	1.6
Antarctosaurus	Titanosauria	Late Cretaceous	14–15	2.3
Nigersaurus	Diplodocoidea	Early Cretaceous	34	4

Table 4. Wear and dimensions (mm) of upper and lower jaw teeth of Tapuiasaurus macedoi (MZSP-PV 807). Codings for wear pattern are: **0**, no wear; **1**, distal wear facet; **2**, both mesial and distal wear; **3**, labial wear; **4**, lingual wear; **5**, both labial and lingual wear; **6**, apex-only wear. Apical-basal height of teeth was measured as exposed; due to preservation, crown-root junction could not be identified. Note that there is one fewer tooth position in the lower jaw (15) compared to the upper jaw (16). Maximum crown breadths were measured orthogonal to height. Abbreviations: **e**, erupting tooth; **i**, incomplete measurement; **L**, left; **R**, right; **rp**, replacing tooth.

element	position	height	breadth	wear
R premaxilla	1	34.3	6.9	0
	2rp	36.8	7.2	5
	3	36.4	7.2	6
	4rp	37.5	6.6	5
R maxilla	5	35.7	7.5	—
	6rp	36.0	7.3	5
	7rp	33.7	7.0	5
	8	32.5	7.0	4
	9	27.6	6.5	6
	10	30.0	6.7	—
	11	27.3	5.8	—
	12	21.7	5.4	6
	13	18.8i	4.8	—
	14	19.6	5.2	—
	15	22.8	4.3	—
	16	16.3	4.2	—
L premaxilla	1e	11.6	5.6	—
	2	41.7	7.3	6
	3	39.3	7.2	4

element	position	height	breadth	wear
	4	36.8	—	0
L maxilla	5	37.2	6.7	0
	6	—	—	2
	7	26.4	—	—
	8	14.0	7.7	—
	9	23.8	—	—
	10	—	—	—
	11	17.3i	—	—
	12	—	4.6	—
	13	12.2i	—	—
	14	—	—	—
	15	11.2i	4.4	—
	16	—	—	—
R dentary	1	27.9	5.9	0
	2	28.7	5.7	3
	3	25.8	6.2	3
	4	22.4i	5.9	—
	5	26.3i	5.9	—
	6	24.0	6.0	0
	7	20.0i	4.9i	—
	8	19.6	5.3	—
	9	16.8	5.6	—
	10	15.6	5.3	3
	11	12.2	5.1	0
	12	—	—	—
	13	—	—	3

element	position	height	breadth	wear
	14	—	—	—
	15	—	—	—
L dentary	1e	23.9	6.0	—
	2	26.1	6.1	—
	3	19.8	5.6	0
	4	23.7	5.5	3
	5	22.1	—	—
	6	19.5i	—	—
	7	19.5i	5.4	—
	8	17.7	5.3	—
	9	20.3	5.1	—
	10	17.7	4.9	—
	11	—	—	—
	12	15.7	4.6	3
	13	16.6	4.4	—
	14	15.9	4.3	1
	15	—	3.2	—

Table 5. Spacing (mm) of upper and lower jaw teeth of Tapuiasaurus macedoi (MZSP-PV 807). Gaps between teeth were measured orthogonal to apico-basal height. There is one fewer tooth in the lower jaw, and thus one fewer gap (marked with an **X**). The first row marks the median gap and is the same for both left and right sides.

position	R upper	L upper	R lower	L lower
	1.0	(same)	1.5	(same)
1				
	1.6	2.5	0.8	1.3
2				
	1.1	2.3	1.2	—
3				
	2.4	1.8	1.6	—
4				
	2.2	3.8	2.6	0.7
5				
	4.5	1.8	4.0	0.0
6				
	3.5	3.0	2.4	0.0
7				
	3.6	1.7	4.6	0.9
8				
	4.8	2.8	2.2	2.1
9				
	1.5	2.0	3.1	2.3
10				
	2.8	2.5	3.1	3.4
11				

position	R upper	L upper	R lower	L lower
	2.4	2.0	—	3.3
12				
	2.0	3.1	—	4.5
13				
	2.8	—	—	3.4
14				
	2.8	—	—	6.8
15				
	2.6	—	X	X
16				

Table 6. Revised character scorings for Tapuiasaurus and Isisaurus used in phylogenetic analysis. Remainder of character-taxon matrix is unchanged from Zaher et al. (2011).

Tapuiasaurus (all characters; 1–246)

00?1011201 0110010101 0-02011111 0111121111 0?10001000 0101101 00?
?00-111101 1210001 10? 111101 1?0- ?1010?1?10 1100110??? ??????????
?????????? ????????10 11??????1? ????0?0??? ????110010 1?????????
????????? ?????1?2?? ?????????? ??????1??? ?????0?11? 1110110111
111111

Isisaurus (cranial characters only; 1–88)

?????????? ????????0? 0?0?0????? ?????????? ??1?0??000 0??1??????
?????????? ?????????? ????????

Table 7. Missing data scores for titanosaur taxa scored in the original phylogenetic analysis presented by Zaher et al. (2011) and the revised analysis presented here. The only scorings that changed between the two analysis are those of Isisaurus and Tapuiasaurus, which are labeled "orig" (original) or "rev" (revised) accordingly. Missing data have been broken down and ranked for total missing data, cranial missing data, and postcranial missing data. Taxa are listed in order of their "Rank Sum," which indicates the sum of the rank scores for total, cranial, and postcranial missing data. Note that each of the four rankings provides a different ordering of taxa.

Taxon	Total		Cranial		Postcranial		Rank Sum
	%	rank	%	rank	%	rank	
Phuwiangosaurus	40.2	1	63.6	5	29.7	2	8
Rapetosaurus	41.5	2	19.3	3	58.6	10	15
Opisthocoelicaudia	42.3	3	100.0	14	11.0	1	18
Tapuiasaurus_rev	45.5	4	4.5	1	74.5	12	17
Saltasaurus	49.2	5	79.5	6	35.9	3	14
Tapuiasaurus_orig	55.7	6	23.9	4	80.0	13	23
Malawisaurus	58.5	7	81.8	7	49.6	6	20
Neuquensaurus	58.9	7	100.0	14	39.3	4	25
Alamosaurus	63.2	9	100.0	14	44.8	5	28
Isisaurus_rev	62.2	9	87.5	8	52.4	7	24
Isisaurus_orig	66.7	11	100	14	52.4	7	32
Nemegtosaurus	68.3	12	11.4	2	100.0	14	28
Diamantinasaurus	75.2	14	100.0	14	66.9	11	39
Tangvayosaurus	68.3	12	100.0	14	55.2	9	35

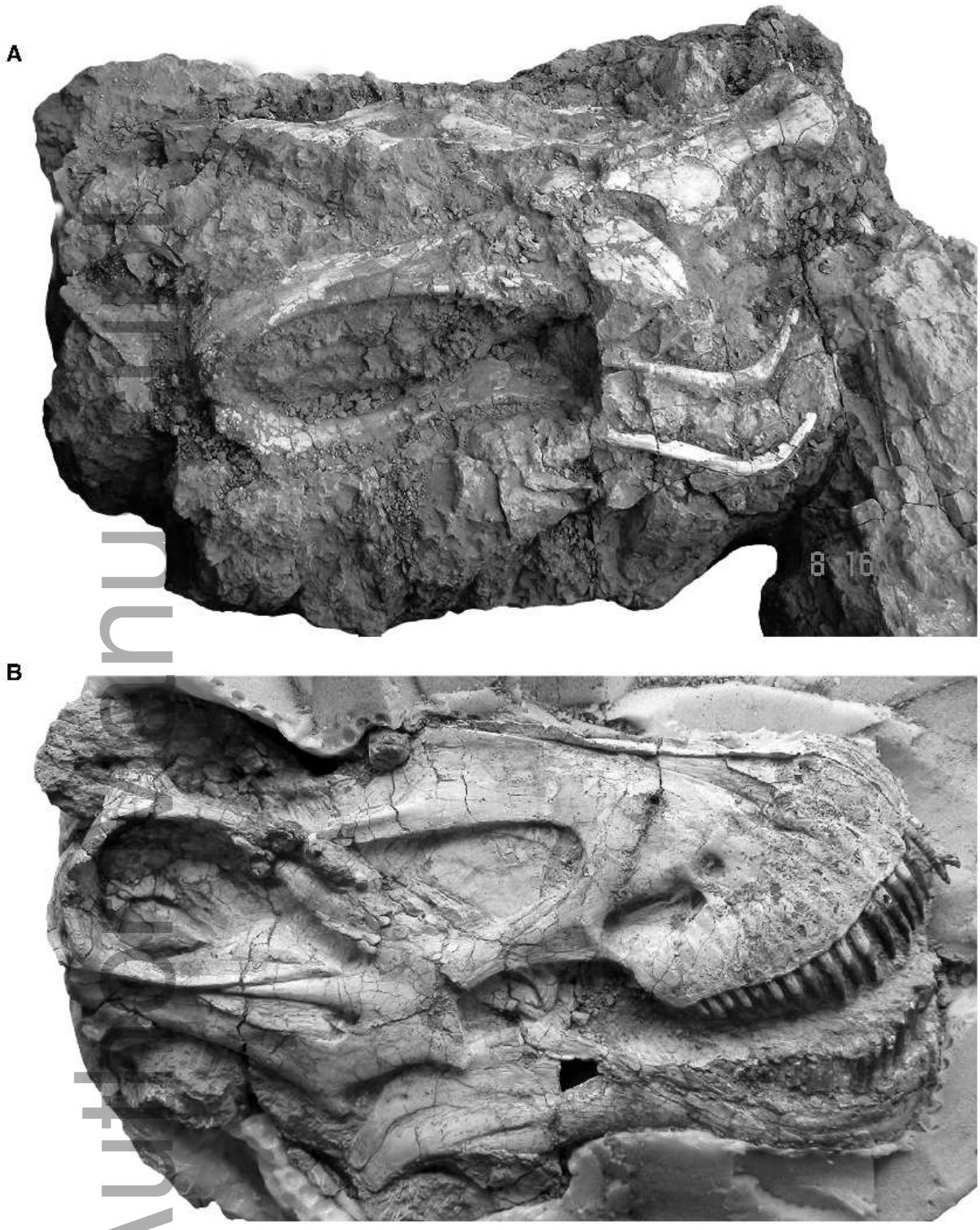

zoj_12420_f1.tif

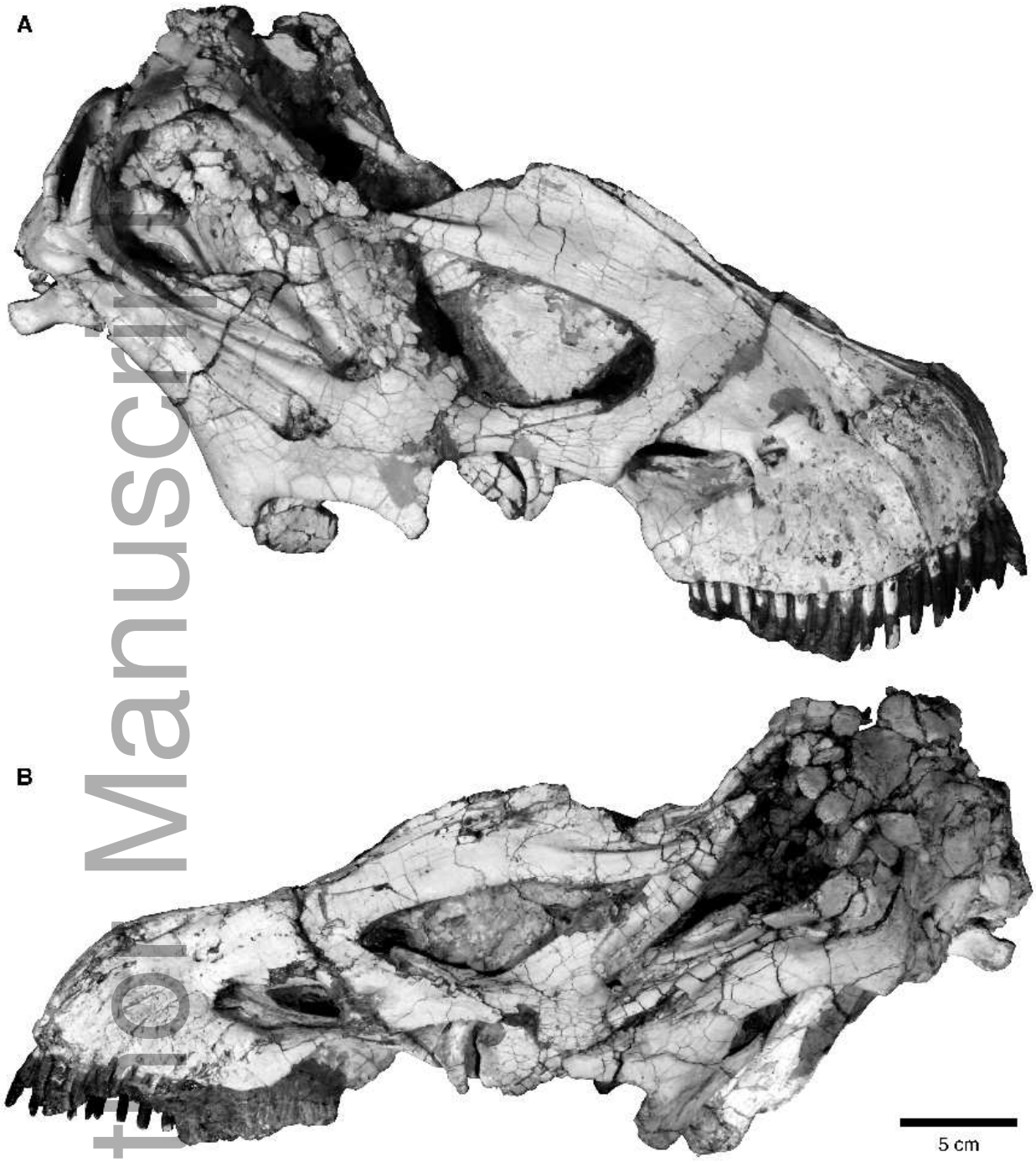

zoj_12420_f2.tif

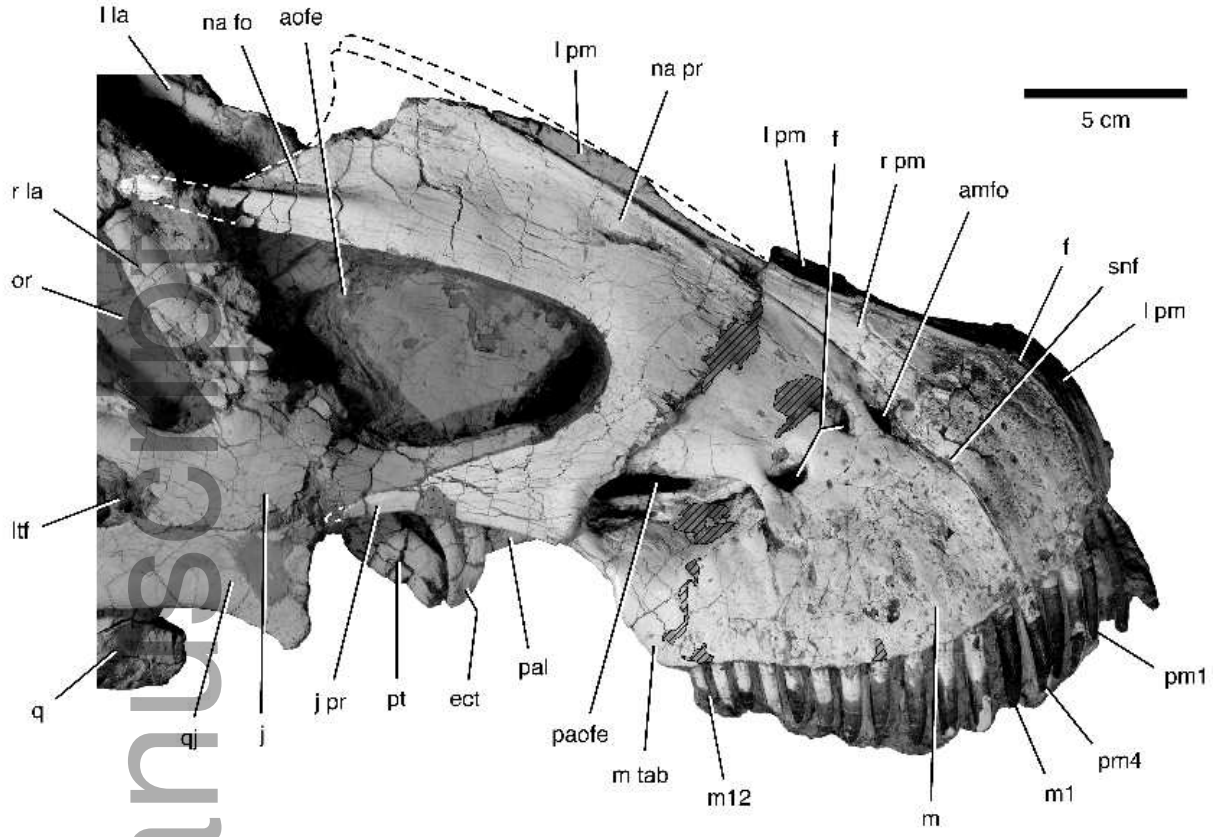

zoj_12420_f3.tif

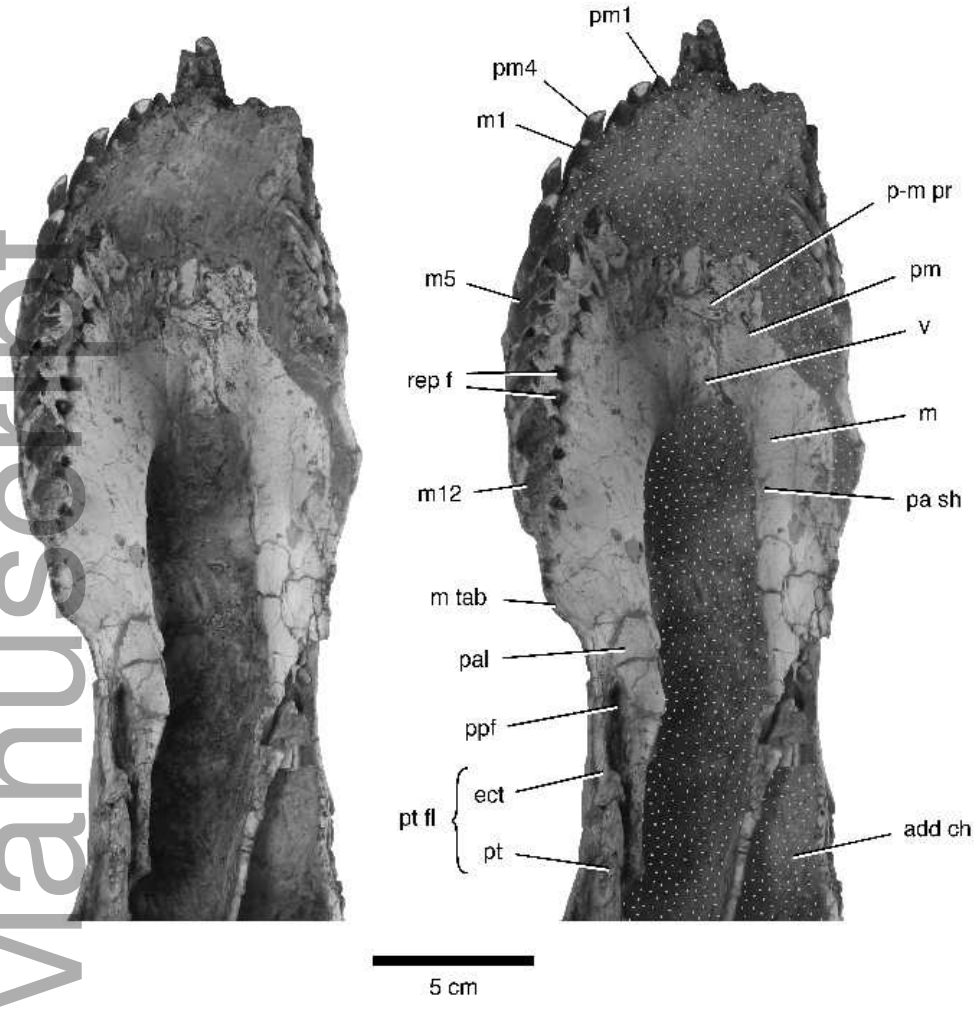

zoj_12420_f4.tif

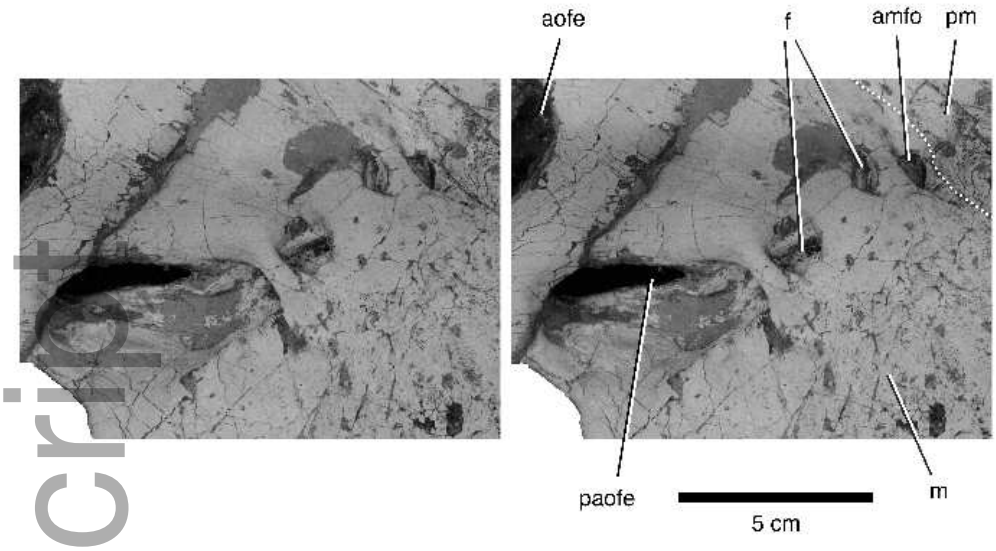

zoj_12420_f5.tif

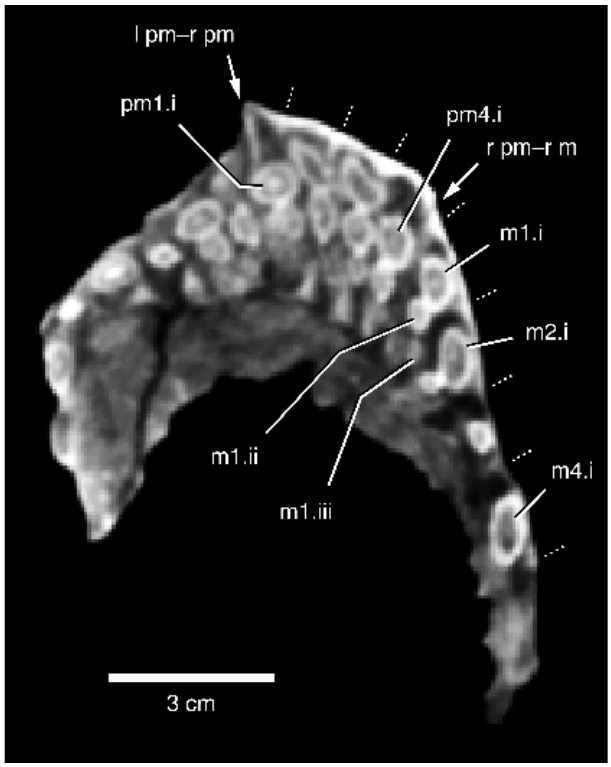

zoj_12420_f6.tif

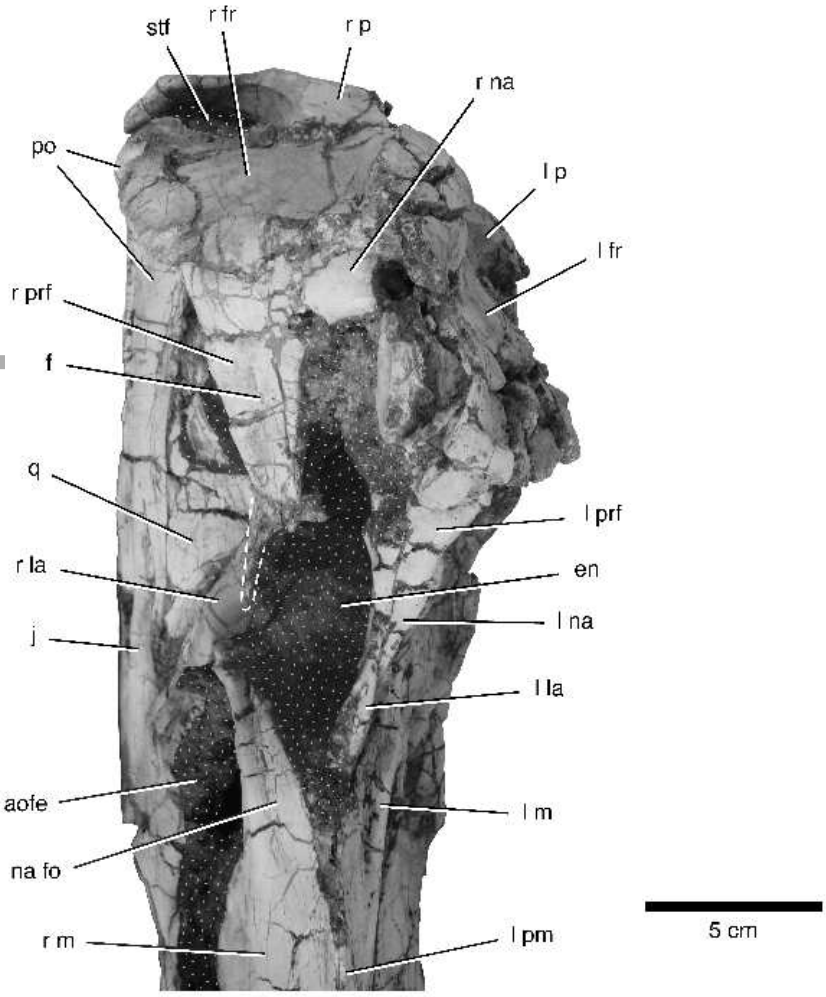

zoj_12420_f7.tif

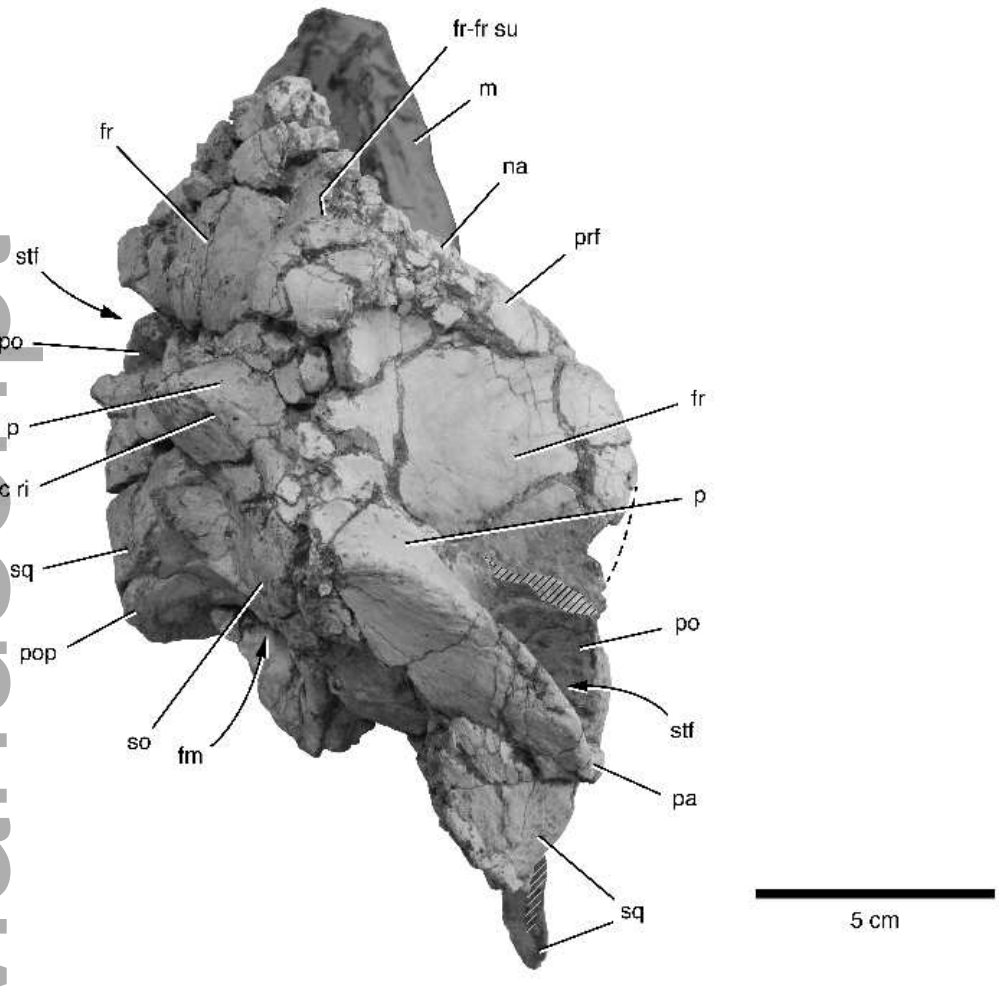

zoj_12420_f8.tif

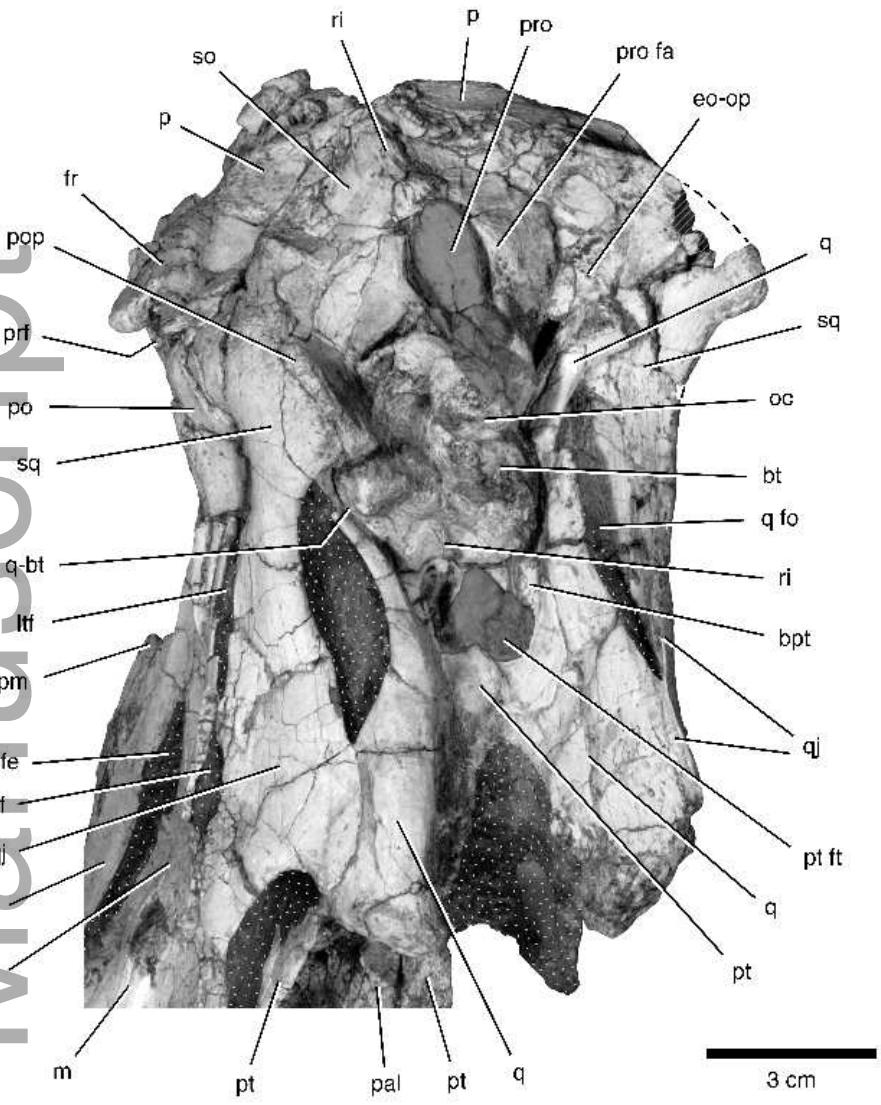

zoj_12420_f9.tif

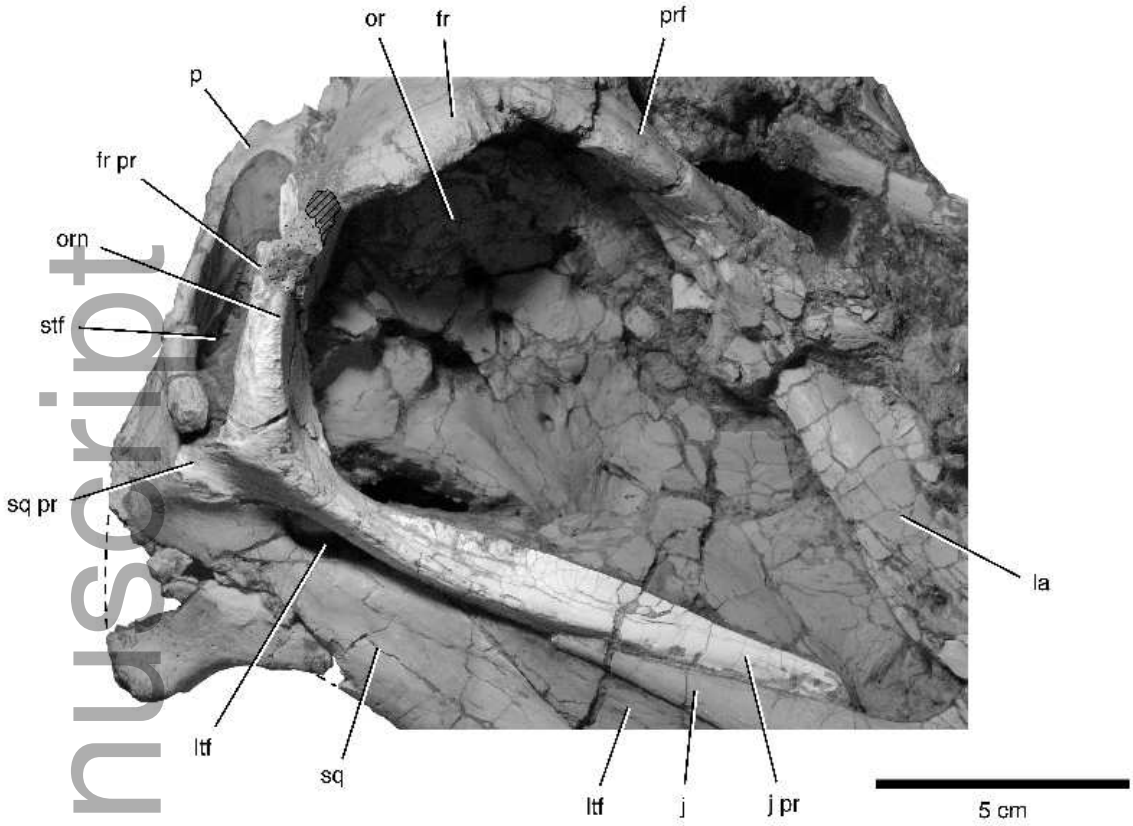

zoj_12420_f10.tif

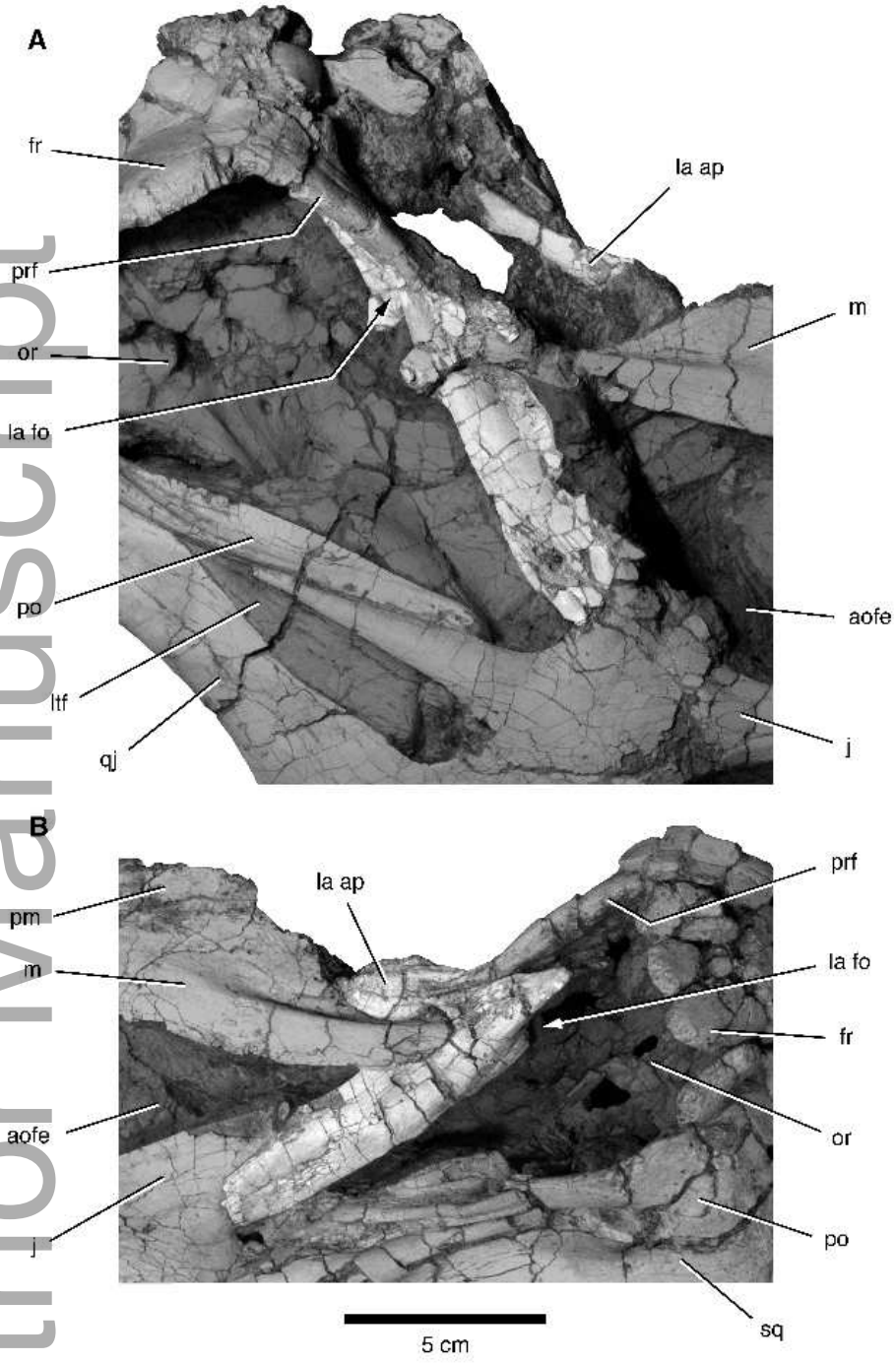

zoj_12420_f11.tif

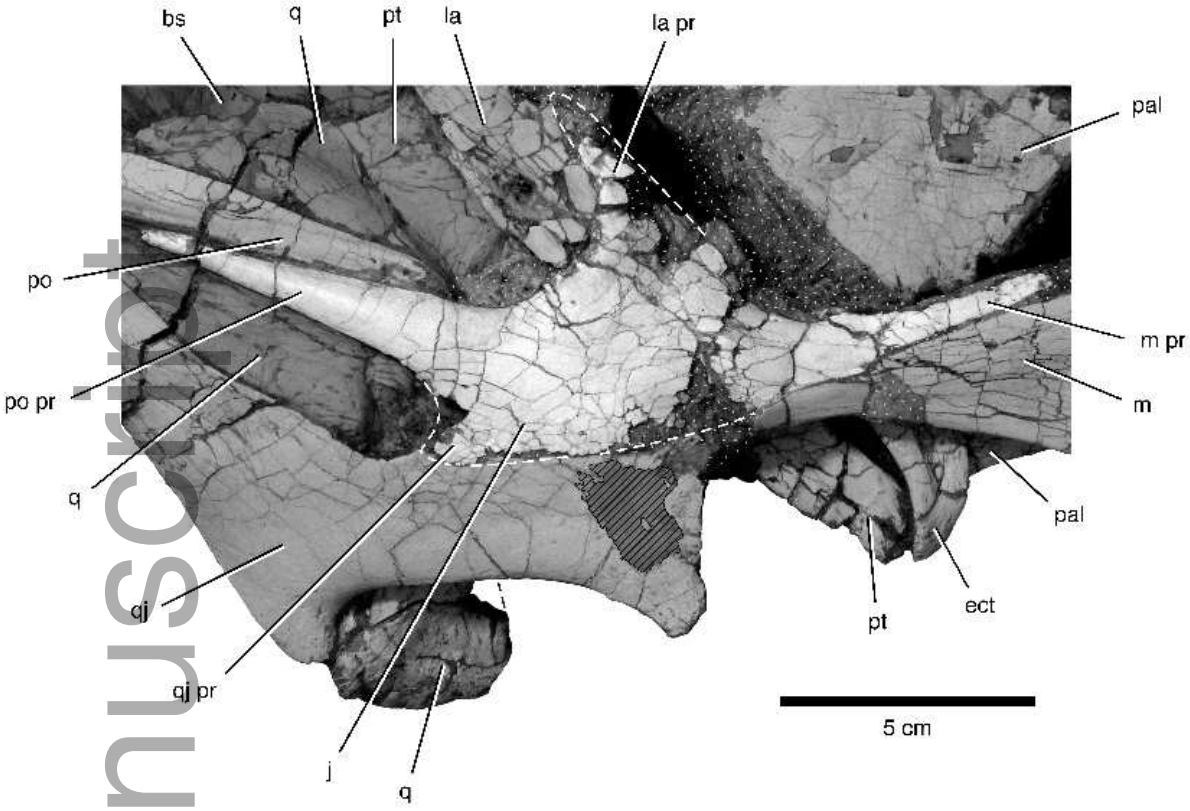

zoj_12420_f12.tif

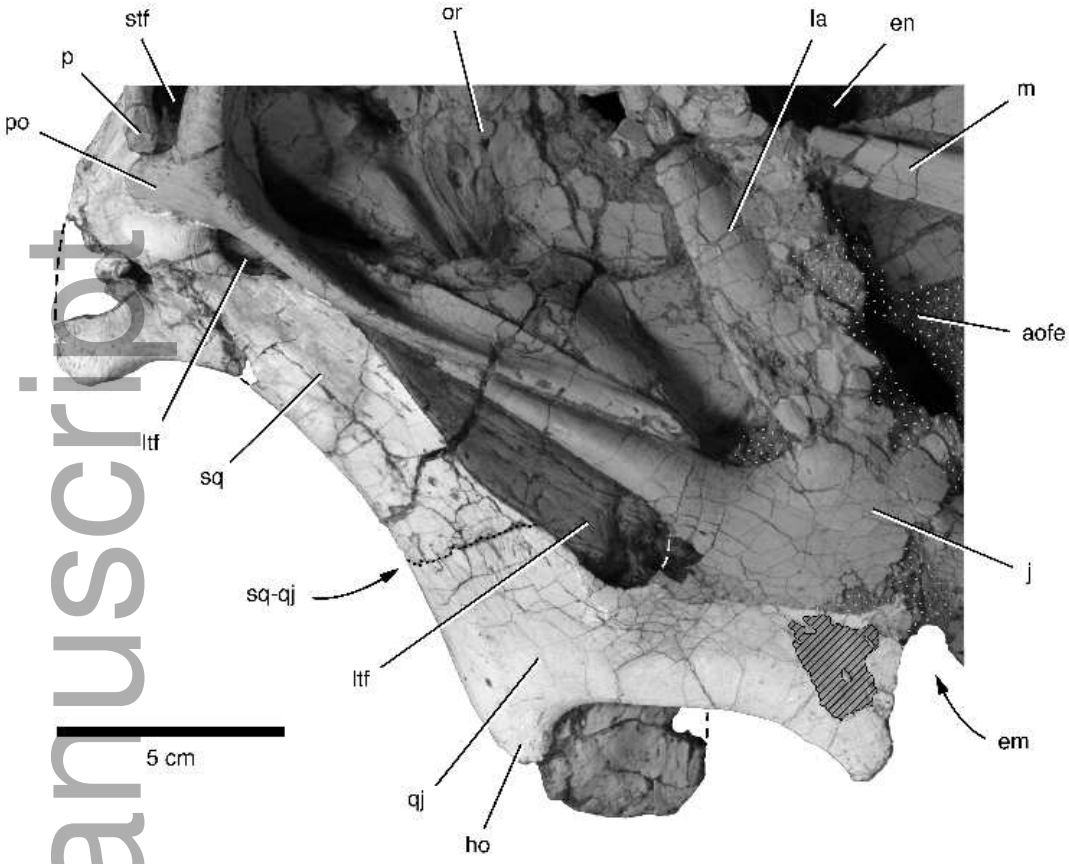

zoj_12420_f13.tif

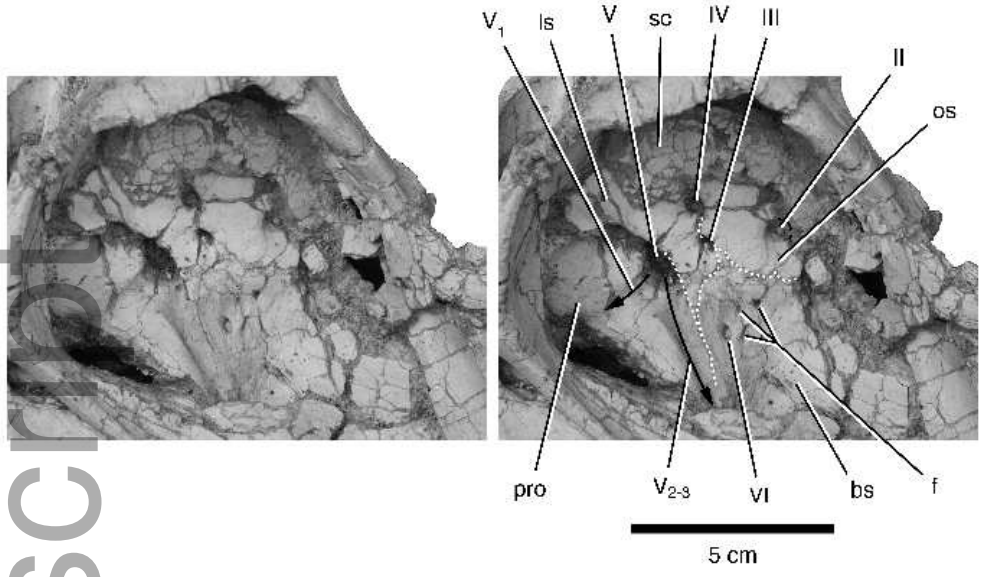

zoj_12420_f14.tif

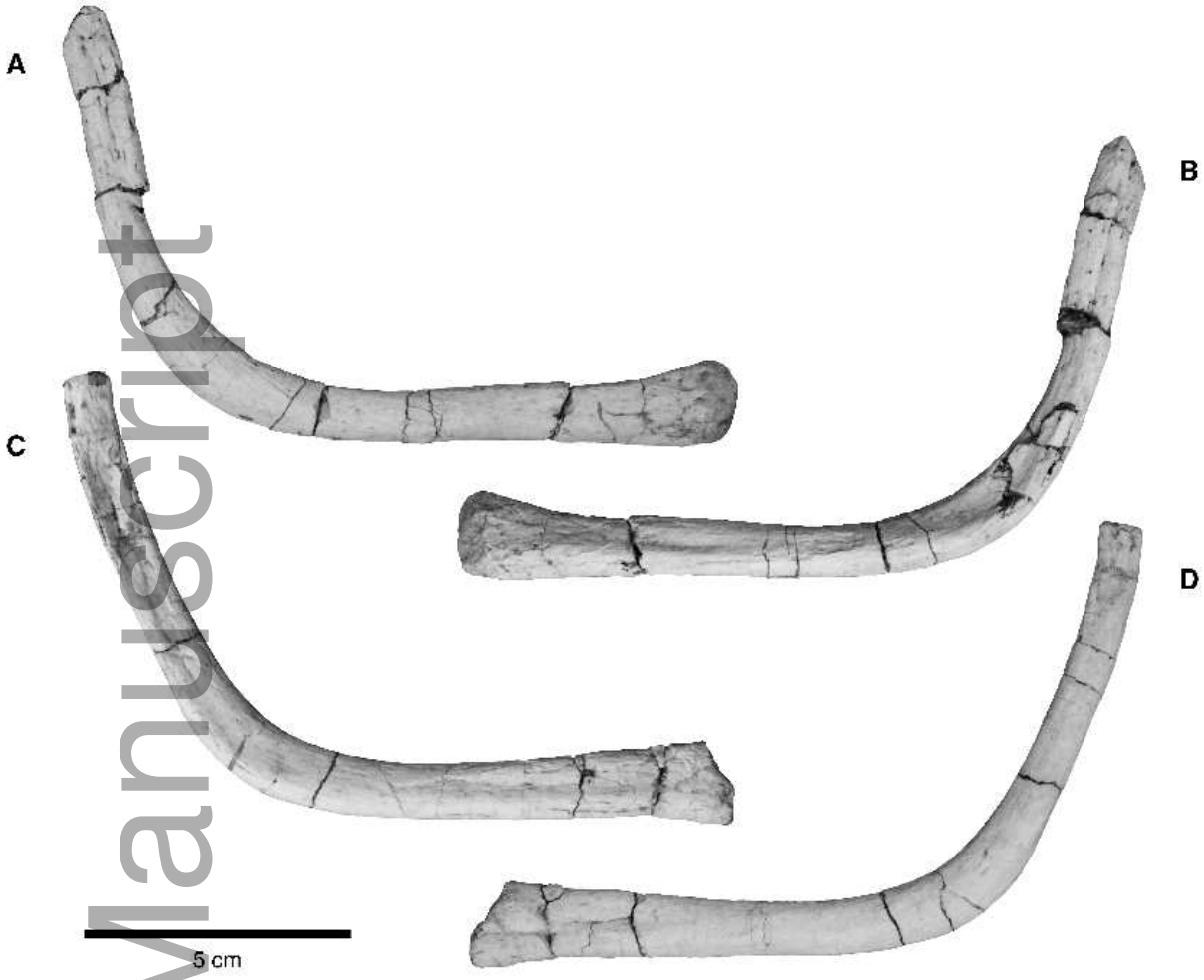

zoj_12420_f15.tif

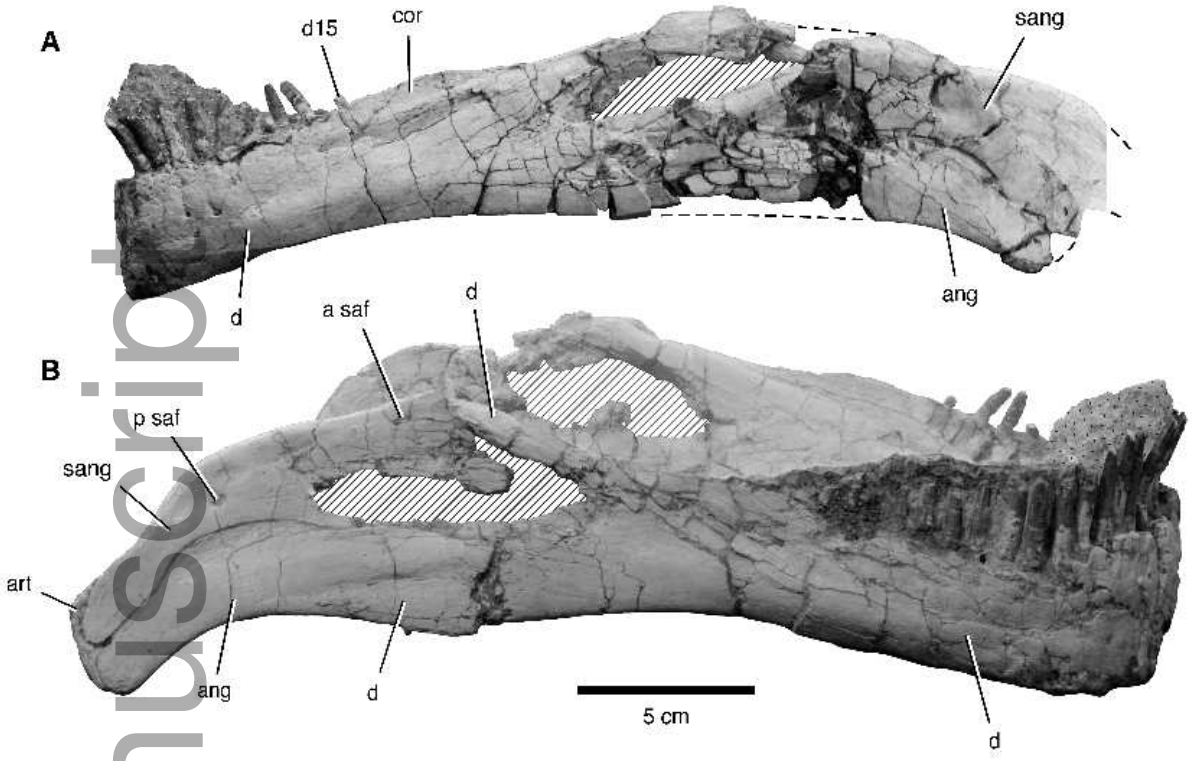

zoj_12420_f16.tif

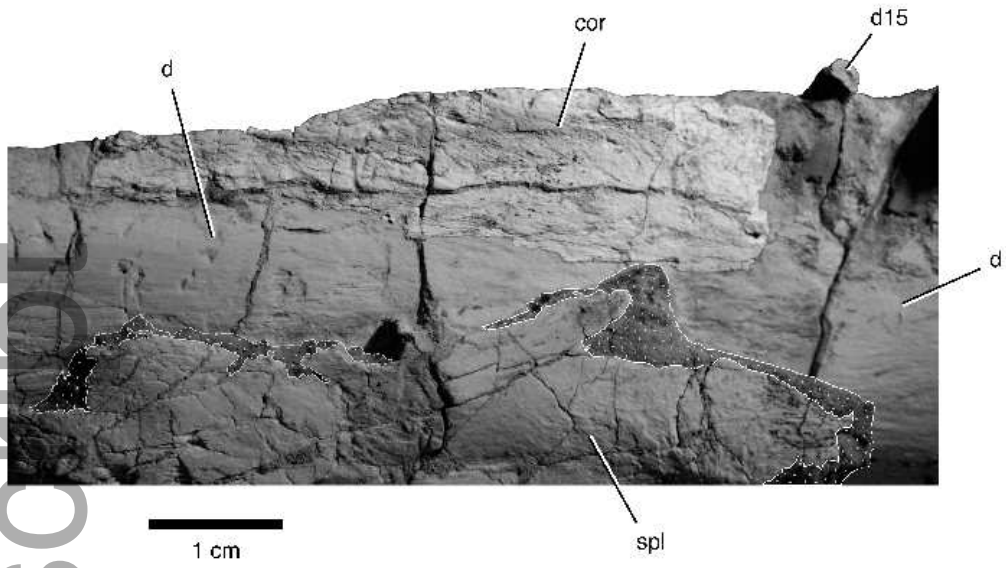

zoj_12420_f17.tif

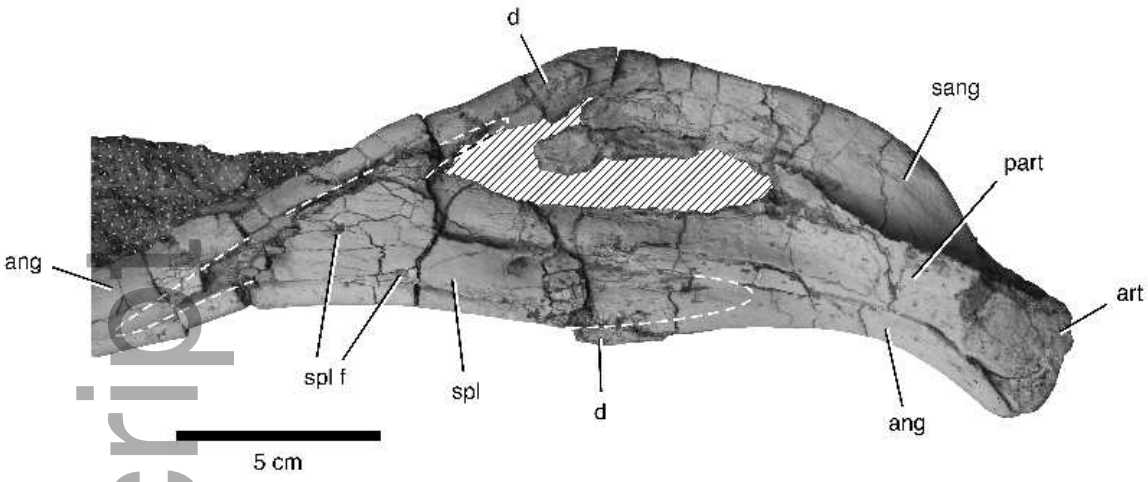

zoj_12420_f18.tif

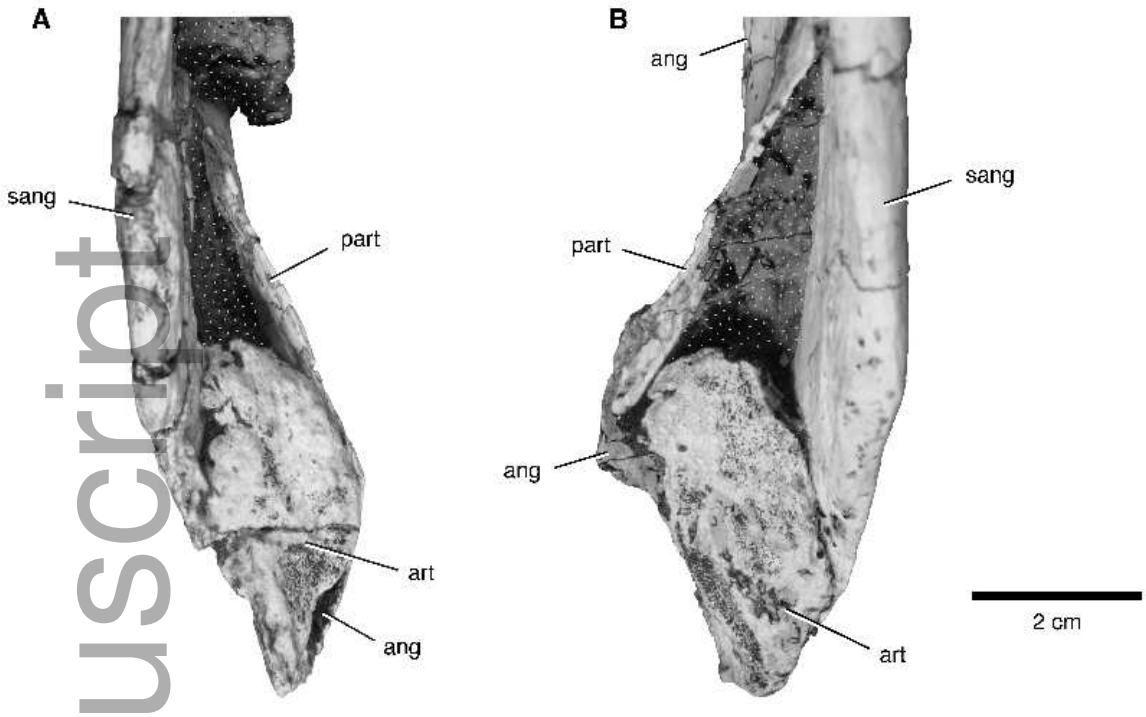

zoj_12420_f19.tif

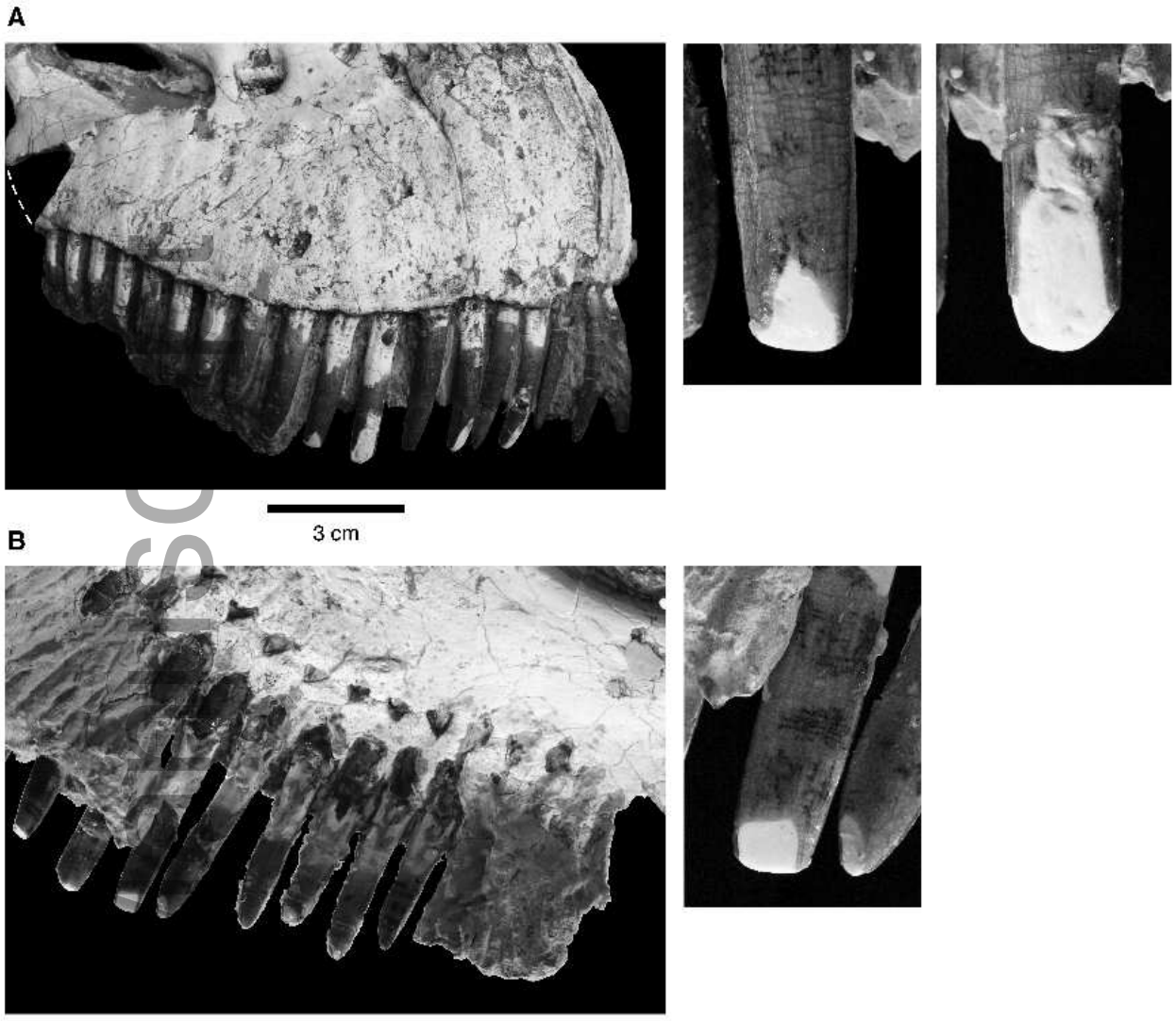

zoj_12420_f20.tif

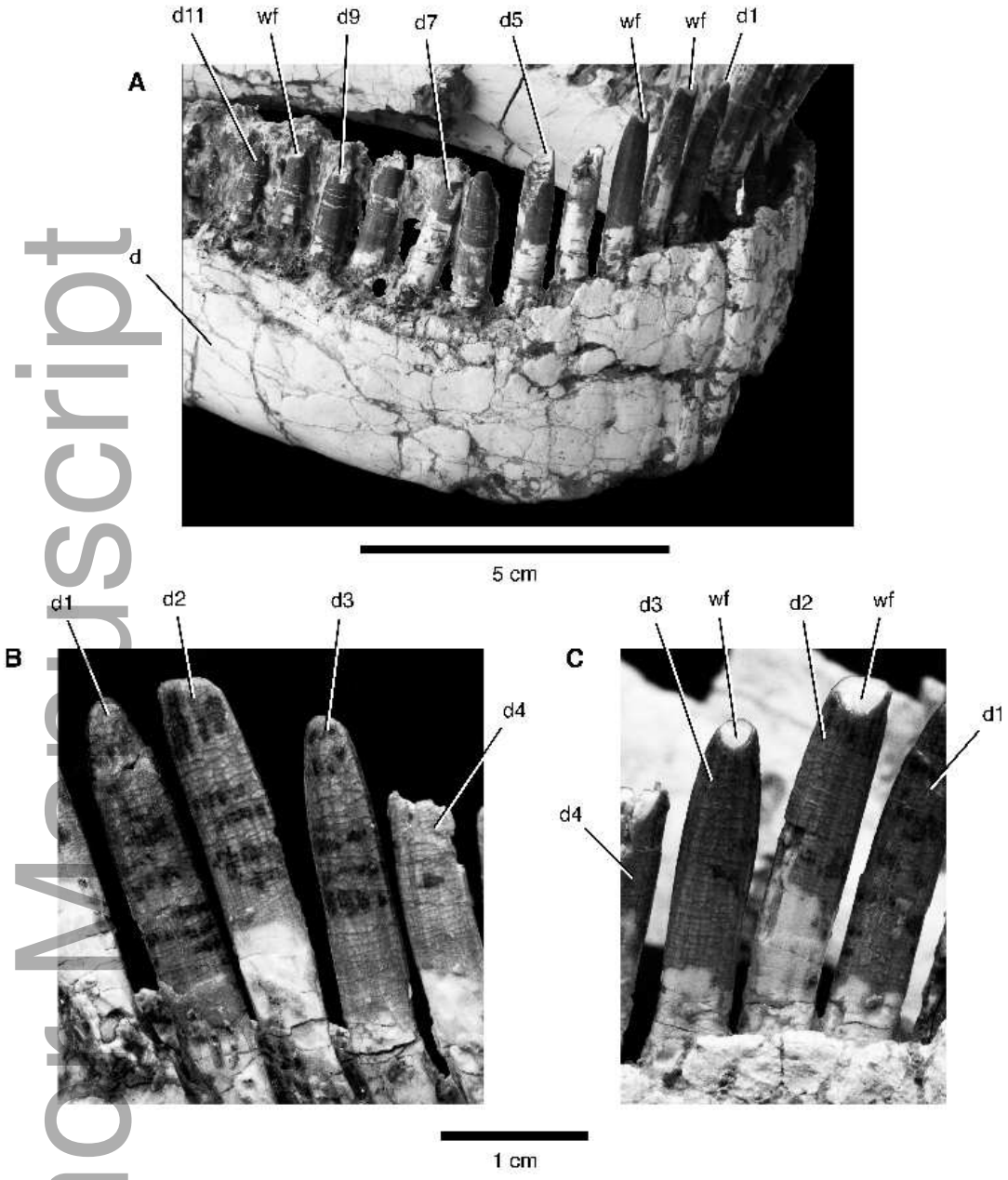

zoj_12420_f21.tif

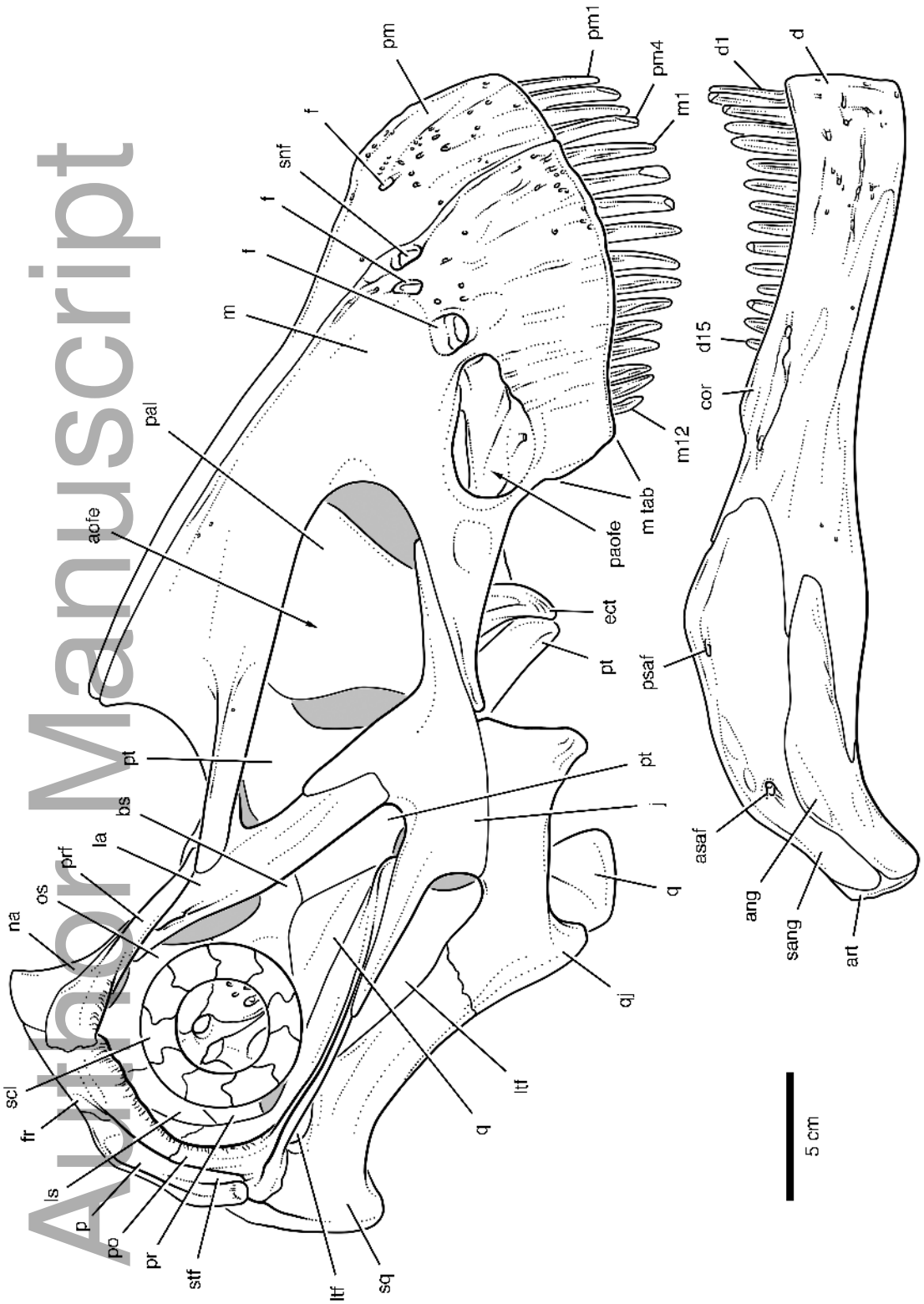

zoj_12420_f22.tif

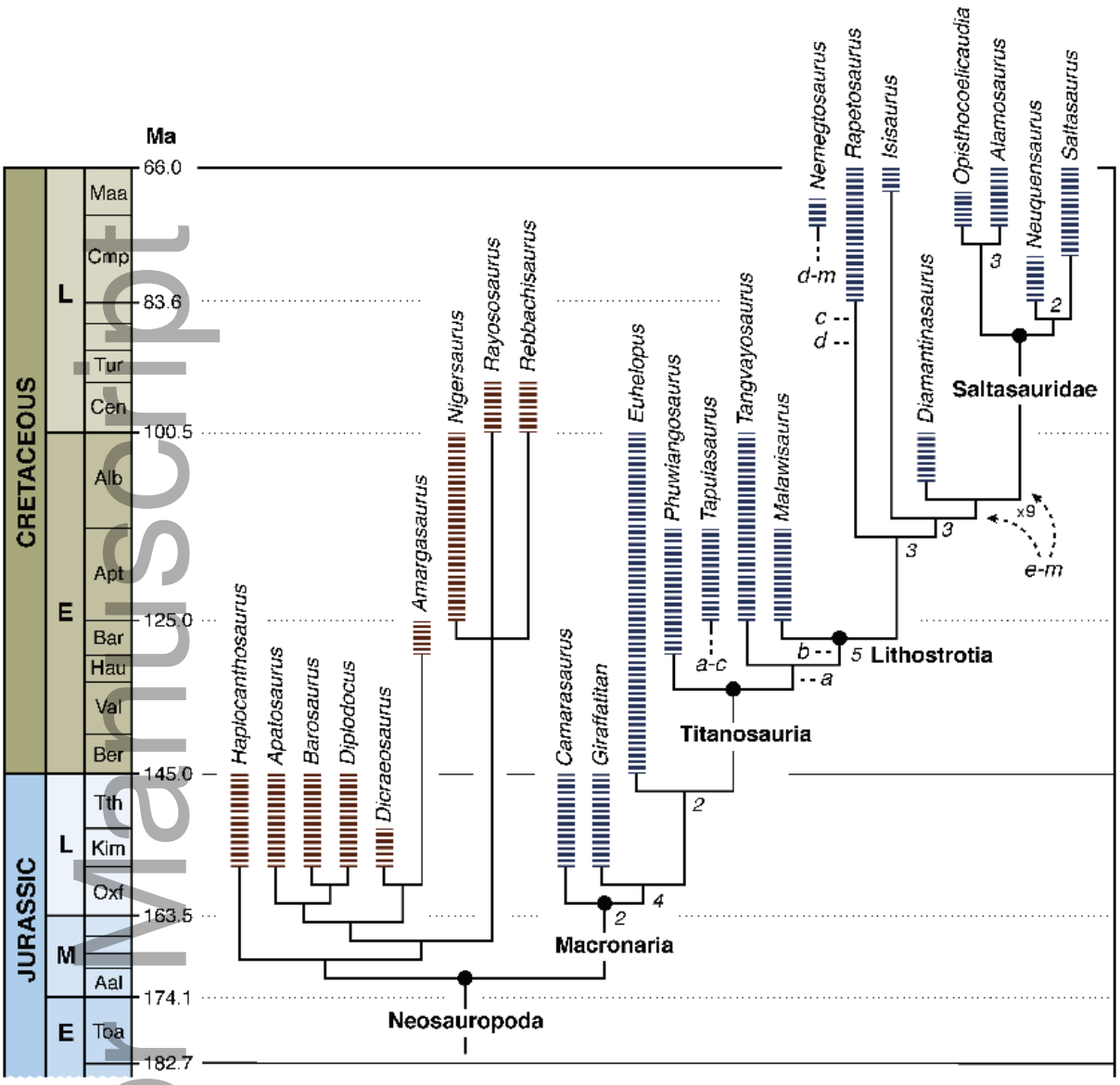

zoj_12420_f23.tif

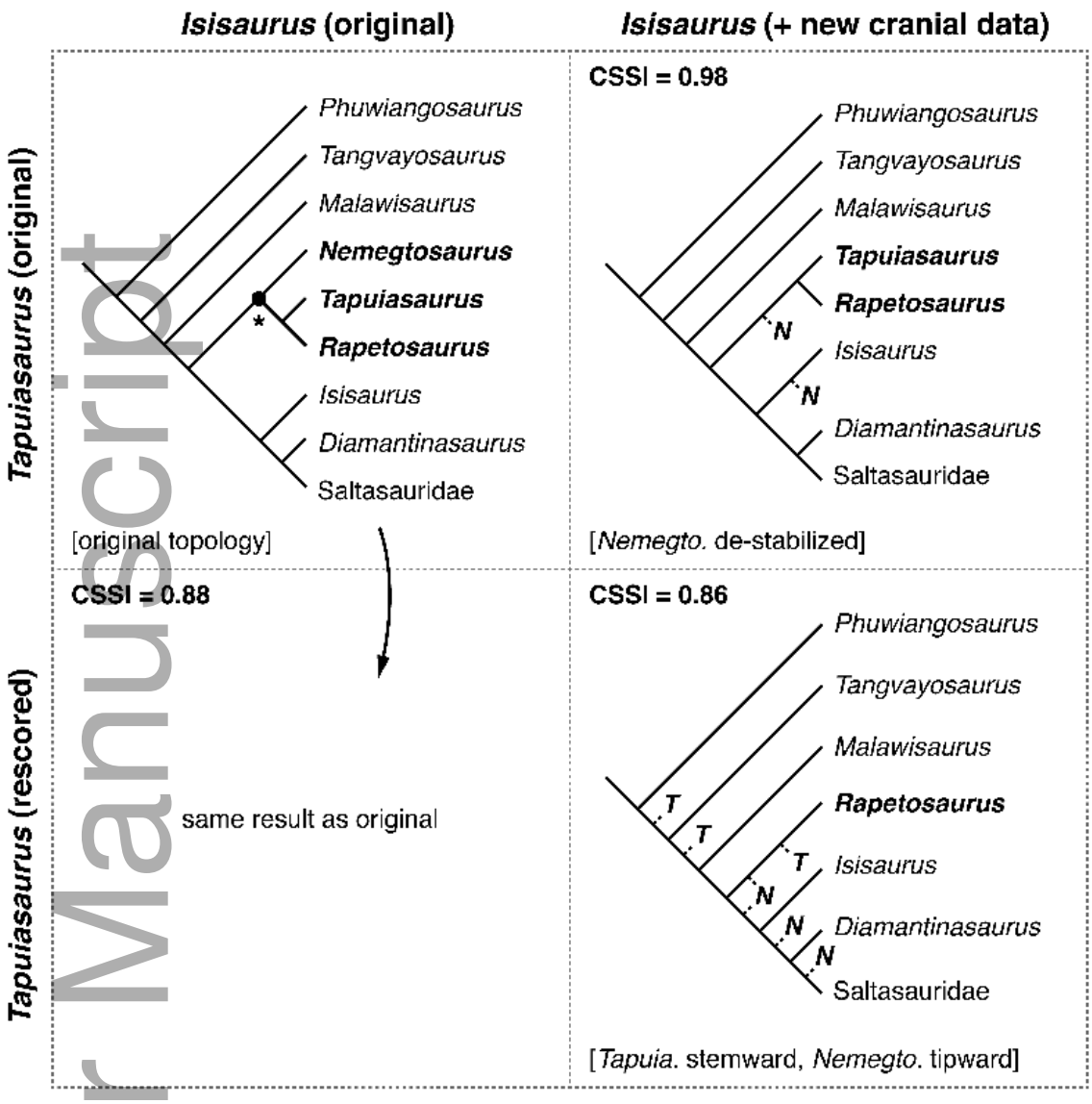

zoj_12420_f24.tif

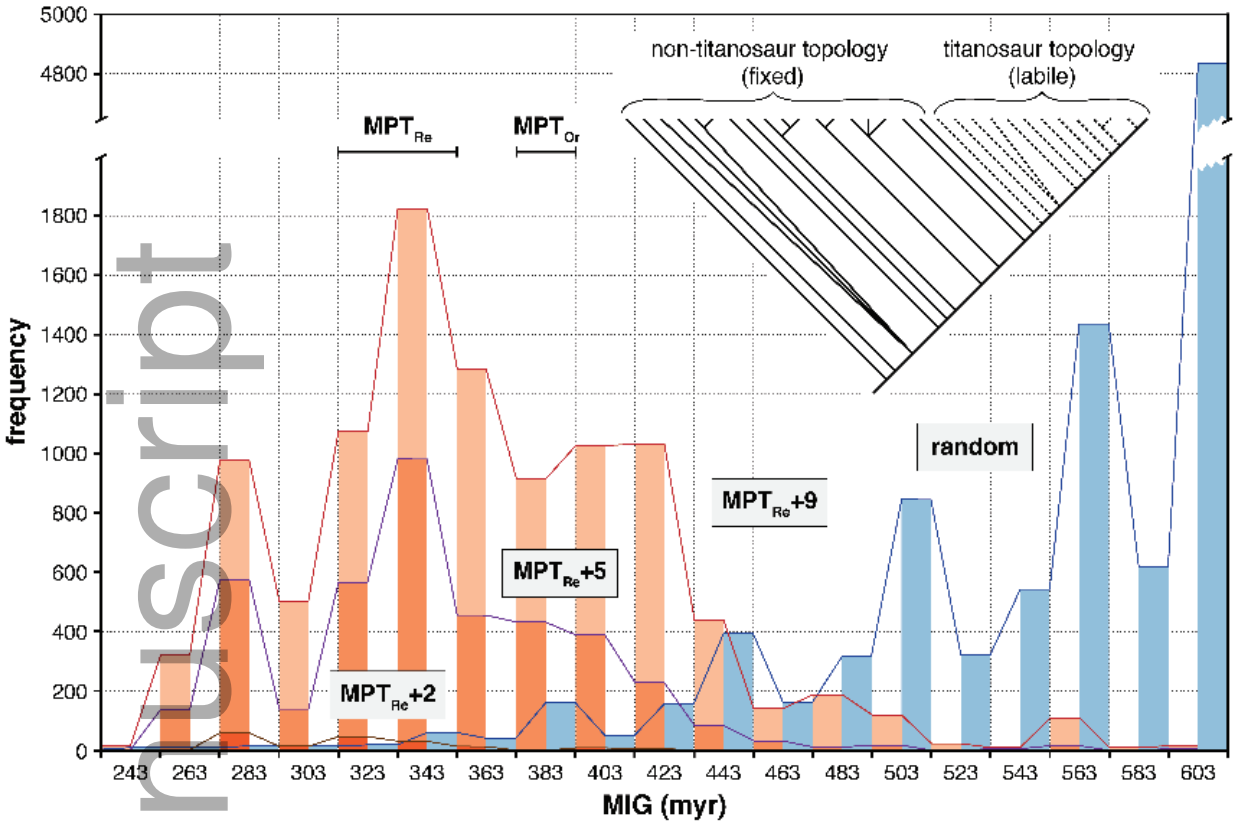

zoj_12420_f25.tif